Effect of Glucose on Human Adipogenesis and its Regulation by Macrophages

Vian Peshdary

A thesis submitted to the Faculty of Graduate and Postroctoral Studies in partial fulfillment of the requirements for the PhD degree in Biochemistry

Biochemistry, Microbiology and Immunology
Faculty of Medicine
University of Ottawa

ABSTRACT

Adipose tissue expands via differentiation of preadipocytes into adipocytes (adipogenesis) and/or hypertrophy of existing adipocytes. A low adipogenic capacity promotes adipocyte hypertrophy, causing inflammatory macrophage accumulation and insulin resistance. Macrophage-conditioned medium (MacCM) inhibits adipogenesis and promotes adipocyte inflammation, but it is unknown if these effects are altered by high glucose (HG) versus normal glucose (NG) concentrations. The effect of HG on adipogenesis was assessed. Human subcutaneous abdominal preadipocytes were induced to differentiate in HG or NG conditions. HG did not affect adipogenesis. HG increased ChREBP-β mRNA and protein levels, and increased GLUT4 mRNA, in differentiated adipocytes. It did not change mRNA levels of ACC, SCD, and FAS. The increase in ChREBP-β mRNA was positively correlated with HG-induced increase in GLUT4 mRNA. The effect of HG-MacCM versus NG-MacCM on human adipogenesis and adipocyte inflammation was compared. Human monocyte-derived macrophages (MDM) were placed in NG or HG glucose for 24 hours to generate MacCM. HG-MacCM, but not NG-MacCM inhibited triacylglycerol accumulation and protein expression of PPARγ during human adipogenesis. Preadipocytes differentiated in HG-MacCM displayed a more pro-inflammatory phenotype, as assessed by increased MCP-1 and IL-6 and reduced adiponectin mRNA expression. HG increased phosphorylation of IKK-β and decreased protein expression of IκBα in MDMs. In addition, HG reduced protein expression of PPARγ in MDMs. The pro-inflammatory effect of HG-MacCM on MCP-1 expression in adipocytes was partially inhibited when MDMs were treated with sc-514 (IKKβ inhibitor). My data demonstrate that HG-induced expression of ChREBP-β in adipocytes may be associated with increased GLUT4 mRNA. The anti-

adipogenic and pro-inflammatory effects of HG-MacCM are more potent than NG-MacCM. This suggests the possibility that adipose tissue cellular remodeling *in vivo* may be altered with hyperglycemia.

ACKNOWLEDGEMENTS

I would like to deeply and sincerely thank my thesis supervisor, Dr. Alexander Sorisky and lab research associate, Dr. AnneMarie Gagnon for all the valuable guidance, unending patience, and the continued support they have provided me throughout my training. I sincerely thank my thesis advisory committee members, Dr. Fraser Scott, Dr. Xiaohui Zha, and Dr. Mary-Ellen Harper for their guidance and support. I thank Anne Landry for all her continued help in and out of the lab. I thank all the old and new lab-mates who have made my journey pleasant and memorable. I would like to thank the patients and surgeons of The Ottawa Hospital for human adipose tissue samples. Finally, I thank my family and friends for their support and encouragement.

TABLE OF CONTENTS

LIST OF ABBREVIATIONS

ABCA1	ATP-binding cassette transporter A1
ACC	Acetyl-CoA carboxylase
AIM	Apoptosis inhibitor of macrophage
Akt	Protein kinase B
AMPK	AMP-activated protein kinase
ANF	Angiogenin
ANOVA	Analysis of variance
AP-1	Activated protein-1
aP2/FABP4	Adipocyte fatty acid binding protein 4
Arg1	Arginase 1
AT	Adipose tissue
ATM	Adipose tissue macrophage
ATP	Adenosine triphosphate
BAT	Brown adipose tissue
BMDM	Bone marrow-derived macrophages
BMI	Body mass index
BSA	Bovine serum albumin
C/EBPα	CCAAT/enhancer binding protein
cAMP	Cyclic adenosine monophosphate
CCL	Chemokine C-C motif ligand
CCR	Chemokine C-C motif receptor
CD	Cluster of differentiation
CDA	Canadian Diabetes Association
CEB	Cytosol Extraction Buffer
ChoRE	Carbohydrate response element
ChREBP	Carbohydrate-responsive element-binding protein
CLS	Crown-like structure
CREB	cAMP response element-binding protein
CXCL5	C-X-C motif chemokine
DAG	Diacylglycerol
DEXA	Dual-energy X-ray absorptiometry
DMEM	Dulbecco's modified Eagle's medium
DMSO	Dimethyl sulfoxide
ECM	Extracellular matrix
EGTA	Ethylene glycol tetraacetic acid
ELISA	Enzyme-linked immunosorbent assay
ERK1/2	Extracellular signal-regulated kinase 1/2
F2-6P2	Fructose -2, 6-P2
FA	Fatty acid
FAS	Fatty acid synthase
FBS	Fetal bovine serum
G6P	Glucose 6-phosphate
GLUT4	Glucose transporter type 4

Gr1	Granulocyte differentiation antigen 1
HG	High glucose
HOMA-IR	Homeostasis model assessment of insulin resistance
HRP	Horseradish peroxidase
IBMX	Isobutylmethylxanthine
ICAM-1	Intercellular adhesion molecule-1
ICAM-3	Intercellular adhesion molecule-3
IFNγ	Interferon gamma
IGF-1	Insulin-like growth factor 1
IKK	Inhibitor of IκB kinase;
IL	Interleukin
IR	Insulin receptor
IRS-1	Insulin receptor substrate-1
IκB	Inhibitor of κB
JNK	c-Jun N-terminal kinase
LD	Lipid droplet
LID	Low-glucose inhibitory domain
LOX-1	Lectin-like oxidized LDL receptor-1
LPL	Lipoprotein lipase
LPS	Lipopolysaccharide
MacCM	Macrophage-conditioned medium
MC4R	Melanocortin 4 receptor
MCP-1	Monocyte chemoattractant protein-1
MDM	Monocyte derived macrophage
MEF	Embryonic fibroblasts
MEK1/2	Mitogen-activated protein kinase kinase
MG	Monoacylglycerol
MIF	Macrophage migration inhibitory factor
Mlx	Max-like protein X
MSC	Mesenchymal stem cells
NEFA	Non-esterified fatty acids
NES	Nuclear export signal
NF-κB	Nuclear factor-κB
NG	Normal glucose
NLS	Nuclear localization signal
NO	Nitric oxide
NOS	Nitric oxide synthase
NOX	Nicotinamide adenine dinucleotide phosphate oxidase
OC	Osmotic control
PBMC	Peripheral blood mononuclear cells
PDGF	Platelet-derived growth factor
PDGFRβ	Platelet-derived growth factor receptor beta
PGD_2	Prostaglandin D_2
PGE_2	Prostaglandin E_2
PKA	Protein kinase A
PKC	Protein kinase C

PPARγ	Peroxisome proliferator-activated receptorγ
ROS	Reactive oxygen species
RPMI	Roswell Park Memorial Institute medium
RQ	Relative quantification
SAT	Subcutaneous adipose tissue
SCD	Stearoyl-CoA desaturase
SDS-PAGE	Sodium dodecyl sulfate polyacrylamide gel electrophoresis
SGBS	Simpson-Golabi-Behmel syndrome
SR-A	Scavenger receptor
SREBP-1	Sterol regulatory enhancer binding protein 1
SVF	Stromal-vascular fraction
T1D	Type 1 diabetes
T2D	Type 2 diabetes
TG	Triacylglycerol
TNFα	Tumor necrosis factor α
UCP-1	Uncoupling protein -1
VAT	Visceral adipose tissue
WHO	World Health Organization
Xu-5P	Xylulose 5-P

LIST OF FIGURES AND ILLUSTRATIONS

LIST OF TABLES

1. INTRODUCTION

1.1 Obesity

1.1.1 *Definition and measurement of obesity*

Obesity is an excess accumulation of body fat that can adversely affect health (Navaneelan and Janz, 2014). We are currently in a worldwide pandemic of obesity (Speakman and O'Rahilly, 2012). Twenty five percent of adult Canadians were reported to be obese in 2011-2012, a 17.5% increase since 2003 (Navaneelan and Janz, 2014). The most common method used to measure obesity is body mass index (BMI), obtained by dividing weight by the height squared (kg/m^2). A BMI equal to or greater than 25 kg/m^2 is considered overweight, and a BMI equal to or greater than 30 kg/m^2 is classified as obese (WHO, 2004). BMI measurement is time/cost-effective and simple to do, however it has important limitations. For instance, BMI does not distinguish between non-fat (bone, muscle, etc.) and fat weight. Therefore, BMI may overestimate body fat in an individual who is very muscular, and it may underestimate body fat in an individual who has lost muscle mass. Furthermore, body fat distribution is not provided by BMI. Other simple measurements can be used along with BMI to assess body fat such as waist circumference. Other more sophisticated adipose tissue assessments exist, including skin calipers, bioelectrical impedance, hydrostatic weighing, DEXA (dual-energy x-ray absorptiometry), or air-displacement plethysmography (Wells and Fewtrell, 2006).

1.1.2 *Etiology of obesity*

Obesity arises due to excess caloric intake and/or decreased energy expenditure. Although the reasons for the development of obesity are complex, the development of

obesity strongly depends on genetic predisposition and/or environmental factors. Genetically predisposed responses to social and environmental behaviours promote calorie-rich food consumption and a sedentary lifestyle (Speakman and O'Rahilly, 2012). Based on twin and adoption studies, genetic factors contribute to 40%-75% of BMI variation within a population (Tung and Yeo, 2011). There are also monogenic forms of obesity, which usually lead to early-onset weight gain. Of these, melanocortin 4 receptor (MC4R) deficiency is the most common, accounting for 5.8% of early-onset severe weight gain. Stimulation of MC4R in the hypothalamus normally leads to decreased food intake (Farooqi et al., 2003).

1.1.3 *Complications of obesity*

Obesity is a severe health concern, as it is associated with complications such as type 2 diabetes (T2D), cardiovascular disease, hypertension, cancer, and mental health disorders like anxiety and depression (Krauss et al., 1998; Gariepy et al., 2010; Atlantis and Baker, 2008; Calle et al., 2003; Wilson et al., 2002). Excess adiposity can blunt the sensitivity of insulin action in peripheral tissues causing local and systemic insulin resistance (Khan and Fleir, 2000). Insulin resistance leads to excessive adipocyte release of non-esterified fatty acids (NEFA), reduced glucose uptake by myocytes, and increased production of glucose and very low density lipoproteins by hepatocytes (Jung and Choi, 2014). One of the major causes of obesity-induced insulin resistance is chronic low-grade inflammation that occurs due to over-production of pro-inflammatory factors within the adipose tissue and their release into the circulation (Johnson and Olefsky, 2013).

1.2 Adipose tissue (AT)

1.2.1 *Adipose tissue types: brown versus white*

There are two types of adipose tissue (AT), white and brown AT (BAT). Each possesses unique features and distinct metabolic functions. BAT contains more capillaries and nerve supply than white AT. The brown colour of BAT is due to high vascularization and high mitochondrial density in the brown adipocytes (Saely et al., 2012). BAT is primarily involved in thermogenesis and is essential for the survival of small mammals in cold environments. Brown adipocytes are uniquely enriched with uncoupling protein -1 (UCP-1) that plays a key role in heat production (Cannon, 1982, Harms and Seale, 2013). Heat is generated when activated UCP-1 in brown adipocytes short circuits the electrochemical gradient that normally supports adenosine triphosphate (ATP) synthesis. In humans, it was classically thought that BAT disappeared after birth, however recent positron emission tomography studies have found BAT in the neck region of adult humans (Cypess et al., 2009; van Marken Lichtenbelt et al., 2009; Virtanen et al., 2009). In response to cold exposure, circulating glucose and NEFA are taken up by BAT. Furthermore, increased uncoupled oxidation of NEFA by BAT upon cold exposure is significantly associated with whole body energy expenditure (Ouellet et al., 2012). BAT is therefore of great interest in humans, as it raises intriguing possibilities for treatment or prevention of obesity.

While BAT dissipates energy as heat, white AT (referred to as AT) stores energy, and it is the form of AT that defines obesity. Unlike brown adipocytes that store lipids in multiple small vacuolae, white adipocytes have a large unilocular lipid droplet. Also, in contrast to BAT, AT has fewer mitochondria and a low oxidative rate. The classical role of AT is regulation of energy homeostasis in times of feeding and fasting. After feeding, insulin

levels rise, promoting the uptake of energy by AT. Energy is stored in AT in the form of triacylglycerol (TG) through insulin stimulated lipogenesis (Fryan et al., 2003). During fasting or periods of exercise, activation of the sympathetic nervous system releases norepinephrine which stimulates lipolysis in AT and release of NEFA into circulation (Fryan et al., 2003).

1.2.2 *Adipose tissue depots*

In humans, the major AT depots are intra-abdominal (visceral AT; VAT) and subcutaneous (SAT) depots. VAT includes fat depots around the omentum, intestine, and perirenal areas. SAT accounts for ~80% of body fat, and is located mainly in abdomen, buttocks, and thighs (Gesta et al., 2007; Wajchenberg, 2000). AT can also be found in many other areas such as the retro-orbital space, within the bone marrow, and on the face (Gesta et al., 2007).

VAT compared to SAT is more vascular, innervated, and contains more inflammatory and immune cells (Ibrahim, 2010). VAT adipocytes are also more metabolically active than SAT adipocytes. VAT adipocytes are more responsive to adrenergic stimulated lipolysis than SAT adipocytes. With obesity, adipocytes from VAT are more insulin-resistant than SAT adipocytes. SAT has a greater capacity for energy storage than VAT. These differences between VAT and SAT may contribute to the positive correlation observed between VAT accumulation and metabolic disorders (e.g. insulin resistance, T2D) (Ibrahim, 2010).

1.2.3 *Adipose tissue endocrine function*

In addition to its classical role in energy homeostasis, AT is also an active endocrine organ, regulating many physiological processes in the body (Galic et al., 2010). As an endocrine organ, AT releases various adipocyte-specific factors known as adipokines, with the two most studied being, leptin and adiponectin (Galic et al., 2010). Leptin is the polypeptide product of the *ob* gene, cloned in 1994 by Freidman and colleagues (Zhang et al., 1994). The cloning of leptin solved the genetic mystery of the obese phenotype of the *ob* mutant mouse, generated in 1950 (Ingalls et al., 1950). Leptin suppresses food intake by acting on its receptor in the hypothalamus (Myers et al., 2008). Leptin also promotes energy expenditure by acting on the central nervous system as well as peripheral tissues (Bjorbaek and Kahn, 2004). Levels of leptin in circulation are proportional to the amount of AT (Myers et al., 2008). Adiponectin is an anti-inflammatory adipokine that plays a major role in whole body insulin sensitivity. It increases fatty acid (FA) oxidation in muscle and liver, and promotes energy expenditure, and suppresses hepatic glucose production (Galic et al., 2010). Unlike leptin, levels of circulating adiponectin are inversely related to obesity (Ukkola and Santaniemi, 2002).

Other factors released by AT that are not adipocyte-specific include anti-inflammatory cytokines (interleukin (IL)-10 and secreted frizzled-related protein 5) and pro-inflammatory cytokines (IL-6, IL-1β, and tumor necrosis factor (TNF) -α), and they also act as autocrine and/or paracrine signals (Bradley et al., 2008; Hotamisligil et al., 1995; Ouchi et al., 2010; Turer and Scherer, 2012). These factors are produced by various cell types in the AT including, adipocytes, preadipocytes, and immune cells.

1.2.4 *Cellular components of adipose tissue*

Adipose tissue is heterogeneous and is composed of many cell types, including adipocytes, preadipocytes, fibroblasts, endothelial cells, mast cells, neurons, and immune cells (Lee et al., 2010). Adipocytes make up about 50-70% of the AT cellular mass. Preadipocytes comprise 20-40%, endothelial cells make up 1-10% and immune cells account for 1-30% of AT cellular mass (Hauner, 2005). The percent composition of other cell types in the AT is unknown but minor.

Adipocytes are mature fat cells that serve as an energy reservoir, with lipid storage capacity of ~3 μg/cell (Danforth, 2000). Lipids are stored as TG within a single lipid droplet in the adipocyte. The lipid droplet consists of phospholipid monolayer encapsulating a neutral lipid core mostly composed of TG with trace amount of cholesteryl ester (Frayn et al., 2003). Preadipocytes are progenitor cells with partial commitment to an adipocyte fate upon differentiation (adipogenesis; discussed below). Endothelial cells and fibroblasts in AT contribute to formation of extensive vasculature and provide structural support respectively. Immune cells in the AT include B-cells, T-cells, monocytes, and macrophages (Lee et al., 2010).

1.3 Adipogenesis

Adipocytes differentiate from mesenchymal stem cells (MSCs), in a process known as adipogenesis. MSCs transition to become committed preadipocytes, which then, upon exposure to adipogenic inducers (discussed in section 1.3.2) undergo terminal differentiation to become mature adipocytes. Much of what is known about adipogenesis is derived from *in vitro* studies using adipogenic cell lines such as mouse 3T3-L1 (embryonic fibroblasts) preadipocytes (Green and Meuth, 1974). Although studies using 3T3-L1 preadipocytes have

been very valuable, they do not fully represent human cells. Primary human stromal preadipocytes are increasingly used for translational research.

1.3.1 *Adipogenic transcriptional machinery*

Adipogenesis is regulated by a complex network of transcriptional activities that gives rise to expression of various proteins involved in establishing a mature adipocyte phenotype. At the core of this elaborate network are two key adipogenic transcription factors, peroxisome proliferator-activated receptor γ (PPARγ) and CCATT-enhancer-binding protein (C/EBP)α that oversee the process of terminal differentiation (Farmer, 2006). PPARγ is viewed as the master regulator of adipogenesis. Without it, C/EBPα alone cannot promote adipogenesis (Rosen et al., 2002). Precursor cells deficient in C/EBPα can undergo terminal differentiation, but these C/EBPα-deficient adipocytes lack insulin-stimulated glucose uptake (Wu et al., 1999). These studies suggest that PPARγ and C/EBPα participate in a single pathway in adipocyte formation; however PPARγ is the dominant one.

PPARγ is a member of the nuclear hormone receptor family. It was first identified by Spiegelman and colleagues in 1994 who were searching for the transcription factor responsible for regulating the expression of adipocyte specific fatty acid binding protein 4 (aP2/FAB4) (Tontonoz et al., 1994). There are two isoforms of PPARγ (PPARγ1 and PPARγ2). The gene products are generated by differential promotor usage and alternative splicing resulting in four distinct transcripts (PPARG1, PPARG2, PPARG3, and PPARG4). PPARG1, PPARG3, and PPARG4 transcripts encode the same protein product, PPARγ1, which is expressed in most tissues. PPARG2 transcript encodes the PPARγ2 protein product, expressed almost exclusively in the AT. PPARγ2 has 30 more amino acids at the N-

terminus, however otherwise it is identical to PPARγ1 (Fajas et al., 1997, Mukherjee et al., 1997). Studies using PPARγ-/- mouse embryonic fibroblasts (MEFs) showed that when PPARγ1 and 2 were expressed ectopically, both isoforms could induce adipogenesis. However, PPARγ2 was able to stimulate a more robust adipogenesis under lower ligand concentrations than PPARγ1 (Mueller et al., 2002). Also, AT selective PPARγ2-/- mouse model displayed impaired insulin sensitivity, suggesting that PPARγ2 may have a selective role in modulating insulin sensitivity (Zhang et al., 2004).

Upon adipogenic stimuli, activation of other transcription factors precedes the expression of PPARγ and C/EBPα. Work by McKnight and his research group propose that two other members of the C/EBP family (C/EBPβ and C/EBPδ) are expressed earlier than PPARγ and C/EBPα during adipogenesis, and that C/EBPβ and C/EBPδ may in fact regulate the expression of C/EBPα (Cao et al., 1991; Yeh et al., 1995). These studies also showed that ectopic expression of C/EBPβ and C/EBPδ in NIH 3T3 (non-adipogenic fibroblasts) cells could force adipogenesis without stimulating C/EBPα expression (Yeh et al., 1995). To elucidate the link between C/EBPs and PPARγ expression during the onset of adipogenesis, other studies showed that inhibiting PPARγ activity in 3T3-L1 preadipocytes, inhibited adipogenesis but also blocked the activation of C/EBPα. This group also showed that ectopically expressed C/EBPβ in Swiss fibroblasts induced the expression of PPARγ independent of C/EBPα (Zuo et al., 2006). Collectively these data indicate that the onset of adipogenesis is a single unidirectional path involving early activation of C/EBPδ and C/EBPβ stimulation of PPARγ, which then activates C/EBPα (Farmer, 2006).

Another transcription factor that plays a key role in adipogenesis is sterol regulatory element-binding protein 1 (SREBP-1). An adipogenic role for SREBP-1 was suggested when a dramatic induction of SREBP-1 mRNA expression was observed during adipogenesis of 3T3-L1 and 3T3-F442A preadipocytes (Kim and Spiegelman, 1996). The work by Spiegelman and colleagues showed that when a dominant-negative form of SREBP-1 was introduced, differentiation of 3T3-L1 cells was inhibited, but this inhibition could be overcome by addition of PPARγ ligand (Kim and Spiegelman 1996; Kim et al., 1998). In addition, overexpression of SREBP-1 in non-adipogenic NIH-3T3 cells significantly increased the adipogenic activity of PPARγ (Kim and Spiegelman 1996). Therefore, SREBP-1 may regulate the activity of PPARγ during adipogenesis. In addition to its involvement in adipogenesis, SREBP-1 is a well-established lipogenic transcription factor that stimulates the expression of many genes necessary for lipogenesis, such as fatty acid synthase (FAS).

1.3.2 *Adipogenic inducers*

Differentiation inducers include insulin (850 nM), dexamethasone (0.5 μM), isobutylmethylxanthine (IBMX; 0.25 mM), and indomethacin (100 μM). During differentiation, insulin acts on insulin receptors to promote Akt-dependent phosphorylation of FoxO1, a forkhead transcription factor. Phosphorylation of FoxO1 prevents its translocation into the nucleus, where FoxO1 would normally suppress the expression of adipogenic genes (Farmer, 2006). Dexamethasone is a synthetic glucocorticoid that, through binding to glucocorticoid receptor, induces the expression of C/EBPδ and acetylation/binding of C/EBPβ to adipogenic target genes (Cristancho and Lazar, 2011). IBMX is a phosphodiesterase inhibitor that leads to increased levels of cAMP. Higher levels of cAMP promote the activation of PKA. PKA phosphorylates and activates CREB and

C/EBPβ. Indomethacin is a PPARγ agonist that then leads to induction of C/EBPα, generating a positive feedback loop with PPARγ (Gregoire, 2001; Cristancho and Lazar, 2011).

1.3.3 *Lipogenesis*

After a meal, lipoproteins (e.g. chylomicrons, very low-density lipoproteins) deliver NEFA to mature adipocytes for storage. NEFA release form lipoproteins is facilitated by adipocyte lipoprotein lipase (LPL), converting TG from lipoproteins into NEFA and glycerol molecules. The action of LPL takes places in the lumen of AT capillaries (Lafontan, 2008). NEFA can also be synthesized *de novo* from glucose entering mature adipocytes via insulin-stimulated glucose transporter type 4 (GLUT4). Glucose can undergo glycolysis, which converts it into two pyruvate molecules. Pyruvate molecules can undergo oxidative decarboxylation to form acetyl-CoA, the building block for fatty acid synthesis (Reshef, 2003). Acetyl-CoA can then be carboxylated to malonyl-CoA by acetyl-CoA carboxylase (ACC): this step is the rate-limiting step in fatty acid synthesis. At this point, FAS facilitates the formation of palmitate using acetyl-CoA and malonyl-CoA. Palmitate may undergo further modifications such as desaturation by stearoyl-CoA desaturase (SCD) and/or further elongation by FAS to generate other NEFA molecules (Steinberg, 2009).

Regardless of the source, three NEFA molecules can be esterified with glycerol phosphate, serving as the "backbone". This esterification action is facilitated by acyltransferases to generate monoacylglycerol phosphate, diacylglycerol phosphate, to eventually form TG. The main source of glycerol phosphate is from the action of glycerol-3-phosphate dehydrogenase on dihydroxyacetone-3-phosphate, a glycolysis metabolite (Proença et al., 2014).

1.4 Adipose tissue remodeling

AT remodeling occurs as a response to nutrient excess or deprivation. Angiogenic and extracellular matrix (ECM) remodeling in the AT play a significant role in maintaining AT plasticity. Remodeling of the AT is an ongoing process, but becomes pathologically accelerated in the obese state, leading to reduced angiogenic capacity, ECM overproduction, and increased immune cell infiltration, resulting in pro-inflammatory fat state (Sun et al., 2011). AT expansion is not always linked to pathological changes; in fact, there are obese individuals who are metabolically healthy (Klöting et al., 2010). A recent study has shown higher anti-inflammatory adiponectin levels are associated with better metabolic health in obese individuals (Ahl et al., 2015). As discussed below, healthy versus unhealthy AT expansion plays a major role in developing metabolically healthy versus metabolically unhealthy obese individual, respectively.

1.4.1 *Hyperplastic vs hypertrophic expansion*

AT expansion is a dynamic process involving two distinct mechanisms: hyperplasia (an increase in adipocyte cell number) and hypertrophy (an increase in adipocyte volume). Hyperplastic AT expansion is mediated by recruitment and/or differentiation of preadipocytes into mature adipocytes. Expansion by hyperplasia allows for even distribution of energy among newly formed adipocytes, which helps maintain metabolically neutral AT. Therefore, fat accumulation via hyperplastic AT expansion is favoured, and it is commonly seen in metabolically healthy obese, representing about 10-25% of obese individuals (Blüher, 2010). AT expansion through hypertrophy on the other hand, leads to excess energy storage in existing adipocytes, resulting in enlargement of the adipocyte cell size (Sun et al.,

2011, Heilbronn et al., 2004). Fat accumulation through hypertrophic expansion is most commonly seen in metabolically unhealthy obese individuals (Klöting et al., 2010).

1.4.2 *Adipocyte turnover*

Adipocyte number increases through puberty, and remains steady in mature AT in rodents and humans. Approximately 10% of adipocytes are renewed annually, independent of age or body mass index (Spalding et al., 2008). The manner by which adipocytes die has been studied by Cinti and colleagues who showed the presence of "crown like structures" (CLS), consisting of macrophages surrounding dead adipocytes in the AT of obese rodents and humans (Cinti et al., 2005). They also showed that CLS increase with adiposity using different animal models of obesity (Cinti et al., 2005).

A study by Strissel and colleagues assessed VAT adipocyte cell number and diameter of mice fed a high fat diet for 20 weeks. The study found a high fat diet led to early adipocyte hypertrophy (by week 4), and by week 16, adipocyte cell number dropped ~80%. Interestingly, at week 20, adipocyte cell number was restored by increased number of smaller adipocytes, along with reduction in cell death (Strissel et al., 2007). These findings showed the existence of temporal coordination between hyperplasia and hypertrophy in AT remodeling. However, they also allude to the idea that adipogenesis plays a critical role in the expansion of functional versus dysfunctional AT (discussed below). An increase in the number of smaller functional adipocytes depends on intact adipogenic capacity.

1.5 Adipose tissue dysfunction

If expansion by adipocyte hyperplasia cannot cope with high energy storage demands, then excessive adipocyte hypertrophy occurs, leading to AT dysfunction (Heilbornn et al., 2004). Impairment of hyperplastic AT expansion may be due to deficits in adipogenic capacity and/or preadipocyte number (Danforth, 2000). A reduction in the number of preadipocytes in AT of obese versus lean humans has been reported (Oñate et al., 2012; Tchoukalova et al., 2007). In addition, in adult obese humans, AT hyperplasia and hypertrophy are strongly related to adipocyte number; a 70% reduction in adipocyte cell number was associated with adipose hypertrophy and insulin resistance (Arner et al., 2010). This suggests that the number of preadipocytes and their ability to differentiate may be a key determinant of AT function.

A recent study identified an unexpected role for a local pro-inflammatory response that allowed adipogenesis to proceed. Adipocyte-specific expression of a dominant-negative form of TNF-α in mice fed a HFD led to a reduced capacity for healthy adipose tissue remodeling compared to WT littermates (Wernstedt Asterholm et al., 2014).

1.5.1 *Molecular basis of adipocyte dysfunction*

Adipocyte hypertrophy is accompanied by alterations in adipokines, shifting towards a pro-inflammatory phenotype, and by disruptions in lipid metabolism (Goossens and Blaak, 2015). Inappropriate release of NEFA (spill-over) from hypertrophied adipocyte results in ectopic fat accumulation in other tissues such as liver and muscle. The intrahepatic and intramyocytic lipid accumulation results in production of toxic lipid-derived molecules, such as fatty acyl-CoA, DAG, and ceramides (Bremer et al., 2012). These toxic lipid metabolites can trigger the activation of serine/threonine kinases (such as protein kinase C (PKC), c-Jun

N-terminal kinase, (JNK), and inhibitor of kappa B kinase beta (IKKβ)) involved in inhibitory phosphorylation of insulin receptor (IR) and insulin receptor substrate 1 (IRS-1), blocking insulin signal transduction. At the tissue/organ level, this leads to insulin resistance, including impairment of insulin-stimulated glucose uptake in myocytes, and a reduction in the ability of insulin to suppress hepatic gluconeogenesis (Bremer et al., 2012).

1.5.2 *Macrophage infiltration into AT*

The AT macrophage (ATM) population ranges between ~ 10-50% varying by 1) degree of adiposity and 2) adipocyte size. Work by Ferrante and group in 2003 showed that in lean mice, ATM content (assessed by reactivity with F4/80 antibody) was less than 10% of total cell nuclei counted in AT in lean mice, but more than 50% in extremely obese mice. This was established using leptin-deficient (*ob/ob*), leptin receptor-deficient (*db/db*), and diet induced obese mouse models. AT from obese humans exhibited similar trends. Ferrante and colleagues also showed that there was a positive relationship between adipocyte size and ATM content in AT of rodents as well as humans, suggesting a link between hypertrophied AT expansion and macrophage infiltration. (Weisberg et al., 2003). In addition to increased adiposity, ATM content has been shown to vary with age, gender, and AT depot (Lumeng et al., 2011; Ortega Martinez de Victoria et al., 2009; Tam et al., 2012). VAT depots have the most ATM and are more numerous in females. ATM numbers increase with age until ~31-33 years old, and then slightly decrease overtime (Ortega Martinez de Victoria et al., 2009).

ATM numbers have also been shown to be positively correlated with the degree of insulin resistance in human obesity (Wentworth et al., 2010). The first indications of a link between ATM and insulin resistance was observed by Chen et al in 2003, who highlighted that when adipocyte hypertrophy reaches a critical threshold, factors derived from adipocytes

induce macrophage infiltration and their activation. They suggested that preadipocytes may also participate in attracting monocytes by secreting chemokines (under stimulation of TNF-α for example). Together, these events participate in amplifying signals that ultimately lead to macrophage infiltration, AT inflammation, impaired adipocyte insulin signaling, and subsequent systemic insulin resistance (Xu et al., 2003).

Bone marrow transplant studies suggested that the accumulation of ATM in diet induced obese mice was due to an influx of bone-marrow-derived precursors (monocytes) into AT, which then different into mature F4/80-expressing macrophages (Weisberg et al., 2003). This was later confirmed by *in vivo* monocyte labeling (using PKH26 dye) (Lumeng et al., 2007A). The monocyte influx from the circulation depends on interactions between AT-secreted monocyte chemoattractant protein 1 (MCP-1) and chemokine C-C motif receptor 2 (CCR2) expressed on the cell surface of monocytes in circulation (Kanda et al., 2006; Weisberg et al., 2006). Selective overexpression of MCP-1 (under the control of aP2 gene promoter) in adipocytes increased macrophage infiltration into AT. Mice deficient in MCP-1 exhibited reduced macrophage infiltration compared to WT under high fat diet (Kanda et al., 2006). Other recruitment systems involving other chemokines (e.g. MCP-2, MCP-3, or chemokine C-C motif ligand 5; CCL5) and their respective receptors (e.g. CCR1, CCR2, and CCR5) have been reported to operate in AT of obese mice and humans (Kitade et al., 2012; Zeyda et al., 2010).

Macrophages are versatile cells that can polarize to either pro- (M1) or anti-inflammatory (M-2) like responses, depending on the surrounding microenvironment and various stimuli. Human and mouse M1 macrophages express CD11c (integrin, alpha X - complement component 3 receptor 4 subunit), nitric oxide synthase (NOS) 2, and tumor

necrosis factor (TNFα). One study demonstrated the importance of CD11c by depleting CD11c+ cells in an obese mouse model; insulin resistance and inflammation improved (Patsouris et al., 2008). Human and mouse M2 macrophages express markers such as arginase 1 (Arg1), CD206 (mannose receptor), and CD301 (macrophage galactose-type C-type lectin 1). Common inducers of an M1 macrophage are interferon γ (IFNγ) or lipopolysaccharide (LPS), which lead to macrophages displaying a pro-inflammatory phenotype (Gordon, 2003). Stimulation with IL-13 or IL-4 induces an M2 macrophage, displaying anti-inflammatory phenotype (Ohashi et al., 2010). M2 macrophages use ATP generated from fatty acid oxidation as their source for energy, whereas M1 macrophages use ATP produced from glycolysis (Vats et al., 2006; Rodriguez-Prados et al., 2010). Alteration in macrophage energy metabolism may influence M1/M2 fate. When energy metabolism was shifted towards glycolysis in macrophages (by means of over expressing GLUT1 in RAW 264.7 macrophages), mRNA and protein expression of inflammatory mediators was enhanced (Freemerman et al., 2014).

Other macrophage subtypes have been recently recognized, including M3 and Mox. M3 macrophages account for a switch phenotype that occurs between M1 and M2 macrophages undergoing phenotypic change (from M1 to M2 or vice versa) depending on the microenvironment (Malyshev and Malyshev, 2015). Mox macrophages are initially found in atherosclerotic lesions of LDL receptor-deficient mice. They are induced by oxidized phospholipids and are characterized by high expression of sulforedoxin-1, thioredoxin-1 reductase, and heme oxygenase 1 (Kadl et al., 2010).

In obesity, the M1 to M2 ratio is commonly used to describe ATMs (Dalmas et al., 2011). Hypertrophied obesity is associated with increased M1 and decreased M2 like

macrophage (Dalmas et al., 2011). In contrast, ATM isolated from AT of lean animals express hallmarks of an M2 like state. Unlike the adverse effects of M1 like ATMs on the function of AT, M2 polarized ATM participate positively in the maintenance of AT homeostasis (Wu et al., 2011). Transition from a lean to an obese state triggers a switch in the activation state of ATM from an M2- to M1-polarized state (Lumeng et al., 2007B). The shift in ATM phenotype with hypertrophied obesity is due to accumulation of pro-inflammatory ATM, rather than local transformation of resident anti-inflammatory ATM to pro-inflammatory ATM (Lumeng et al., 2008).

It is not yet clear whether infiltrating monocytes acquire a pro-inflammatory phenotype within the AT microenvironment, or whether they are predisposed to a pro-inflammatory consequence. *In vivo* monocyte tracking studies have shown that circulating monocytes only gain pro-inflammatory activity once they have been recruited to the AT (Oh et al., 2012). Indeed, various factors are present in the obese AT microenvironment that may promote the activation of recruited monocytes. Some of these factors include pro-inflammatory cytokines, TNFα, IFNγ, and IL-1β, or adipocyte derived NEFA (Ouchi et al., 2011; Suganami et al., 2005). However, suggestions in support of pro-inflammatory predisposition among circulating blood monocytes have been reported in rodents and humans. For example, Gr1+ (granulocyte differentiation antigen 1) murine and CD14+CD16+ human monocytes have inflammatory properties, thus may have a propensity to differentiate into pro-inflammatory ATM. Gr1- murine and $CD14^{dim}$CD16+ human monocytes display patrolling properties, which may predispose to a more M2 macrophage like phenotype once differentiated (van de Veerdonk and Netea, 2010).

1.5.3 *Macrophage and adipogenesis*

ATM can influence AT remodeling and function via paracrine signaling. ATM accumulation in AT is associated with hypertrophied expansion, indicating that macrophages may decrease the adipogenic capacity, survival and/or proliferation response of preadipocytes. Constant *et al*. reported that medium conditioned by human or mouse macrophage cell lines (macrophage conditioned medium; MacCM) attenuated adipogenesis of human and mouse 3T3-L1 preadipocytes, as assessed by protein expression of adipogenic markers and lipid accumulation (Constant et al., 2006). An anti-adipogenic effects of MacCM generated from LPS- activated human monocyte derived macrophage (MDMs) and adipose tissue derived macrophages was further established by Clement and her research group (Lacasa et al., 2007). These authors also demonstrated that secreted factors, from LPS-activated MDMs, enhanced gene mRNA expression and protein levels of inflammatory markers in human preadipocytes, (Lacasa et al., 2007). Determining the particular macrophage secreted anti-adipogenic factor(s) is a subject of ongoing investigations. Size fractionation and heat treatment studies using human THP-1 macrophages have revealed that the anti-adipogenic factor(s) is between 3-50 kDa in size and that it is heat sensitive (Gagnon et al., 2013).

Several anti-adipogenic candidates released by macrophages have been proposed such as IL-1β, TNFα, and Wnt-5a (Suzawa et al., 2003; Ruan et al., 2002; Bilkovski et al., 2011). Using mouse 3T3-L1 preadipocytes, anti-adipogenic response of medium conditioned by mouse J774A.1 was shown to be attenuated by growth hormone, and this correlated with the amount of IL-1β produced by macrophages. These authors did not directly assess whether IL-1β in MacCM was required for the anti-adipogenic effect (Lu et al., 2010).

Others using human THP-1 macrophages and human preadipocytes showed that human recombinant IL-1β alone was sufficient to inhibit human adipogenesis. However, when IL-1β was immunedepleted from MacCM, the anti-adipogenic effect of MacCM was not reversed, suggesting that IL-1β is not required for the MacCM-induced anti-adipogenic effect (Gagnon et al., 2013). TNFα, another inflammatory cytokine has also been investigated as a potential macrophage secreted anti-adipogenic factor.

Immunoneutralization of TNFα from LPS-treated human MacCM marginally reversed the anti-adipogenic effect; however it did robustly attenuate MacCM-mediated inflammatory preadipocyte responses (Lacasa et al., 2007). Recently, wnt-5a (secreted glycoprotein; inhibitory to adipogenesis) was found to be expressed by ATM and circulating monocytes in obese and type 2 diabetic human subjects. Functional analysis using mouse J774A.1 macrophage and 3T3-L1 preadipocytes models showed that wnt-5a may be a plausible macrophage secreted anti-adipogenic factor (Bilkovski et al., 2011). Our lab was not able to detect wnt-5a in human THP-1 MacCM (unpublished data), and it remains unclear whether this intercellular communication occurs in human systems.

Taking a different approach to understand the paracrine effects of macrophages on preadipocytes, studies have examined activation of signaling networks in preadipocytes by MacCM, and whether they are implicated in the anti-adipogenic action of MacCM. Medium conditioned by human THP-1 macrophages acutely stimulated ERK1/2 phosphorylation in mouse 3T3-L1 preadipocytes. Inhibition of MEK-ERK1/2 pathway in 3T3-L1 preadipocytes partially blocked the anti-adipogenic effect of THP-1 MacCM (Constant et al., 2008). Studies using human preadipocyte model systems demonstrated that the activation of NF-κB pathway was associated with anti-adipogenic effect of MacCM (Yarmo et al., 2010; Lacasa

et al., 2007; O'Hara et al., 2012). Sc-514, a selective inhibitor of IKKβ, which is an upstream activator of NF-κB almost fully abrogated the ability of THP-1 MacCM to inhibit human adipogenesis (Yarmo et al., 2010).

Coincident with their action in inhibiting adipogenesis, macrophage secreted factors also promote a profibrotic phenotype in human preadipocytes (Keophiphath et al., 2009). Factors derived from macrophages regulate levels of collagen I/III and fibronectin in human preadipocytes (Gagnon et al., 2012). Fibrillar collagen I/III and fibronectin make up most of ECM surrounding preadipocytes, and upon differentiation, these proteins are down regulated (Gregoire et al., 1998). Studies have shown that direct manipulation of ECM is sufficient to inhibit adipogenesis (Smas and Sul, 1995; Spiegelman and Ginty, 1983).

1.5.4 *Macrophages and adipocytes*

Although not the focus of my thesis, it should be noted that several studies have examined the effects of macrophage-derived factors on mature adipocytes. MacCM blocked insulin-stimulated glucose uptake in mature adipocytes by down-regulating GLUT4 and inhibiting insulin receptor substrate-1 (IRS-1) tyrosine phosphorylation. These results were observed using the mouse J774A.1 macrophage and differentiated mouse 3T3-L1 adipocytes (Lumeng et al., 2007C). Others have shown that macrophage-derived factors endocytosed by adipocytes disrupt lipid synthesis by impairing FAS activity and concomitantly inducing lipolysis (Kurokawa et al., 2010). Adipocyte-derived NEFA can then act on macrophages to further activate them to release more inflammatory cytokines. These actions create a pro-inflammatory paracrine loop between macrophage and adipocyte (Suganami et al., 2005). On the other hand, conditioned medium from alternatively activated mouse RAW264.7

macrophages (anti-inflammatory) can neutralize the inhibitory effect of pro-inflammatory MacCM on mouse 3T3-L1 preadipocyte differentiation (Stienstra et al., 2008).

1.6 Diabetes

1.6.1 *Definition and evaluation of diabetes*

Under normal conditions, blood glucose concentration is ~5 mM, and it is tightly regulated by release of insulin from pancreatic β-cells. Normally, when glucose levels are elevated in circulation (i.e. after a meal), insulin is released from the pancreatic β-cells, to stimulate glucose uptake, mainly by muscle and to suppress hepatic gluconeogenesis, bringing the circulating glucose concentrations back to ~ 5 mM. Diabetes occurs when blood glucose levels rise (hyperglycemia) due to impaired insulin secretion, impaired insulin action or both. A diagnosis of diabetes is made if the blood glucose concentration is ≥ 7 mM in a fasting state, ≥ 11.1 mM 2 hours after a glucose challenge, and/or levels of glycated hemoglobin called A1C are ≥ 6.5% (CDA, 2013)

There are two major forms of diabetes, type 1 (T1D) and type 2 diabetes (T2D) representing 10% and 90% of cases respectively. Another common type of diabetes is gestational diabetes, which occurs during pregnancy. In T1D, insulin-producing pancreatic β-cells fail to produce insulin due to autoimmune destruction, leading to absolute insulin deficiency. In T2D, there is the loss of insulin sensitivity of insulin-target tissues, which leads to elevated insulin secretion to compensate. This is referred to as "insulin resistance", meaning greater than normal levels of insulin are needed to maintain normal blood glucose. Eventually, the hypersecretion of insulin fails, and blood glucose levels rise. Both types of diabetes are caused by a combination of genetic and environmental risk factors (Saini, 2010).

In gestational diabetes, it is believed that insulin resistance occurs due to pregnancy-related hormonal changes (Agha-Jaffar et al., 2016).

In Canada, 9.3% of Canadians have diabetes (Canadian Diabetes Cost Model, 2015). Complications of diabetes are associated with premature death. Among Canadian adults, it was estimated that 1 in 10 deaths was attributed to diabetes in 2008-2009 (Public Health Agency of Canada, 2011). Compared to the general population, individuals with diabetes are 4 times more likely to have cardiovascular complications, 12 times more likely to have end-stage renal disease, and 20 times more likely to be hospitalized for a non-traumatic lower limb amputation (CDA, 2013). T2D is strongly linked to obesity. It is estimated that about 80-90% of individuals with diabetes are obese (Lau et al., 2013).

1.7 Hyperglycemia and effects on adipose tissue functions

1.7.1 *Effect of high glucose (HG) on adipogenesis*

The effect of HG concentrations on adipogenesis has not been clearly established. The standard protocol for the differentiation of 3T3-L1 mouse preadipocyte cell line uses high glucose (25 mM; HG), and our lab reported that differentiation of these cells in normal glucose (5 mM; NG) enhanced adipogenic insulin signal transduction and markers of adipocyte differentiation (Gagnon and Sorisky 1998). Others subsequently noted that differentiating these cells in 25 mM versus 5 mM glucose resulted in more inflamed, insulin-resistant adipocytes (Lin et al., 2005). These studies suggest HG has a negative influence on adipogenesis. However, using mouse bone marrow-derived mesenchymal stem cells, HG promoted the adipogenic fate (Chuang et al., 2007).

There have been a few investigations of the effects of glucose concentration on human preadipocyte models. One human preadipocyte cell line is derived from the adipose

tissue of an infant with Simpson Golabi Behmel syndrome (SGBS), termed the SGBS cell line. SGBS is a congenital syndrome of unknown etiology that leads to abnormal weight gain (Wabitsch et al., 2001). Using this cell line, one study saw no effect of HG on adipogenesis, but the duration of exposure was only 24 hours, which may not have been enough time for any changes to be observed (Verrijn Stuart et al., 2012). Others, using primary human adipose progenitor cells but without adipogenic inducers, reported that HG augmented spontaneous adipogenesis (limited extent of differentiation) , as evidenced by more lipid accumulation as well as enhanced gene expression of SREBP-1c, PPARγ, LPL, adiponectin, and GLUT4 (Aguiari et al., 2008). Another study suggests that exposure of HG (17.5 mM) to human preadipocytes undergoing differentiation resulted in comparable TG accumulation versus NG. Adipogenic markers were not assessed in this study. (Collins et al., 2011).

VAT progenitor cells isolated from individuals with T2D versus non-diabetic controls have higher levels of stemness markers CD105 and CD90, OCT4 and NANOG (stem cell self-renewal), and reactive oxygen species (ROS). When VAT progenitor cells were treated with HG (25 mM), ROS levels and cell proliferation increased. ROS production and AKT activation drove proliferation of diabetic, but not non-diabetic progenitor cells (Dentelli et al., 2013). This suggests that HG conditions may regulate the fate or functional behaviour of preadipocytes by activating downstream signals. Adipogenesis was not assessed by this group. HG appears to promote an adipogenic fate when non-preadipocyte cell lines were used. When human osteoblastic MG-63 cells are placed in HG, they switch from osteoblastic to adipogenic differentiation, through activation of the cAMP/PKA/ERK pathway (Wang et al., 2010). HG also promotes the trans-differentiation of murine muscle stem cells into adipocytes via ROS-activated protein kinase C (PKC) β (Aguiari et al., 2008).

1.7.2 *Hyperglycemia and ChREBP*

Glucose not only serves as an energy source and a basic anabolic building block used to synthesize different macromolecules, it can also act as a signaling molecule in the liver and AT (Girard et al., 1997; Foufelle et al., 1992). Glucose signaling occurs via activation of the glucose-responsive transcription factor, carbohydrate response element-binding protein (ChREBP), which belongs to the family of basic helix-loop-helix leucine sipper transcription factors (Yamashita et al., 2001). Glucose-regulated genes share a conserved consensus sequence, called the carbohydrate response element (ChoRE) (Thompson and Towle, 1991). ChREBP expression is most abundant in liver, white/brown AT, small intestine, kidney, and pancreatic islets (Iizuka et al., 2004). ChREBP possesses an obligatory functional partner, Max-like protein X (Mlx) (Ma et al., 2005). Two Mlx-ChREBP heterodimers bind two E boxes of the ChoRE motif to form a transcriptional complex regulated by glucose (Ma et al., 2006). In hepatocytes, ChREBP regulates the expression of lipogenic enzymes, but its role in adipocytes is less well understood, especially in the setting of obesity.

Liver biopsies from lean and obese human subjects show that ChREBP mRNA and protein expression is enhanced in obese subjects compared to lean. In contrast, the expression of ChREBP in VAT and SAT of these individuals was reduced in the obese compared to lean. These data suggest that in obesity, ChREBP may be regulated differently in the liver versus AT, which is consistent with the increased hepatic lipogenesis and decrease AT lipogenesis seen develop with obesity. Also, ChREBP mRNA and protein dramatically increased during differentiation of human primary preadipocytes (from obese VAT and SAT), suggesting there may be a possible role for ChREBP in adipogenesis. The

increase in ChREBP mRNA was much more pronounced in differentiated adipocytes from SAT compared to VAT (Hurtado del Pozo et al., 2011).

Several phosphorylation sites have been identified on ChREBP that regulate its activity. Under low glucose conditions, serine 196 on the N-terminus is phosphorylated by cAMP dependent PKA, leading to sequestration of ChREBP to the cytosol, rendering it inactive (Sakiyama et al., 2008). Also, in the cytosol, the N-terminus of ChREBP is associated with 14.3.3 protein which stabilizes ChREBP, preventing proteolytic degradation and maintaining an inactive state (Ge et al., 2012). The mechanism by which glucose activates ChREBP is complicated and several models have been proposed. Three glucose metabolites are involved, including, xylulose 5-P (Xu-5P; derived from pentose phosphate pathway; PPP), glucose 6-phosphate (G6P; the first intermediate when glucose enters the cell), and fructose -2, 6-P2 (F2-6P2; regulator of glycolysis and gluconeogenesis) (Kabashima et al., 2003; Li et al., 2010; Arden et al., 2012).

There are reports that under HG concentrations, Xu-5P levels rise, leading to activation of protein phosphatase 2A (PP2A) which in turn dephosphorylates ChREBP, allowing its entry into the nucleus (Kabashima et al., 2003). This model has been challenged since PPP is not active in β-cells, where ChREBP is expressed and is active (Collier et al., 2007). To address this, others have shown that G6P was sufficient to activate ChREBP in β-cells (Li et al., 2012). Furthermore, overexpressing G6P dehydrogenase in hepatocytes also demonstrated that G6P, and not Xu-5P, was needed for activation and nuclear translocation of ChREBP in response to glucose (Dentin et al., 2012). A third potential glucose metabolite may be involved in ChREBP activation. Selective depletion of F2-6P2 was shown to inhibit

glucose-induced recruitment of ChREBP to promoter sites of target genes (Arden et al., 2012).

The role of ChREBP in the AT is not very well understood. A transgenic mouse model overexpressing GLUT4 selectively in adipocytes exhibited higher levels of ChREBP target genes (e.g. FAS, SCD, ACC, etc.) and the reverse was true when GLUT4 was deleted in adipocytes. These authors concluded that GLUT4 regulates ChREBP activity in the AT (Herman et al., 2012). They identified a novel ChREBP isoform, ChREBP-β (the conventional isoform named ChREBP-α thereafter) in adipocytes. ChREBP-β is a truncated form of ChREBP-α, missing 177 amino acids from the N-terminus, containing the low-glucose inhibitory domain (LID). LID includes two nuclear export signal (NES) domains and one nuclear localization signal (NLS) domain. The transcriptional activity of ChREBP-β is 20 fold greater than ChREBP-α. ChREBP-β is predominantly found in the nucleus, whereas ChREBP-α is mainly found in the cytoplasm, under both low and high glucose concentrations. Herman *et al*. suggested that glucose metabolites stimulate ChREBP-α activity and lead to the induction of ChREBP-β (Herman et al., 2012). The expression of ChREBP-β, but not -α mRNA, in VAT of obese and obese with T2D was significantly lower compared to non-obese individuals. These authors observed an inverse correlation between VAT ChREBP-β mRNA expression and homeostasis model assessment of insulin resistance (HOMA-IR), suggesting that ChREBP-β in AT is associated with systemic insulin sensitivity (Eissing et al., 2013). Also, others have suggested that ChREBP-β in SAT is the major isoform predicting systemic insulin sensitivity (Kursawe et al., 2013).

1.7.3 *Hyperglycemia and macrophage activation/responses*

In the vast majority of patients with T2D, obesity co-exists with hyperglycemia. Despite this fact, very little has been published on how HG concentrations might affect macrophage-preadipocyte interactions. Studies using various macrophage models have been used to assess the effects of HG on macrophages, in the context of macrophages, diabetes, and atherosclerosis. Using bone marrow-derived macrophages (BMDM), HG reduced the mRNA and protein expression of ATP-binding cassette transporter A1 (ABCA1) in a dose and time dependant manner (Chang et al., 2013). ABCA1 is an atheroprotective protein that regulates the export of cholesterol from macrophages (Oram and Vaughan, 2006). In BMDM cultures, HG-induced ROS production and activated the ERK pathway, which in turn down-regulated ABCA1 mRNA and protein levels (Chang et al., 2013). Exposure of LPS-activated RAW 264.7 mouse macrophages to HG (25 mM) versus NG (5.5 mM), enhanced nitric oxide (NO) production, inducible NO synthase (iNOS) protein expression, and IL-1β secretion. These effects were not seen with HG alone, suggesting that HG may aggravate the effects of LPS (Hua et al., 2012). In another study, HG with or without LPS impaired migration of RAW 264.7 macrophages (Moura et al., 2013). When RAW 264.7 macrophages were stably transfected to overexpress GLUT1, the rate limiting glucose transporter in activated macrophages, increased PPP with complimentary suppression in cellular oxygen consumption rates. Also, mRNA and protein expression of inflammatory mediators were enhanced in these macrophages overexpressing GLUT1 compared to control (Freemerman et al., 2014).

Others showed that THP-1 macrophages in HG increased to C-reactive protein (CRP) protein production in a dose dependant manner (Kaplan, 2010). Human MDMs exposed to

HG conditions produce factors that promote endothelial cell responses, including increases in the expression and secretion of E-selectin. (Chen et al., 2011). HG treatment of human MDMs increases the production of reactive oxygen species (ROS), leading to increased expression of lectin-like oxidized LDL receptor-1 (LOX-1) and scavenger receptor –A (SR-A). Antioxidants and NADPH oxidase inhibitors reverse these HG-induced effects (Li et al., 2004; Fukuhara-Takaki et al., 2005). HG-induced ROS production activates nuclear factor-κB (NF-κB) and activated protein-1 (AP-1) in human MDMs (Li et al., 2004). HG also activates protein kinase C (PKC) in human MDMs, increasing expression of platelet-derived growth factor (PDGF)-β receptor. PKC inhibition reverses this effect (Ibana et al., 1996). Other studies have shown that HG exposure to human MDMs leads to over-production of the inflammatory cytokine, tumor necrosis factor-α (TNF-α) and reduction in mRNA expression of anti-inflammatory peroxisome proliferator-activated receptor γ (PPARγ) (Sartippour et al., 1998; Sartippour et al., 2000; Ni et al., 2010). However, others reported that HG exposure to human MDMs did not elicit any changes in pro-inflammatory cytokine IL-1β or PPARγ mRNA expression (Kratz et al., 2014; Senanayake et al., 2007).

RATIONALE

Adipose tissue dysfunction in obesity, associated with inadequate adipogenesis, is linked to hypertrophic low-grade inflammation and macrophage infiltration (Sun et al., 2011). In the vast majority of patients with T2D, obesity co-exists with hyperglycemia. Despite this fact, very little has been published on how HG concentrations might affect macrophage-preadipocyte interactions. Our lab and others have shown that macrophage secreted factors inhibit adipogenesis, however the effect of HG concentrations on the anti-adipogenic effect is yet to be investigated (Constant et al., 2006; Lacasa et al., 2007; Keophiphath et al., 2009; Ide et al., 2011). I **hypothesize that exposure of macrophages to HG levels increases their release of anti-adipogenic factors that will inhibit human adipogenesis**. I propose to address this hypothesis with the following specific aims.

SPECIFIC AIMS:

Aim 1: Examine the effects of HG on human adipogenesis.

Aim 2: Determine mechanisms by which HG modulates the anti-adipogenic properties of macrophages.

Aim 2A: Evaluate the effect of HG on the ability of macrophage-conditioned medium (MacCM) to inhibit adipogenesis.

Aim 2B: Determine which macrophage factors induced by HG are responsible for the anti-adipogenic effect.

Aim 2C: Explore signaling pathways in macrophages that are activated by HG leading to generation of anti-adipogenic factors.

MODEL SYSTEMS USED

Human stromal preadipocytes

Human primary preadipocytes were obtained from the stromal vascular fraction (SVF) of human SAT (Skurk and Hauner, 2012). Adherent cells from SVF have fibroblastic like morphology and are documented as CD14-/CD34+/CD31- (Decaunes et al., 2011). Upon exposure to adipogenic inducers, these preadipocytes can effectively differentiate into mature adipocytes (Skurk and Hauner, 2012). Cell responses can be variable due to donor heterogeneity.

Monocyte-derived macrophages (MDM)

Human MDMs were isolated from the peripheral blood mononuclear cell (PBMC) layer after Ficoll-density gradient centrifugation of whole blood (Johnson et al., 1977). Monocytes were allowed to differentiate into macrophages (Norris et al., 1979). Human MDMs that differentiate from adherent monocytes exhibit two morphologically distinct subtypes, spindle and round (Eligini et al., 2012). Spindle-shaped macrophages exhibit functional traits similar to M1 macrophages profile, whereas round-shaped MDMs show similarities to that of M2 macrophage (Eligini et al., 2012; Eligini 2015). Human MDM responses can be variable due to donor heterogeneity.

2. MATERIALS AND METHODS

2.1 Isolation and culture of human abdominal subcutaneous stromal preadipocytes

Human subcutaneous abdominal adipose tissue samples were obtained from 10 weight-stable females undergoing elective abdominal surgery (approved by the Ottawa Health Science Network Research Ethics Board). Patients on insulin or glucocorticoid steroids were excluded. Mean age (±SD) of patients was 58±6.4 years and mean BMI (±SD) was 32±9 kg/m^2 (**Table 1**). Adipose tissue was dissected to remove connective tissue and blood vessels, then digested with collagenase CLS type 1 (600U/g of tissue; Worthington Biochemical Corporation, Lakewood, NJ, USA) for 1 hour at 37°C on a rotator shaker. Samples were filtered through 200 μm nylon filters to exclude any undigested debris or connective tissue. Filtered samples were centrifuged (200 x g) for 20 minutes. After centrifugation, the part of the supernatant containing floating mature adipocytes was removed and the remainder was processed by progressive size filtration through 100 μm, 50 μm and 25 μm nylon filters to exclude any remaining connective tissue, debris, or mature adipocytes. Samples were then centrifuged again (200 x g) for 20 minutes to pellet the stromal vascular fraction (SVF). The SVF was exposed to erythrocyte lysis buffer (155 mM NH4Cl, 5.7 mM K2HPO4, 0.1 mM EDTA; pH 7.3) for 5 minutes. Preadipocytes were grown in Dulbecco's modified Eagle's medium (DMEM) supplemented with 10% FBS, antibiotics (100 U/ml penicillin, 0.1 mg/ml streptomycin; Life Technologies Inc., Burlington, ON, Canada), and an antifungal agent (50 U/mL nystatin; Calbiochem, Etobicoke, ON, CA) (designated growth medium). Preadipocytes were cultured in growth medium and the medium was replaced every 2 days. Cells were passaged up to 3 times by

Donor	Age	Sex	BMI (kg/m^2)	Surgery
H713	61	F	44.7	Hysterectomy
H754	49	F	30.6	TRAM flap
H755	51	F	27.2	TRAM flap
H762	55	F	20.8	TRAM flap
H764	56	F	27.9	TRAM flap
H765	65	F	31.0	TRAM flap
H766	64	F	30.4	TRAM flap
H768	63	F	30.2	TRAM flap and abdominoplasty
H760	63	F	50.9	Bariatric surgery
H767	49	F	24.1	TRAM flap

Table 1. Adipose tissue donor information chart. Human subcutaneous abdominal adipose tissue samples were obtained from 10 weight-stable women undergoing elective abdominal surgery (approved by the Ottawa Health Science Network Research Ethics Board). The following table lists all fat tissue donor's age, sex, BMI (kg/m^2), and surgery performed. TRAM flap refers to breast reconstructive surgery.

addition of 0.5 mL 1X TrypLE reagent (Life Technologies Inc., Burlington, ON, Canada) for 3-4 minutes at 37 °C (Gagnon et al., 2013).

2.2 Isolation of human monocytes and differentiation into macrophages

Blood was obtained from 13-healthy non-diabetic volunteers (4 males and 9 females; approved by the Ottawa Health Science Network Research Board). Mean age (±SD) of donors was 29±10 years and mean BMI (±SD) was 24.6±3.6 kg/m^2. Blood was diluted (1:2) with PBS supplemented with 2 mM EDTA and layered onto Ficoll-Hypaque (GE Healthcare; Uppsala, Sweden) and centrifuged (400 x g) for 30 minutes. Upon density-gradient centrifugation, peripheral blood mononuclear cells (PBMCs) were isolated from the buffy coat, washed with PBS, and centrifuged (300 x g) for 5 minutes. Pellets containing PBMCs were resuspended in Roswell Park Memorial Institute 1640 medium (RPMI 1640; Thermo Fisher Scientific) supplemented with antibiotics (100U/ml penicillin and 0.1mg/ml streptomycin; Life Technologies Inc., Burlington, ON, Canada), designated monocyte-derived macrophage (MDM) growth medium, with normal glucose concentration (NG; 5 mM). PBMC blood counts for donors ranged from 80-100 cells/mL. PBMCs were seeded at a density of 1.1×10^5 cells/cm^2 and monocytes within PBMC pool were allowed to adhere for 1 hour in serum-free MDM growth medium with NG. Adherent monocytes were washed twice with PBS and then left in MDM growth medium with NG, supplemented with 10% FBS for 7 days. Medium was changed every day for the first 3 days and every second day thereafter for 7 days. Mature MDMs were photographed using a Nikon Coolpix 995 digital camera mounted on Nikon Eclipse TS-100 microscope at 200X magnification.

2.3 Macrophage-conditioned medium (MacCM) preparation

MDMs differentiated for 7 days in MDM growth medium supplemented with 10% FBS in NG conditions were lifted by using 0.5 mL 1X TrypLE reagent (Life Technologies Inc., Burlington, ON, Canada) for 5-6 minutes 37°C and by subsequent gentle scraping. The number of MDMs ranged from 1.4 x 10^7 - 1.8 x 10^7 cells per donor. About 50-60% of MDMs were round shaped, whereas 40-50% was spindle shaped. Detached MDMs were pooled and centrifuged (180 x g) for 5 minutes. The pelleted MDMs were resuspended in MDM growth medium containing NG and supplemented with 10% FBS. MDMs were enumerated using Neubauer hemocytometer and seeded at a density of 1.3 x 10^5 cells/cm^2 and were placed in MDM growth medium (1 mL per 5 x10^5 cells) containing NG, supplemented with 10% FBS for 24 hours to allow cells to adhere and recover from any stress introduced during trypsinization/scraping. After 24 hours, medium was gently removed and replaced with fresh MDM growth medium (1mL per 5 x10^5 cells) supplemented with 10% FBS containing NG, high glucose (HG; 25 mM), or osmotic control (OC; 5 mM glucose/20 mM mannitol) for 24 hours. For some experiments, 1 μM sc-514 (#401485; EMD Millipore) or vehicle (DMSO) was added at the start of this 24 hour conditioning period. After 24 hours MacCM was collected and centrifuged (180 x g) for 5 minutes to pellet any floating cells or debris. MacCM was then stored at - 20°C for later use for adipogenesis experiments or human cytokine array analysis. Human cytokine array analysis was performed using Human XL Cytokine Array Kit (R&D Systems, Inc.), as per the manufacturer's instructions (see section 2.4). Control medium, not exposed to cells was processed in parallel.

2.4 Human cytokine array analysis

Membranes from Human XL Cytokine Array Kit (R&D Systems, Inc) were blocked with Array Buffer 6 for 1 hour at room temperature on a rocking platform shaker. After blocking, membranes were incubated with NG-MacCM or HG-MacCM overnight at 4°C on Labquake rotator. The following day, membranes were washed three times with Wash Buffer for 10 minutes at room temperature. Membranes were then incubated with 1.5 mL Detection Antibody Cocktail diluted in 1X Array Buffer4/6 for 1 hour at room temperature on a rocking platform shaker. Upon incubation, membranes were washed three times with Wash Buffer for 10 minutes at room temperature. Membranes were then incubated with 1X Streptavidin-HRP for 30 minutes at room temperature on a rocking platform shaker and then washed again three times with Wash Buffer for 10 minutes. After the final wash, membranes were incubated with 1 mL Chemi Reagent Mix for one minute. Membranes were then exposed to film, which was processed using a Feature-SRX-101A developer (Konica Minolta, Chiyoda, Tokyo, Japan). Relative cytokine spot intensity was quantified and expressed as integrated optical density (IOD) units using the AlphaImager imaging system (Alpha Innotech Co., San Leandro, CA, USA).

2.5 Culture and differentiation of human subcutaneous preadipocytes

For differentiation, cells were enumerated using a Neubauer hemocytometer and seeded at a density of 3×10^4 cells/cm^2 in growth medium and grown to confluence. Differentiation was induced in growth medium containing NG, HG, or OC and supplemented with adipogenic inducers 850 nM insulin (Roche, Laval, QC, Canada); 0.5 μM dexamethasone (Steraloids, Newport, RI, USA); 0.25 mM isobutylmethylxanthine; and 100

μM indomethacin (both from Sigma-Aldrich, St. Louis, MO, USA) for 14 days. Alternatively, preadipocytes were differentiated in NG-MacCM, HG-MacCM, OC-MacCM, or control medium with adipogenic inducers. Every 3 days 50% of medium were changed with fresh medium (including differentiation inducers) for 14 days. After 14 days, cultures were photographed using a Nikon Coolpix 995 digital camera mounted on Nikon Eclipse TS-100 microscope at 200X magnification (Gagnon et al., 2013).

2.6 Triglyceride (TG) extraction and quantification

After adipocyte differentiation, medium was gently removed and cells were rinsed with PBS (500 μL). Cellular lipids were extracted using isopropanol/heptane (2:3; v /v) in a two-step procedure. Cells were incubated in isopropanol/heptane (500 μL) for 30 minutes at room temperature. After incubation, the isopropanol/heptane solution containing extracted lipid was collected in a glass test tube. This was repeated a second time: cells were incubated in isopropanol/heptane for an additional 15 minutes at room temperature, and again, the isopropanol/heptane solution containing extracted lipids was collected and combined with the first batch. Samples were immediately dried under N_2 stream using N-EVAP model 112 (Organomation Associates Inc., Manual, NV, USA) and lipid extracts were stored at -20°C for quantification at a later time.

Lipid extracts were resuspended in isopropanol (300 μL). TG was quantified using triolein (MP Biomedicals Inc., Santa Ana, CA, USA) as a standard. Samples were assayed in triplicates and diluted using isopropanol. Sample dilutions ranged from undiluted to 1:6 dilution in a final volume of 60 μL, depending on the degree of adipocyte differentiation for each sample. TG was quantified biochemically for some experiments and enzymatically for others.

Biochemically, samples were diluted when necessary (up to 1:6 dilution in a final volume of 60 µL) directly in a 96 well plate followed by addition of 60 µL saponification solution (18 M KOH in 25% isopropanol) to each sample. Samples were incubated with saponification solution for 10 minutes at room temperature. After incubation 60 µL of 3 mM sodium metaperiodate solution (3 mM sodium metaperiodate, 100 mM ammonium acetate; in 6% acetic acid) and 60 µL of acetylacetone solution were added to the plate. The plate was incubated for 15 minutes at 65 °C and then left to cool down to room temperature. Absorbance were read at a wavelength of 405 nm using FLUOstar Galaxy spectrophotometer and TG in µg was normalized to protein content in mg, determined by the modified Lowry assay.

For some experiments TG accumulation was quantified enzymatically (Infinity Triglyceride Liquid Stable Reagent, Thermo Scientific). Sample dilutions, when necessary, were prepared (up to 1:6 dilution in a final volume of 60 µL) in 1.5 mL Eppendorf tubes and dried using a SpeedVac (CentriVap Benchtop Vacuum Concentrators, Labconco, Kansas City, MO, USA) for 1.5 hours at room temperature. As per manufacturer's instructions, dried lipid samples were resuspended in 250 µL of Infinity TG reagent and incubated on a rotary shaker for 1.5 hours at 37 °C. Samples were loaded onto 96 well plate and absorbance was read at a wavelength of 540 nm using FLUOstar Galaxy spectrophotometer and TG in µg was normalized to protein content in mg, determined by the modified Lowry assay.

2.7 Modified Lowry protein assay

After TG was extracted from differentiated human adipocytes, the cellular remains were solubilized in Laemmli buffer (2% SDS, 10% glycerol, 60 mM Tris pH 6.8, 0.002% bromophenol blue) (Laemmli, 1970). For human MDMs, cultures were rinsed with ice cold

PBS and then solubilized in Laemmli buffer (Laemmli, 1970) containing 1 mM sodium orthovanadate, 50 mM sodium fluoride, 5 mM sodium pyrophosphate, and 5 mM EGTA on ice. Lysates from either cell type were scraped, collected with a 26G syringe, and were boiled for 5 minutes. Samples were stored at -20°C for later quantification and use for immunoblot analysis.

Protein was quantified using the modified Lowry assay (Bio-Rad Protein Assay Kit, Hercules, CA, USA) with bovine serum albumin (BSA) as a standard. Lysates were thawed and assayed in triplicate. Samples were diluted using water and dilutions ranged from 1:45-1:90 in final volume of 200 µL in 1.5 mL Eppendorf tubes. Once sample dilutions were prepared, 20 µL deoxycholate (1.5 mg/mL) were added and mixed by vortexing followed by a 10 minute incubation at room temperature. Subsequently, 20 µL trichloroacetic acid (72% v/v) were added to each sample and mixed by vortexing. Precipitated proteins were pelleted by centrifugation (21 000 x g) for 10 minutes at room temperature. After centrifugation, supernatants were removed and pellets were air dried for 1 hour. Pellets were resuspended in Bio-Rad Reagent A' (commercially available reagents S and A in 1:50 dilution) and incubated for 5 minutes at room temperature, followed by 200 µL addition of Bio-Rad Reagent B. Samples were incubated for 15 minutes at room temperature and 200 µL of sample were transferred to 96 well microplate. Absorbance was read at wavelength of 750 nm using FLUOstar Galaxy spectrophotometer.

2.8 Nuclear and cytosolic fraction preparation

Nuclear and cytosolic fractions from differentiated human adipocytes were prepared using Nuclear/Cytosol Fractionation Kit (BioVision, Milpitas, CA, USA). Differentiated human adipocytes were lifted by using 0.5 mL 1 X TrypLE reagen Life Technologies Inc.,

Burlington, ON, Canada) for 5-6 minutes at 37°C and by subsequent gentle scraping. As per manufacturer's protocol, detached cells were pooled and centrifuged (600 x g) for 5 minutes at 4°C. The pelleted cells were resuspended in Cytosol Extraction Buffer A Mix (CEB-A Mix) supplemented with DTT and Protease Inhibitors. Samples were vortexed for 15 seconds and then incubated for 10 minutes on ice. After incubation, ice-cold CEB-B was added and samples were vortexed for 5 seconds. Samples were incubated for 1 minute on ice and then vortexed once more for 5 seconds. Subsequently, samples were centrifuged (16 000 x g) for 5 minutes. After centrifugation, supernatants containing the cytoplasmic fraction were transferred to new pre-chilled tubes. The remaining pellets (containing nuclei) were resuspended in ice-cold Nuclear Extraction Buffer Mix. Samples were incubated on ice for 40 minutes, and every 10 minutes, samples were vigorously vortexed for 15 seconds. Finally, samples were centrifuged (16 000 x g) for 10 minutes. After centrifugation, the supernatants containing the nuclear fraction were transferred to a new pre-chilled tubes. Samples were stored at -20°C until modified Lowry assay analysis were performed.

2.9 Immunoblot analysis

Solubilized cellular proteins (5 – 25 µg depending on the experiment) were resolved by SDS–PAGE (7.5% – 12.5% acrylamide) at 200 V for 50 minutes to 1 hour. Gels were then electrophoretically transferred onto a nitrocellulose membrane (Bio-Rad, Mississauga, ON, Canada) at 70 V for 1 hour and 15 minutes to 1 hour and 45 minutes, depending on molecular weight of protein(s) being assessed. After transfer, non-specific binding sites on the membrane were blocked by 5% non-fat milk in PBS/0.1% Tween20 for 1 hour at room temperature. Membranes were rinsed with PBS and probed overnight at 4°C on Labquake rotator with the following antibodies directed against: adipocyte fatty acid-binding protein

(aP2; 0.1 mg/ml; R&D Systems), AMP-activated protein kinase (AMPK; 1:1000), carbohydrate-responsive element-binding (ChREBP; 1:1000; Thermo Fisher Scientific), ERK1/2 (0.25 mg/ml; EMD Millipore), fatty acid synthase (FAS; 1:1000; BD Biosciences), inhibitor of κB (IκB) α (1:1000), inhibitor of κB kinase (IKKβ, 1:500; EMD Millipore), peroxisome proliferator-activated receptor γ (PPARγ; 1:500), phospho-AMPK (Thr172) (1:1000), phospho-IKKα/β (Ser 176/180) (1:250), phospho-ERK (Thr202/Tyr204) (1:1000), phosphoserine PKC substrate (1:1000), sterol regulatory enhancer binding protein 1 (SREBP-1; 1:1000; Santa Cruz Biotechnology), all from Cell Signaling Technology unless otherwise indicated. After incubation with primary antibody overnight, membranes were washed twice with PBS/0.1% Tween20 for 15 minutes at room temperature. Membranes were then incubated with the appropriate horseradish peroxidase (HRP)-conjugated secondary antibodies (anti-rabbit, anti-mouse, or anti-goat, 1:5000 – 1:50,000) diluted in 5% non-fat milk in PBS for 1 hour at room temperature. Following incubation with secondary antibody, membranes were washed once for 15 minutes and three times for 10 minutes in PBS/0.01% Tween20. Membranes were rinsed five times with PBS and then covered with chemiluminescent HRP substrate detection solution (EMD Millipore, Billerica, MA, USA) for 5 minutes at room temperature. Membranes were exposed to film, which was processed using a Feature-SRX-101A developer (Konica Minolta, Chiyoda, Tokyo, Japan). Relative band intensity was quantified and expressed as integrated optical density (IOD) units using the AlphaImager imaging system (Alpha Innotech Co., San Leandro, CA, USA).

Membranes were stripped to re-probe for a second or third target on the same membrane, as follows. First, membranes were washed twice for 10 minutes in PBS/0.01% Tween20. Membranes were then incubated with stripping buffer (100 mM β-

mercaptoethanol, 2% SDS, 62.5 mM Tris HCl pH 6.8) at 50 °C for 30 minutes and agitated every 5 minutes. After incubation with stripping buffer, membranes were washed three times for 10 minutes in PBS/0.01% Tween20 at room temperature. Finally, membranes were blocked with 5% non-fat milk in PBS/0.1% Tween20 for 1 hour at room temperature and then re-probed with primary antibodies as described above.

2.10 RNA isolation and DNase I treatment

Human preadipocytes, differentiated human adipocytes and MDMs were lysed in 1 mL Qiazol (Qiagen, Venlo, Limburg, Netherlands) for 5-7 minutes at room temperature. Lysed samples were collected, transferred to 1.5 mL Eppendorf tubes, and flash-frozen in liquid nitrogen for storage at -80°C. For RNA isolation, Qiazol treated samples were thawed at room temperature. Once samples were completely thawed, 100 µL chloroform was added and samples were mixed by inversion for 3 minutes at room temperature. After mixing, samples were centrifuged (10 000 x g) for 10 minutes at 4°C. After centrifugation, the upper aqueous phase containing RNA was carefully removed and transferred to a new 1.5 mL Eppendorf tubes containing 500 µL isopropanol. Afterwards, 500 µL isopropanol was added to the aqueous phase and samples were mixed by inversion. Samples were then incubated for 10 minutes at room temperature and subsequently centrifuged (10 000 x g) for 10 minutes at 4°C. After centrifugation, the supernatant was removed and discarded and the remaining pellet was washed by adding 1 mL of 75% ethanol (in DEPC-treated water), mixing by inversion and centrifuging (7 500 x g) for 5 minutes at 4°C. After the supernatants were removed and discarded, the pellets were air dried for 3 minutes and then resuspended in 50 µL DEPC-treated water. Samples were then incubated at 65°C for 10 minutes and then cooled on ice, followed by DNaseI treatment to remove any contaminating DNA. DNaseI

treatment was conducted using DNA Treatment & Removal kit (Life Technologies Inc., Burlington, ON, Canada). As per manufacturer's protocol, 1 µL rDNaseI and 5 µL 10X DNaseI buffer were added to all samples and mixed gently by tapping. Samples were then incubated for 30 minutes at 37°C, and after incubation, 5 µL of DNaseI inactivation buffer was added to all samples. Samples were mixed by inversion for 2 minutes and then centrifuged (7 500 x g) for 5 minutes at 4°C. After centrifugation supernatants were transferred to new pre-chilled 1.5 mL Eppendorf tubes. DNaseI-treated RNA was stored at -80°C until later quantification analysis.

2.11 RNA quantification and quality analysis

RNA quantification was performed using Quant-it Ribogreen RNA assay kit (Life Technologies Inc., Burlington, ON, Canada), using 16S/23S rRNA as a standard. DNaseI-treated RNA samples were thawed on ice and diluted (1:100) in 1X Tris-EDTA (TE) buffer. Samples were assayed in triplicates: 1 µL of diluted RNA was added to 99 µL TE buffer in a black-bottomed 96- well plate, followed by addition of 100 µL of Ribogreen reagent to each well. Fluorescence readings (excitation: 485 nm, emission: 520 nm) were measured using a FLUOstar Galaxy spectrophotometer (BMG Labtech, Ortenberg, Germany). For quality control, 1 µg of RNA was run on 1 % denaturing formaldehyde agarose gel to detect any possible RNA degradation. Ethidium Bromide was used as a visualizing agent and gels were imaged using Chemi Doc-It TS2 Imaging System (Ultra-Violet Products Ltd., Upland, CA, USA).

2.12 Reverse transcription and real-time PCR analysis

Total RNA (1.5-2 µg per sample) was added to nuclease-free water to a final volume of 25 µL. Samples were mixed by tapping, and 5 µL of 0.5 µg/µL random primers (Life Technologies Inc., Burlington, ON, Canada) were added. Samples were mixed and incubated at 85°C for 3 minutes and then cooled on ice. Once cooled, 12 µL of sample were added to 8 µL of reverse transcription mixture (1.25 mM dNTP, 1.4 U/µL RNase OUT, 12.5 U/µL MMLV-Reverse Transcriptase, in 1X RT buffer; all from Life Technologies Inc., Burlington, ON, Canada) or negative control mixture (missing MMLV- Reverse Transcriptase). Samples were mixed by tapping and incubated for 1 hour at 42°C. After the incubation, MMLV-Reverse Transcriptase was heat inactivated by incubating samples for 10 minutes at 92°C. Newly synthesized cDNA was then stored at -20°C until later use for real-time PCR.

Real-time PCR assays were performed using the QuantiTect SYBR Green real-time PCR kit (for target genes) or the QuantiTect Probe real-time PCR kit (for 18S rRNA used for endogenous control) (both from Qiagen) Sample cDNA (2 µL) was added to primers (100 nM final concentration, see **Table 2** for primer sequences of target genes) and QuantiTect SYBR Green PCR master mix (Qiagen) to a final volume of 20 µL. For 18S rRNA detection, diluted (1:1000) samples (2 µL) were added to 18S primers (Applied Life Technologies) and QuantiTect Probe real-time PCR mix to a final volume of 20 µL. PCR was performed using Light Cycler Carousel (Roche, Laval, QC, Canada), with the following parameters: 10 minutes at 95°C, followed by 45 cycles each of 15 seconds at 95°C and 1 minute at 60°C. Data were analyzed with Light Cycler Software, version 3.0 (Roche, Laval, QC, Canada) by relative quantification (RQ) using 18S rRNA as a reference.

The real-time PCR efficiency of both methods (probe- vs SYBR-based) for IL-6, MCP-1 and adiponectin was similar (90-95%). However, the PCR efficiency of other target genes was not formally compared to the probe method. All real-time PCR analyses yielded a single melting curve corresponding to expected amplicon length.

2.13 Statistical analysis

Two-way ANOVA, followed by Tukey's post-hoc test was used when comparing multiple means within an experiment. Student's t-test was used when comparing two means. Pearson R correlation was used when assessing linear dependence between two data sets (Excel 2010, version 14.0.7; Microsoft). All data were verified to be of normal distribution. Significance was defined as $p<0.05$.

Target		Primer sequence
ACC	Forward	5'-TTTAAGGGGTGAAGAGGGTGC-3'
	Reverse	5'-CCAAAAAGACCTAGCCCTCAAG-3'
Adiponectin	Forward	5'-GCAGAGATGGCACCCCTG-3'
	Reverse	5'-GGTTTCACCGATGTCTCCCTTA-3'
ANG	Forward	5'-TTGTTCTGAGGCCGAGGAGC'3'
	Reverse	5'-TGTCTTTGCAGGGTGAGGTC-3'
CD36	Forward	5'-ATGTAACCCAGGACGCTGAG-3'
	Reverse	5'-GTCGCAGTGACTTTCCCAAT-3'
ChREBP-α*	Forward	5’-AGTGCTTGAGCCTGGCCTAC-3’
	Reverse	5’-TTGTTCAGGCGGATCTTGTC-3’
ChREBP-β*	Forward	5-AGCGGATTCCAGGTGAGG-3
	Reverse	5’-TTGTTCAGGCGGATCTTGTC-3’
CXCL-5	Forward	5'-AATCTTCGCTCCTCCAATCTCC-3'
	Reverse	5'-TCAGGGAGGCTACCACTTC-3'
FAS	Forward	5’-CAGAGCAGCCATGGAGGAG-3’
	Reverse	5’-AATCTGGGTTGATGCCTCCG-3’
GLUT4	Forward	5'-ACTGGCCATTGTTATCGGCA-3'
	Reverse	5'-GTCAGGCGCTTCAGACTCTT-3'
ICAM-1	Forward	5'-CAGCCAGATGCAATCAATGC-3'
	Reverse	5'-GTGGTCCATGGAATCCTGAA-3'
ICAM-3	Forward	5'-GACCAGCCTCACGGTGGTGC-3'
	Reverse	5'-ACGGGCAGGACAAAGGTTCGG-3'
IL-1β	Forward	5'-GATGAAGTGCTCCTTCCAGGACCT-3'
	Reverse	5'-TGCTGTGAGTCCCGGAGCGT-3'
IL-6	Forward	5'-TCCACAAGCGCCTTCGGTCC-3'
	Reverse	5'-TGTCTGTGTGGGGCGGCTACA-3'
IL-8	Forward	5'-CAGAGACAGCAGAGCACACA-3'
	Reverse	5'-GGCAAAACTGCACCTTCACA-3'
MCP-1	Forward	5'-CAGCCAGATGCAATCAATGC-3'
	Reverse	5'-GTGGTCCATGGAATCCTGAA-3'
MIF	Forward	5'-CCCGGACAGGGTCTACATCAAC-3'
	Reverse	5'-CCGTTTATTTCTCCCCACCAGA-3'
Perilipin 2	Forward	5'-AGTGGAAAAGGAGCATTGGA-3'
	Reverse	5'-GTCTCCTGGCTGCTCTTGTC-3'
SCD	Forward	5'-CCAGAGGAGGTACTACAAACCTG-3'
	Reverse	5'-TGGTGGTAGTTGTGGAAGCC-3'
SREBP-1c	Forward	5'-GACCGACATCGAAGACATGC-3'
	Reverse	5'-GGCATGGACGGGTACATCTT-3'
TNFα	Forward	5'-GCCCCCAGAGGGAAGAGTTCCC-3'
	Reverse	5'-CAGCTCCACGCCATTGGCCA-3'

*primer sets were obtained from (Herman et al., 2012)

Table 2. Primer sequences used for real time PCR analysis of target genes. The following table lists forward and reverse primer sequences used to perform real time PCR analysis to assess relative mRNA levels of target genes. Unless otherwise indicated, primers were obtained using NCBI primer selection software.

3. RESULTS

3.1 Effect of high glucose (HG) on adipogenic markers

The first aim of this study was to determine if HG affects adipogenesis. Human abdominal subcutaneous preadipocytes were induced to differentiate in the presence of normal (5 mM; NG) or high (25 mM; HG) glucose conditions. A time course was conducted. At days 0, 6, 10 and 14 of differentiation, triacylglycerol (TG) accumulation and adipogenic protein levels were assessed. TG levels gradually rose upon the course of differentiation, and this increase was similar in NG or HG (**Figure 1**). The protein levels of adipogenic markers, FAS, SREBP-1, PPARγ, and aP2 all increased with differentiation. PPARγ showed the most rapid rise, and aP2 had the most prolonged response. All of these proteins increased similarly in NG or HG conditions (**Figure 2**).

3.2 Effect of HG on ChREBP

To assess the effects of HG on the mRNA expression of ChREBP during adipogenesis, a time course was conducted. Human abdominal subcutaneous preadipocytes were induced to differentiate in the presence of NG or HG for 0, 6, 10, and 14 days. At the indicated time points, total RNA was collected, reverse-transcribed and mRNA expression of ChREBP-α and -β isoforms were quantified by real-time PCR. Under NG conditions, the mRNA expression of ChREBP-α increased very rapidly by day 6 of differentiation compared to day 0. This increase of ChREBP-α mRNA expression under NG was maintained until day 14 of differentiation (**Figure 3A**). ChREBP-β mRNA expression under NG conditions rose gradually during adipogenesis, however this increase did not reach

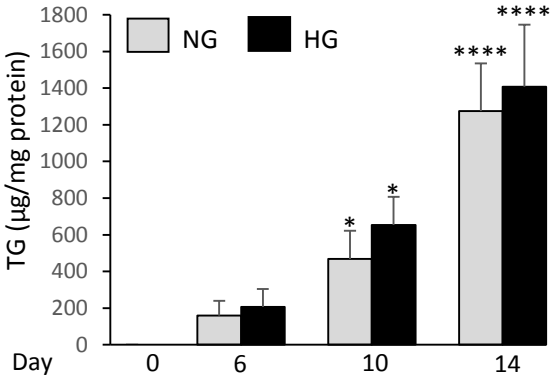
1800
1600
1400
1200
1000
800
600
400
200
0
TG (µg/mg protein)
NG
HG
****
****
*
*
Day
0
6
10
14

Figure 1. HG does not affect TG accumulation during human adipogenesis. Human subcutaneous abdominal preadipocytes were induced to differentiate in 5 mM (NG) or 25 mM (HG) glucose for 0, 6, 10 and 14 days. TG was extracted, quantified, and normalized to protein content. Results are the means ± S.E.M. of 3 separate patient samples; each patient sample was assessed in an individual experiment. **** denotes $p < 0.0001$ and * denotes $p < 0.05$ for each condition compared to day 0, as assessed by two-way ANOVA with Tukey post-hoc tests

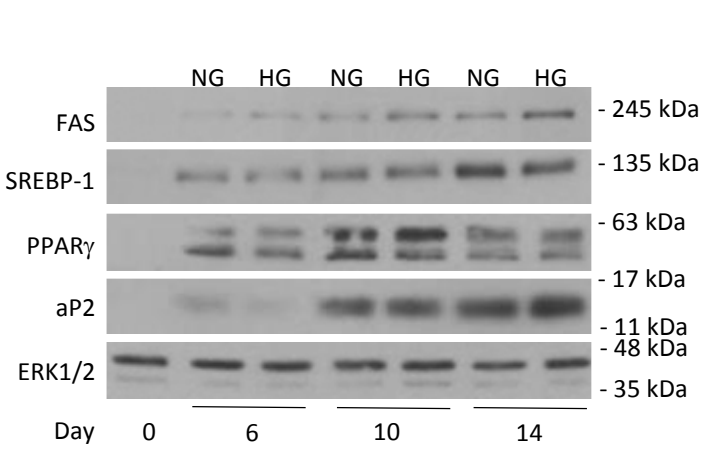
NG
HG
NG
HG
NG
HG
FAS
SREBP-1
PPARγ
aP2
ERK1/2
- 245 kDa
- 135 kDa
- 63 kDa
- 17 kDa
- 11 kDa
- 48 kDa
- 35 kDa
Day
0
6
10
14

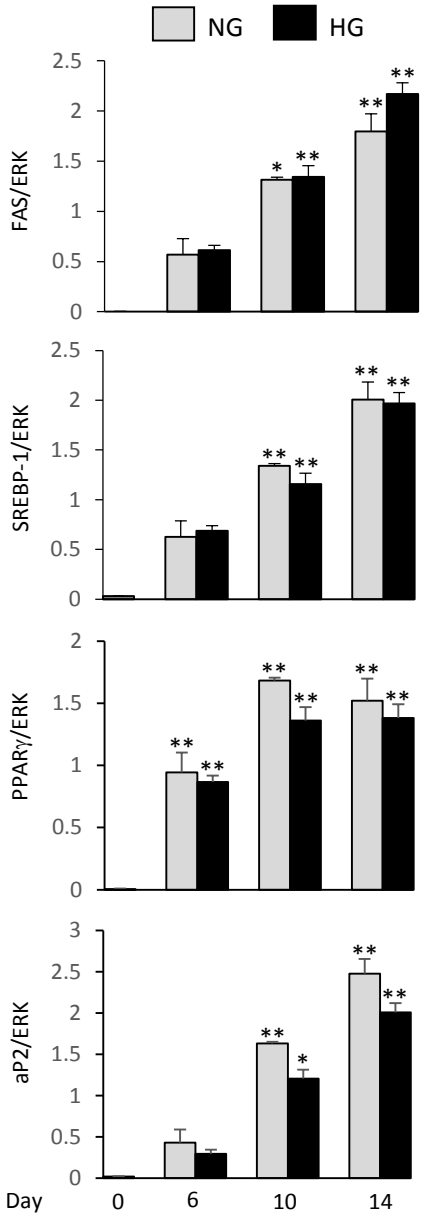
NG
HG
FAS/ERK
SREBP-1/ERK
PPARγ/ERK
aP2/ERK
Day
0
6
10
14

Figure 2. HG does not affect adipogenic protein levels during human adipogenesis. Human subcutaneous abdominal preadipocytes were induced to differentiate in 5 mM (NG) or 25 mM (HG) glucose for 0, 6, 10 and 14 days. Equal amounts of solubilized cellular protein were separated by SDS-PAGE and immunoblotted with the indicated antibodies. ERK1/2 serves as a loading control. Immunoblots from one patient sample are shown. Densitometric data from 3 separate patient samples, normalized to loading control, are graphically presented as means ± S.E.M. Each patient sample was assessed in an individual experiment. ** denotes $p < 0.01$, and * denotes $p < 0.05$ for each condition compared to day 0, as assessed by two-way ANOVA with Tukey post-hoc tests.

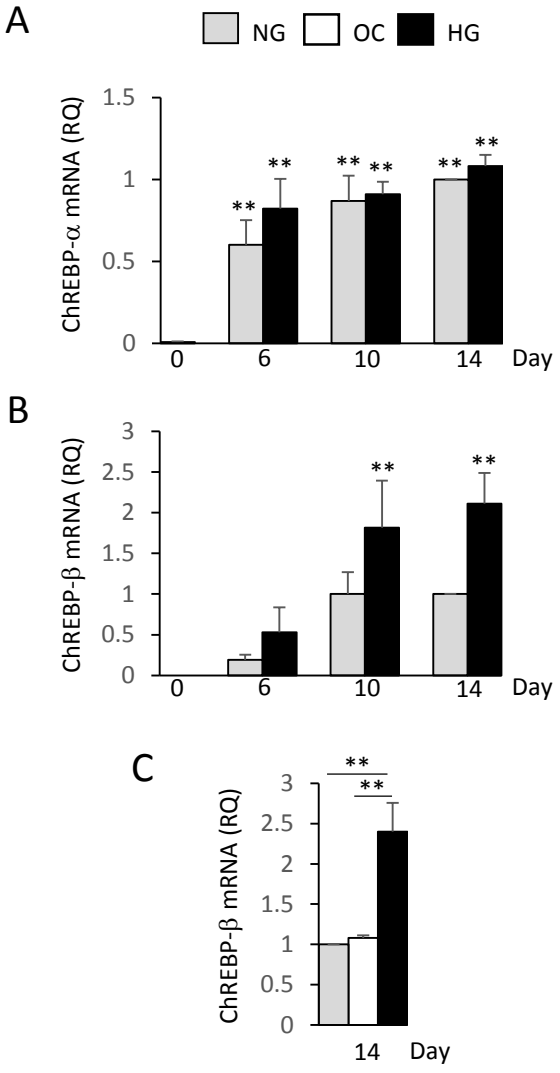
A
NG
OC
HG
ChREBP-α mRNA (RQ)
1.5
1
0.5
0
**
0
6
10
14
Day
B
ChREBP-β mRNA (RQ)
3
2.5
2
1.5
1
0.5
0
C

Figure 3. HG enhances ChREBP-β mRNA expression in differentiated adipocytes. Human subcutaneous abdominal preadipocytes were induced to differentiate in 5 mM (NG), 5 mM glucose/20 mM mannitol (OC), or 25 mM (HG) glucose for 0, 6, 10 or 14 days. RNA was isolated, and then quantified by real-time PCR, using indicated primers. Levels were normalized to endogenous 18S RNA, and expressed as a function of the NG control condition at day 14. Results from 5 (A and B) or 3 (C) separate patient samples are graphically presented as means ± S.E.M. Each patient sample was assessed in an individual experiment. ** denotes $p < 0.01$ for each condition compared to day 0 (A and B) or between indicated pairs (C), as assessed by two-way ANOVA with Tukey post-hoc tests. RQ stands for relative quantification.

statistical significance (**Figure 3A**). When preadipocytes were differentiated in HG conditions, ChREBP-α mRNA expression increased very rapidly by day 6 compared to day 0, and levels remained high through differentiation (**Figure 3A**). ChREBP-β mRNA expression under HG conditions increased with differentiation, compared to day 0 (**Figure 3B**). The increase in ChREBP-α mRNA during adipogenesis was similar under HG versus NG conditions (**Figure 3A**). However, by the last day of differentiation, ChREBP-β mRNA enhancement was greater under HG conditions compared to NG (**Figure 3C**). There was no effect with osmolality control conditions (**Figure 3C**).

ChREBP-α and -β protein levels in adipocytes, differentiated under HG versus NG, were assessed to determine if the pattern seen at the mRNA level occurs at the protein level. Human abdominal subcutaneous preadipocytes were induced to differentiate under NG or HG conditions for 14 days. At day 14, the nuclear and cytosolic fractions of these cultures were extracted and protein levels of ChREBP were analysed by immunoblot.

ChREBP-α protein was detected in both cytosolic and nuclear fractions, and there was no difference in NG versus HG conditions. Under both conditions, NG and HG, ChREBP-β protein was detected only in the nuclear fraction, and its levels increased by 1.6 fold under HG conditions compared to NG (**Figure 4**).

The mRNA expression of ChREBP target genes, acetyl-CoA carboxylase 1 (ACC1), stearoyl-CoA desaturase (SCD), and FAS were assessed in adipocytes differentiated in HG versus NG conditions. Although ChREBP-β gene and protein expression were enhanced by HG (**Figure 3 and 4**), the mRNA expression of target genes did not change in adipocytes differentiated in HG versus NG. (**Figure 5A**).

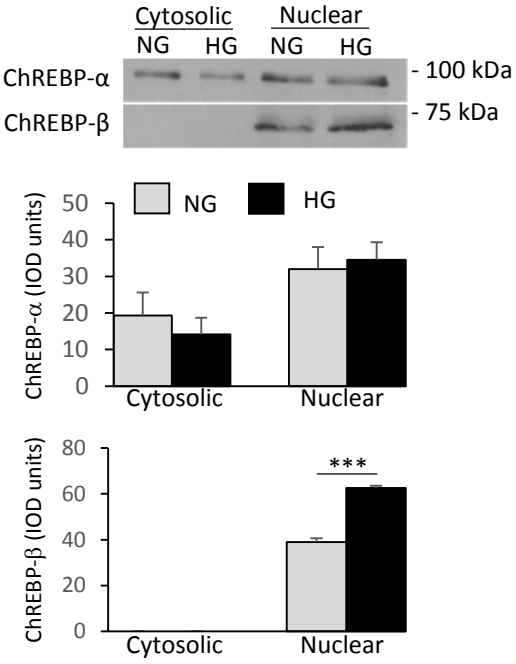
Cytosolic
Nuclear
NG
HG
NG
HG
ChREBP-α
ChREBP-β
- 100 kDa
- 75 kDa
NG
HG
ChREBP-α (IOD units)
50
40
30
20
10
0
Cytosolic
Nuclear
ChREBP-β (IOD units)
80
60
40
20
0
***
Cytosolic
Nuclear

Figure 4. HG increases ChREBP-β protein levels in nuclear fractions of differentiated adipocytes. Human subcutaneous abdominal preadipocytes were induced to differentiate in 5 mM (NG) or 25 mM (HG) glucose for 14 days. Equal amounts of solubilized nuclear and cytosolic protein were separated by SDS-PAGE and immunoblotted with the indicated antibodies. Immunoblots from one patient sample are shown. Densitometric data from 3 separate patient samples, normalized to loading control, are graphically presented as means ± S.E.M. Each patient sample was assessed in an individual experiment. *** denotes $p < 0.001$ between indicated pairs by two-way ANOVA with Tukey post-hoc tests.

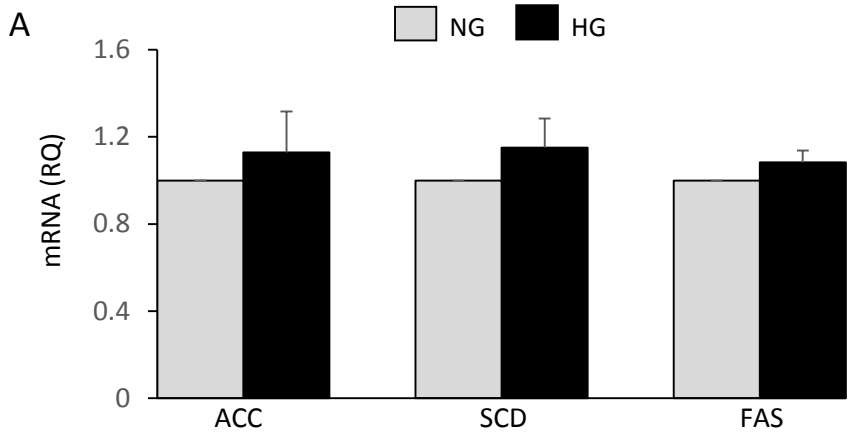
A
NG
HG
1.6
1.2
0.8
0.4
0
mRNA (RQ)
ACC
SCD
FAS

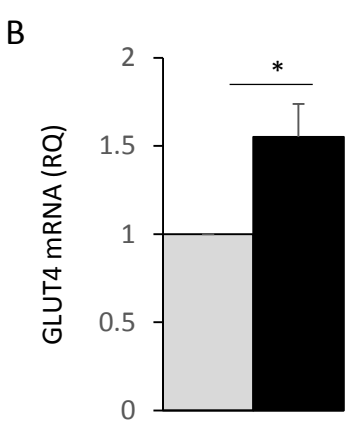
B
2
1.5
1
0.5
0
GLUT4 mRNA (RQ)
*

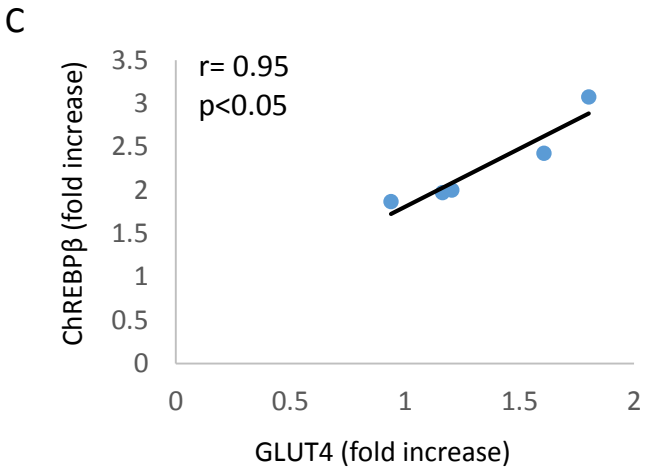
C
r= 0.95
p<0.05
3.5
3
2.5
2
1.5
1
0.5
0
ChREBPβ (fold increase)
0
0.5
1
1.5
2
GLUT4 (fold increase)

Figure 5. HG increases GLUT4 gene expression but does not affect lipogenic genes. Human subcutaneous abdominal preadipocytes were induced to differentiate in 5 mM (NG) or 25 mM (HG) glucose for 14 days. RNA was isolated, and then quantified by real-time PCR, using indicated primers. Levels were normalized to endogenous 18S RNA, and expressed as a function of the NG control condition. Results from 3 (A) or 5 (B and C) separate patient samples are graphically presented as means ± S.E.M. Each patient sample was assessed in an individual experiment. * denotes $p < 0.05$ between indicated pairs, as assessed by paired t-test (B) and Pearson R correlation (C). RQ stands for relative quantification.

Next, mRNA expression of GLUT4 in adipocytes differentiated in HG versus NG was assessed. GLUT4 mRNA expression in HG conditions was significantly enhanced (1.6 fold) compared to NG conditions (**Figure 5B**). Also, the fold-increase of ChREBP-β mRNA expression was positively and significantly correlated to the fold-increase of GLUT4 mRNA (r=0.95) (**Figure 5C**).

3.3 Effect of HG-MacCM on adipogenesis

The next objective was to assess whether HG modulates the anti-adipogenic effects of MacCM. MDMs (prepared as described in section **2.2**) were placed in medium containing either NG (5 mM glucose) or HG (25 mM glucose) for 24 hours. MacCM for either treatment (NG- or HG-MacCM) was prepared as described in section **2.3**. Confluent human abdominal subcutaneous preadipocytes were induced to differentiate for 14 days with either control medium (NG or HG), NG-MacCM, or HG-MacCM. TG accumulation and adipogenic protein markers, FAS, SREBP-1, PPARγ, and aP2 were assessed at day 14.

HG-MacCM significantly reduced TG accumulation versus control-HG by 28% (**Figure 6**). There was a weaker reduction in TG accumulation with NG-MacCM versus control that did not reach statistical significance (**Figure 6**). HG-MacCM, but not NG-MacCM, significantly reduced the protein levels of PPARγ by 50% compared to control medium conditions (**Figure 7**). FAS levels were significantly decreased in NG-MacCM and HG-MacCM by 40% and 43%, respectively, compared to control medium conditions. SREBP-1 and aP2 levels remained stable in either MacCM condition (**Figure 7**). There was a downward trend in aP2 levels under HG-MacCM compared to control that did not reach significance. Control studies demonstrated no effect of osmolality (**Figure 8**).

A

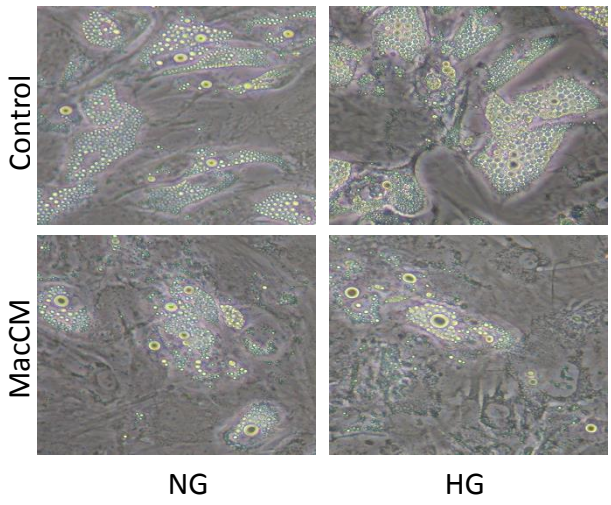
Control
MacCM
NG
HG

B

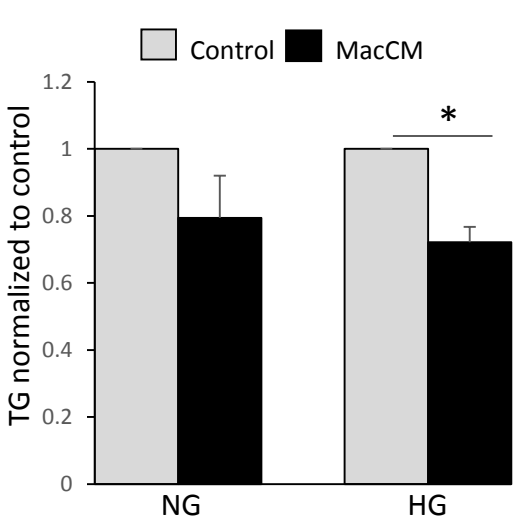
Control
MacCM
TG normalized to control
1.2
1
0.8
0.6
0.4
0.2
0
*
NG
HG

Figure 6. HG-MacCM inhibits TG accumulation in differentiated human adipocytes. MDM-conditioned media (MacCM) and control media were generated over 24 hours in 5 mM (NG) or 25 mM (HG) glucose. Human abdominal subcutaneous preadipocytes were then induced to differentiate for 14 days in control (NG or HG) medium, NG-MacCM, or HG-MacCM (A) Representative photomicrographs from one patient sample are shown (200 X magnifications). (B) TG was extracted, quantified, and adjusted for protein content. Data, normalized to their respective control condition, are graphically presented as means ± S.E.M. of 6 separate patient samples; each patient sample was assessed in an individual experiment. * denotes $p < 0.05$ between indicated pair, as assessed by two-way ANOVA with Tukey post-hoc tests.

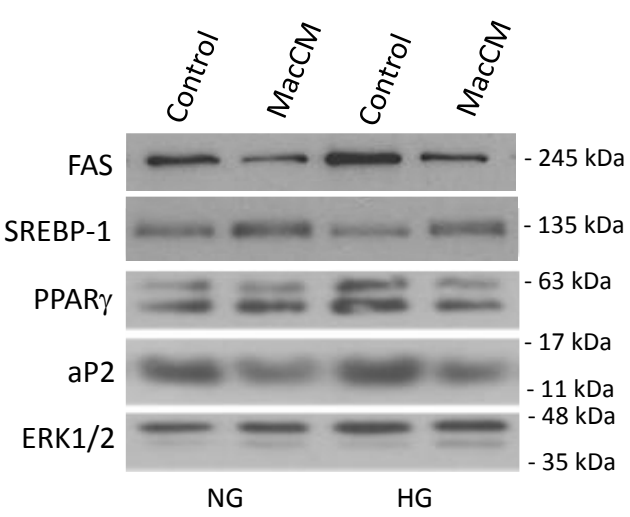
Control
MacCM
Control
MacCM
FAS
SREBP-1
PPARγ
aP2
ERK1/2
- 245 kDa
- 135 kDa
- 63 kDa
- 17 kDa
- 11 kDa
- 48 kDa
- 35 kDa
NG
HG

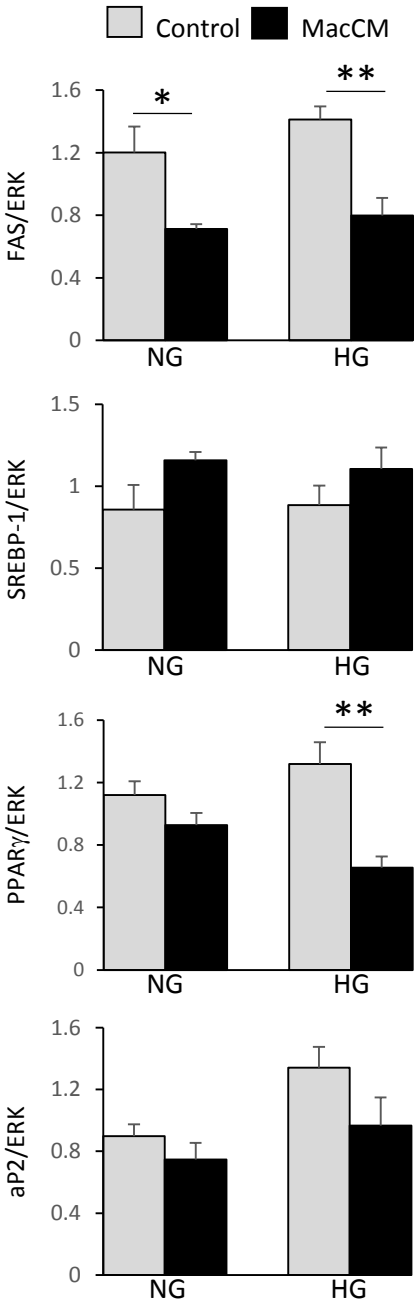
Control
MacCM
FAS/ERK
SREBP-1/ERK
PPARγ/ERK
aP2/ERK
NG
HG
*
**

Figure 7. HG-MacCM reduces PPARγ protein expression in differentiating human adipocytes. MDM-conditioned media (MacCM) and control media were generated over 24 hours in 5 mM (NG) or 25 mM (HG) glucose. Human abdominal subcutaneous preadipocytes were induced to differentiate for 14 days with control (NG or HG) medium, NG-MacCM, or HG-MacCM. Equal amounts of solubilized cellular protein were separated by SDS-PAGE and immunoblotted with the indicated antibodies. ERK1/2 serves as a loading control. Immunoblots from one patient sample are shown. Densitometric data from 6 separate patient samples, normalized to loading control, are graphically presented as means ± S.E.M. Each patient sample was assessed in an individual experiment. ** denotes $p < 0.01$, and * denotes $p < 0.05$ between indicated pairs, as assessed by two-way ANOVA with Tukey post-hoc tests.

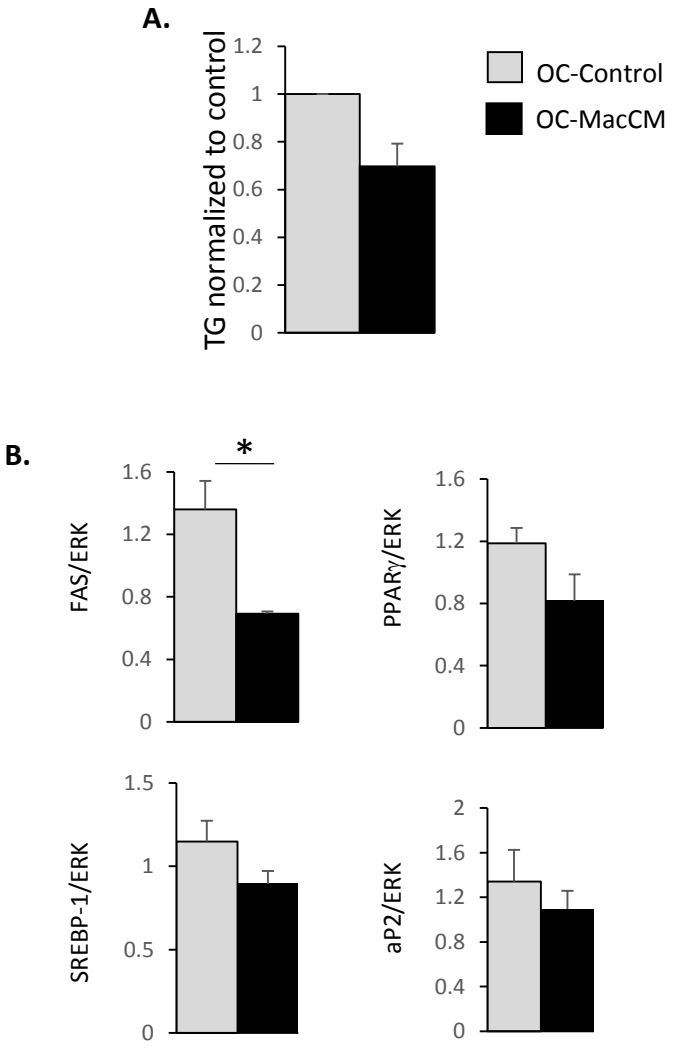
A.
TG normalized to control
1.2
1
0.8
0.6
0.4
0.2
0
OC-Control
OC-MacCM
B.
*
FAS/ERK
1.6
1.2
0.8
0.4
0
PPARγ/ERK
1.6
1.2
0.8
0.4
0
SREBP-1/ERK
1.5
1
0.5
0
aP2/ERK
2
1.6
1.2
0.8
0.4
0

Figure 8. Effect of OC-MacCM on adipogenic responses. MDM-conditioned media (MacCM) and control media were generated over 24 hours in 5 mM glucose and 20 mM mannitol (OC)). Human abdominal subcutaneous preadipocytes were induced to differentiate for 14 days with OC medium, or OC-MacCM. (A) TG was extracted, quantified, and adjusted for protein content. Data, normalized to control condition. (B) Equal amounts of solubilized cellular protein were separated by SDS-PAGE and immunoblotted with the indicated antibodies. ERK1/2 serves as a loading control. Densitometric data from 3 separate patient samples, normalized to loading control, are graphically presented as means ± S.E.M. Each patient sample was assessed in an individual experiment. * denotes $p < 0.05$ between indicated pairs, as assessed by paired student's t-test.

3.4 Effect of HG-MacCM on inflammatory gene expression of differentiated adipocytes

To assess whether HG-MacCM affects the inflammatory state of differentiated adipocytes, human abdominal subcutaneous preadipocytes were induced to differentiate over 14 days in control medium (NG or HG), NG-MacCM, or HG-MacCM. At day 14 of differentiation, total RNA was collected, reverse-transcribed and gene expression levels of pro-inflammatory cytokines, IL-6, MCP-1, IL-1β, IL-8 and anti-inflammatory adiponectin were quantified by real-time PCR.

With control medium (NG versus HG), there was no effect of glucose on the expression of these markers (**Figure 9**). HG-MacCM significantly enhanced the mRNA expression level of IL-6 by 3.6-fold, compared to control medium, whereas NG-MacCM had no effect compared to control medium. With respect to MCP-1 mRNA expression, HG-MacCM was a significantly more potent inducer than was NG-MacCM, with an increase of 4.5- versus 3.2- fold, respectively. IL-1β expression was not changed with MacCM at either glucose concentration. IL-8 expression was enhanced by 5.2-fold with HG-MacCM versus 1.6-fold with NG-MacCM compared to controls; however this trend did not reach statistical significance. The mRNA expression of anti-inflammatory adiponectin was significantly reduced by 57% in HG-MacCM versus control. A weaker reduction of adiponectin mRNA expression in NG-MacCM did not reach significance compared to control was also observed that did not reach significance (**Figure 9**).

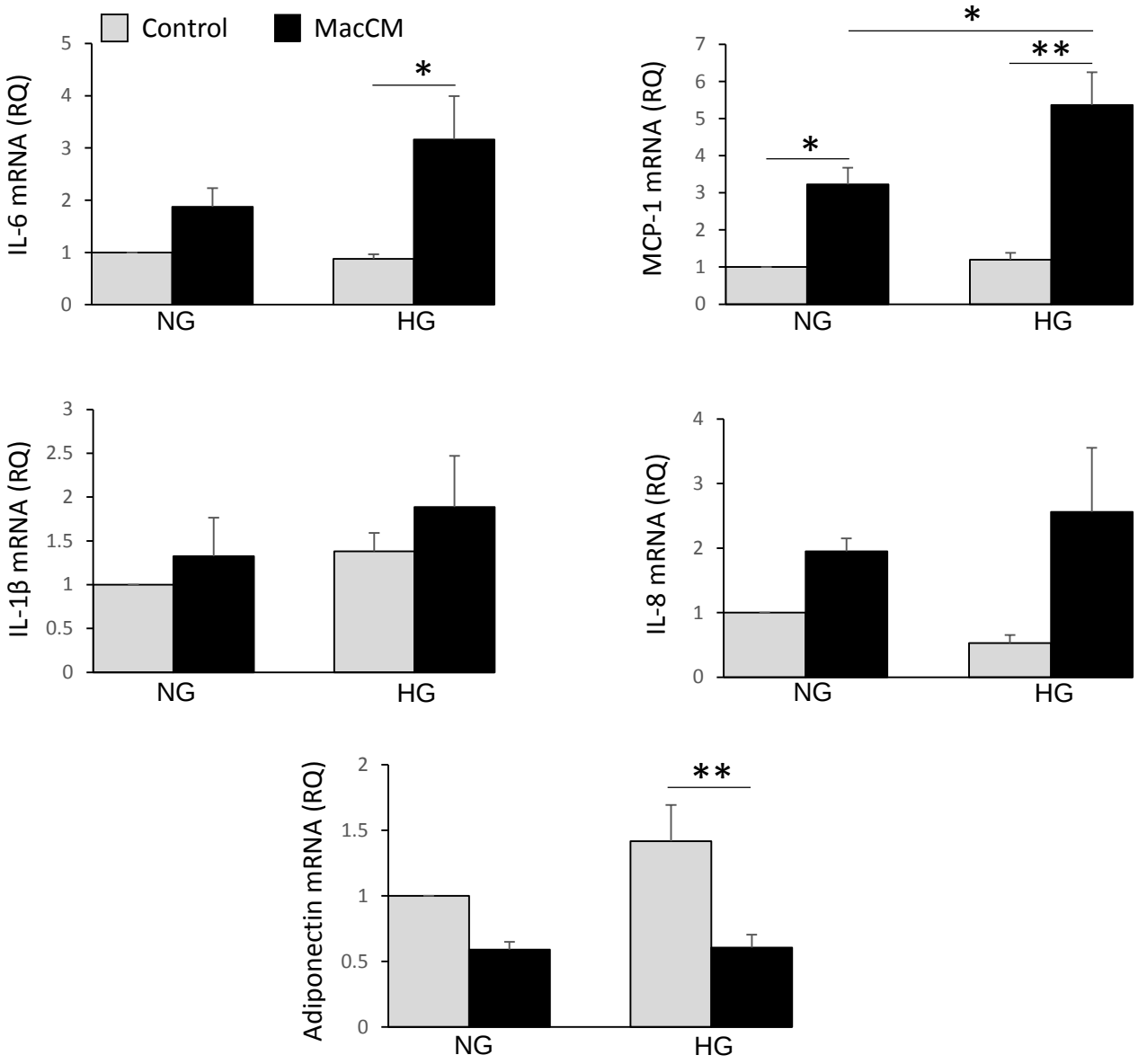
Control
MacCM
IL-6 mRNA (RQ)
MCP-1 mRNA (RQ)
IL-1β mRNA (RQ)
IL-8 mRNA (RQ)
Adiponectin mRNA (RQ)
NG
HG
*
**

Figure 9. HG-MacCM increases pro-inflammatory gene expression in human differentiated adipocytes. MDM-conditioned medium (MacCM) and control medium were generated over 24 hours in 5 mM (NG) or 25 mM glucose (HG). Human abdominal subcutaneous preadipocytes were induced to differentiate for 14 days with control (NG or HG) medium, NG-MacCM, or HG-MacCM. RNA was isolated, then quantified by real time PCR, using indicated primers. Levels were normalized to endogenous 18S RNA, and expressed as a function of the NG control condition. Results from 5 (A-C, E) and 4 (D) separate patient samples are graphically presented as means ± S.E.M. Each patient sample was assessed in an individual experiment. ** denotes $p < 0.01$, and * denotes $p < 0.05$ between indicated pairs, as assessed by two-way ANOVA with Tukey post-hoc tests. RQ stands for relative quantification.

3.5 Identifying anti-adipogenic factors secreted by MDMs upon HG exposure.

Before analysing potential secreted MDM factors, I first assessed a panel of inflammatory and metabolic genes in response to exposure to HG. To address this, MDMs were exposed to NG or HG for 6, 12, and 24 hours. At each time point, total RNA was collected, reverse-transcribed and gene expression levels of adhesion (ICAM-1 and ICAM-3), inflammatory (IL-1β, MCP-1, and TNFα) and metabolic (CD36, perilipin 2, and SREBP-1c) genes were quantified by real-time PCR.

The mRNA expression of adhesion molecules ICAM-1 and ICAM-3 was significantly enhanced under HG conditions after 6 hours, although only modestly by 1.1-fold and 1.2-fold, respectively (**Figure 10A**). The mRNA expression of pro-inflammatory genes, IL-1β, MCP-1, and TNF-α at 6, 12, and 24 hours did not change with HG versus NG (**Figure 10A**). The expression levels of metabolic genes, CD36, perilipin 2, SREBP-1c also did not change with HG versus NG (**Figure 10B**). However, anti-inflammatory PPARγ protein levels in MDMs exposed to HG for 24 hours were significantly decreased by 44% compared to NG (**Figure 11**).

A human cytokine array was performed comparing HG-MacCM versus NG-MacCM, each generated over 24 hours. A total of 30 cytokines were detected in both HG- and NG-MacCM. Five cytokines appeared to be enhanced in HG compared to NG conditions: angiogenin (ANG), macrophage migration inhibitory factor (MIF), C-X-C motif chemokine 5 (CXCL-5), nterleukin-18-binding protein (IL-18Bpa), and interleukin-17 (IL-17) (**Figure 12A**). To confirm these changes, the gene expression of these cytokines was assessed at the mRNA level by real-time PCR at 6 and 24 hours of HG versus NG treatment of MDMs.

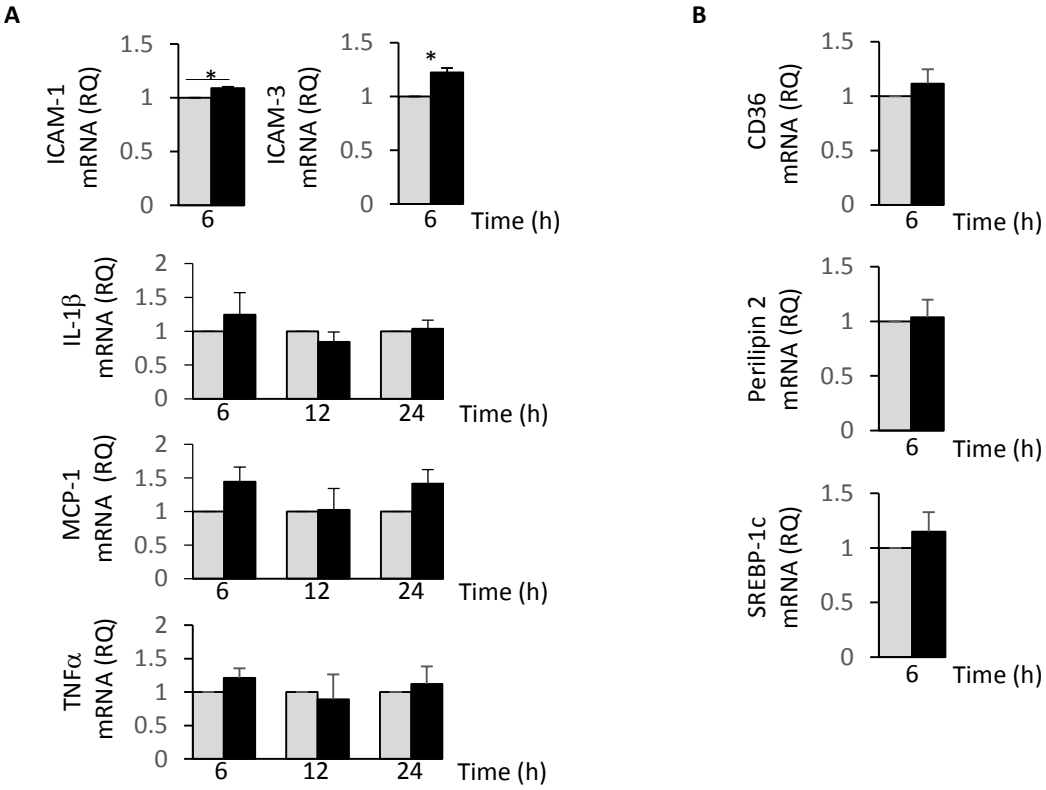
A
ICAM-1 mRNA (RQ)
ICAM-3 mRNA (RQ)
IL-1β mRNA (RQ)
MCP-1 mRNA (RQ)
TNFα mRNA (RQ)
Time (h)
B
CD36 mRNA (RQ)
Perilipin 2 mRNA (RQ)
SREBP-1c mRNA (RQ)
Time (h)

Figure 10. HG modestly enhances the gene expression of ICAM-1 and ICAM-3, but it does not affect pro-inflammatory and metabolic gene expressions in MDMs. Human MDMs were exposed to 5 mM (NG) or 25 mM (HG) glucose for 6-24 hours. RNA was isolated, and then quantified by real-time PCR, using indicated primers. Levels were normalized to endogenous 18S RNA, and expressed as a function of the NG control. Results are graphically presented as means ± S.E.M. of 3-5 separate donor samples; each donor sample was assessed in an individual experiment. * denotes $p < 0.05$ by paired t-test. RQ stands for relative quantification.

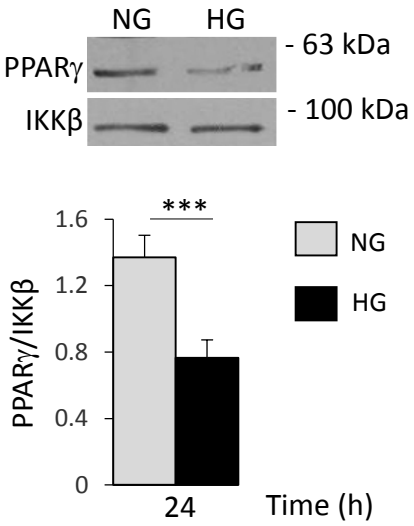
NG
HG
PPARγ
- 63 kDa
IKKβ
- 100 kDa
***
1.6
1.2
0.8
0.4
0
PPARγ/IKKβ
NG
HG
24
Time (h)

Figure 11. HG suppresses PPARγ protein expression in human MDMs. Human MDMs were exposed to 5 mM (NG) or 25 mM (HG) glucose for 24 hours. Equal amounts of solubilized protein were separated by SDS-PAGE and immunoblotted with the indicated antibodies. IKKβ serves as loading control. Immunoblots from one donor sample are shown. Densitometric data from 4 separate donor samples, normalized to loading control, are graphically presented as means ± S.E.M. Each donor sample was assessed in an individual experiment. *** denotes $p < 0.001$ between indicated pairs, as assessed by paired t-test.

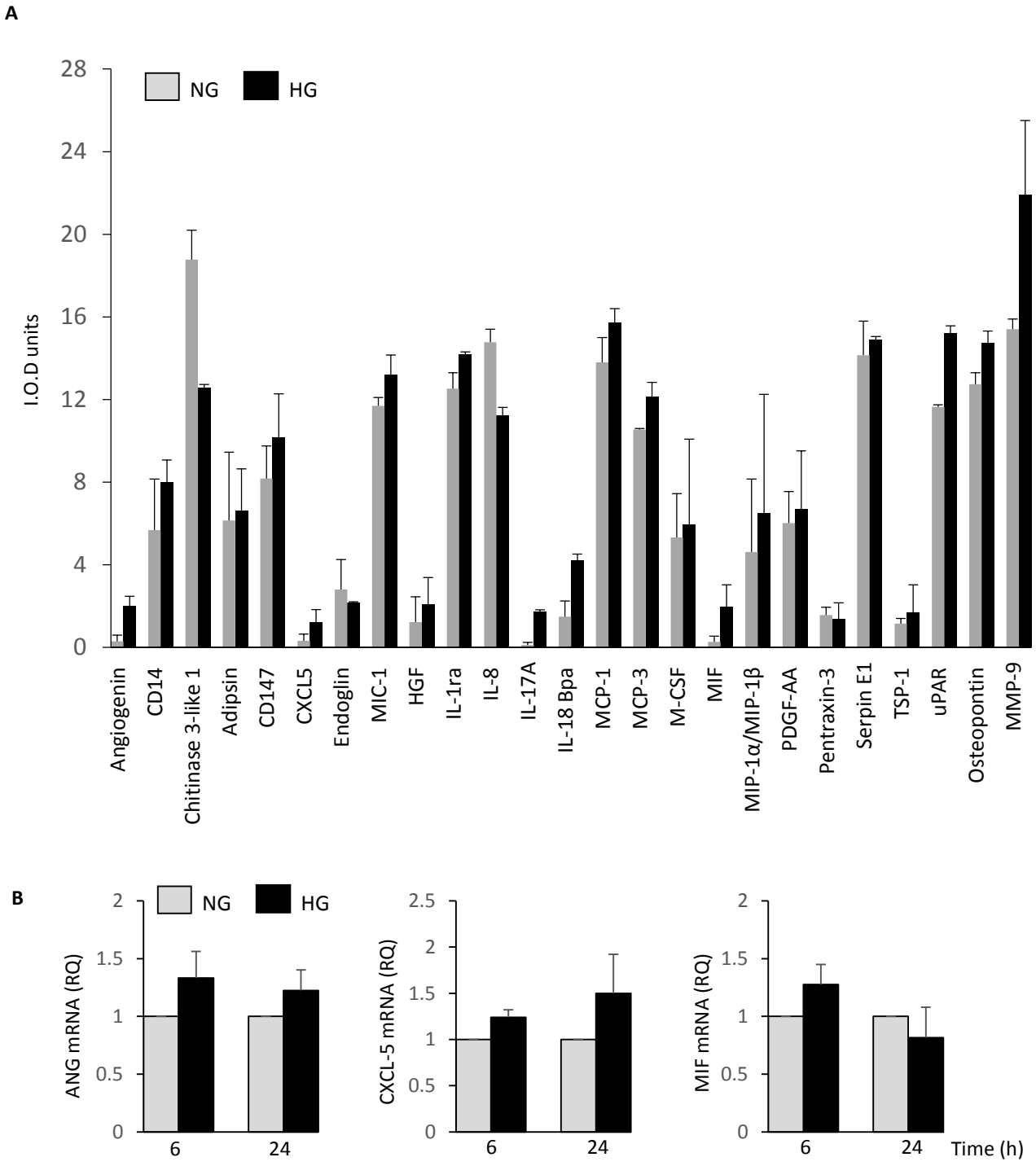
A
NG
HG
I.O.D units
28
24
20
16
12
8
4
0
Angiogenin
CD14
Chitinase 3-like 1
Adipsin
CD147
CXCL5
Endoglin
MIC-1
HGF
IL-1ra
IL-8
IL-17A
IL-18 Bpa
MCP-1
MCP-3
M-CSF
MIF
MIP-1α/MIP-1β
PDGF-AA
Pentraxin-3
Serpin E1
TSP-1
uPAR
Osteopontin
MMP-9
B
NG
HG
ANG mRNA (RQ)
2
1.5
1
0.5
0
6
24
CXCL-5 mRNA (RQ)
2.5
2
1.5
1
0.5
0
6
24
MIF mRNA (RQ)
2
1.5
1
0.5
0
6
24
Time (h)

\

Figure 12. Human cytokine array analysis. Human MDMs were exposed to 5 mM (NG) or 25 mM (HG) glucose for 6-24 hours. (A) After 24 h, human cytokine array analysis was performed on the conditioned media. Densitometric analysis for 25 detected cytokines are shown from two separate experiments presented as means ± range. (B) RNA was isolated and quantified by real-time PCR, using indicated primers. Levels were normalized to endogenous 18S RNA, and expressed as a function of the NG control. Results are graphically presented as means ± S.E.M. of 3 separate donor samples; each donor sample was assessed in an individual experiment. RQ stands for relative quantification.

Only the mRNA expression of ANG, MIF, and CXCL-5 could be detected by real-time PCR analysis and unlike the cytokine array protein data, they did not show a significant enhancement in HG conditions compared to NG (**Figure 12B**). ANG showed a 1.3-fold trend towards enhancement in HG compared to NG at 6 and 24 hours.

To see if ANG could reduce TG accumulation and reduce the protein levels of PPARγ during human adipogenesis, a dose-response analysis using human recombinant ANG (rANG) was performed. Confluent human abdominal subcutaneous preadipocytes were induced to differentiate for 14 days with differentiation medium containing 0, 0.1 µg/mL, 0.3 µg/mL, 0.5 µg/mL, 1 µg/mL rANG , or vehicle (0.1% BSA in PBS) in NG or HG conditions. TG accumulation and protein expression of PPARγ were not affected by rANG at any of the concentrations tested under NG or HG conditions (**Figure 13**).

Enzyme-linked immunosorbent assay (ELISA) was performed to quantify IL-17A protein levels in MacCM generated under NG versus HG conditions. IL-17A protein was not detected in either NG-MacCM or HG-MacCM.

3.6 Explore signaling pathways in macrophages that are activated by HG leading to generation of anti-adipogenic factors.

The final objective of this study was to identify possible HG-induced signaling pathways in MDMs that may contribute to generating factors that lead to the observed responses in differentiated adipocytes. To address this objective, MDMs were exposed to NG or HG for 3, 6, 18, and 24 hours. At each time point, cell lysates were collected and assessed the phosphorylation levels of IKKβ, ERK1/2, AMPK, and PKC substrates by immunoblot analysis.

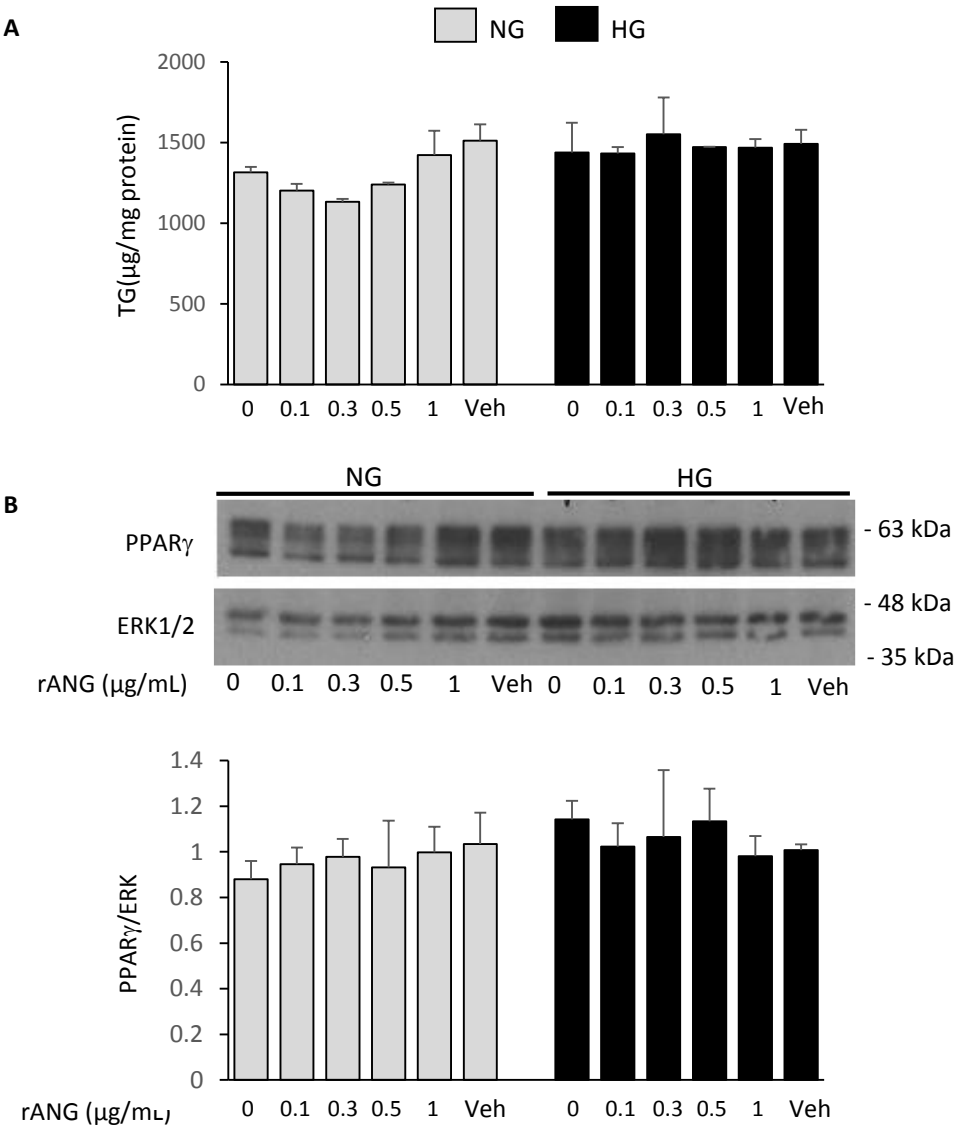
A
NG
HG
TG(μg/mg protein)
2000
1500
1000
500
0
0 0.1 0.3 0.5 1 Veh 0 0.1 0.3 0.5 1 Veh
B
NG
HG
PPARγ
- 63 kDa
ERK1/2
- 48 kDa
- 35 kDa
rANG (μg/mL) 0 0.1 0.3 0.5 1 Veh 0 0.1 0.3 0.5 1 Veh
PPARγ/ERK
1.4
1.2
1
0.8
0.6
0.4
0.2
0
rANG (μg/mL) 0 0.1 0.3 0.5 1 Veh 0 0.1 0.3 0.5 1 Veh

Figure 13. Recombinant ANG (rANG) does not affect TG accumulation or PPARγ protein expression in differentiated human adipocytes. Human subcutaneous abdominal preadipocytes were induced to differentiate in 5 mM (NG) glucose or 25 mM (HG), supplemented with rANG (at the indicated doses) or vehicle for 14 days. (A) TG was extracted, quantified, and normalized to protein content. Results are the means ± S.E.M. of 3 separate patient samples. (B) Equal amounts of solubilized cellular protein were separated by SDS-PAGE and immunoblotted with the indicated antibodies. ERK1/2 serves as a loading control. Immunoblots from one patient sample are shown. Densitometric data from 3 separate patient samples, normalized to loading control, are graphically presented as means ± S.E.M. Each patient sample was assessed in an individual experiment.

MDMs exposed to HG demonstrated significant 1.8 fold more IKKβ phosphorylation at 3 hours compared to NG. The HG-induced enhancement of IKKβ phosphorylation seen after 3 hour exposure was reduced by 52% at 24 hours. Activation of IKKβ leads to phosphorylation and subsequent degradation of IκBα, therefore, IκBα protein levels were also assessed in these cultures. At the 24 hour time point, IκBα levels were significantly decreased by 52% in MDMs treated with HG compared to NG (**Figure 14**). The phosphorylation levels of ERK1/2, AMPK, and PKC substrates in MDMs exposed to HG or NG did not change over time. The phosphorylation levels of these molecules did not change under NG versus HG conditions (**Figure 15**).

Since HG led to an increase in IKKβ phosphorylation in MDMs, the effect of IKKβ inhibitor sc-514 on the HG-MacCM-induced changes in IL-6, MCP-1, and adiponectin gene expression in differentiated adipocytes described above was assessed. Sc-514 significantly reduced HG-MacCM-dependent enhancement of MCP-1 gene expression by 38% compared to vehicle conditions. There was no effect of sc-514 on HG- or NG-MacCM-induced changes in IL-6 or adiponectin gene expression in differentiated adipocytes (**Figure 16**).

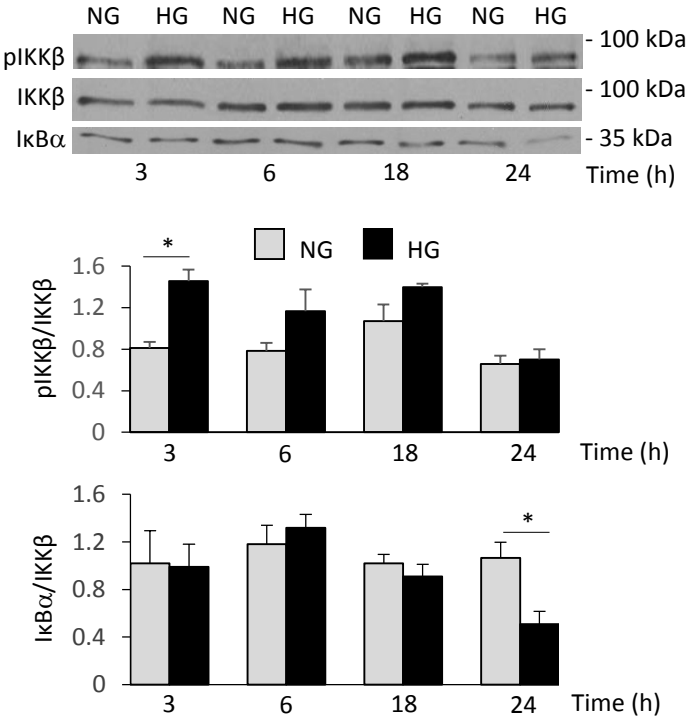
NG HG NG HG NG HG NG HG
pIKKβ
IKKβ
IκBα
- 100 kDa
- 100 kDa
- 35 kDa
3 6 18 24
Time (h)
NG
HG
*
pIKKβ/IKKβ
1.6
1.2
0.8
0.4
0
3 6 18 24
Time (h)
IκBα/IKKβ
*
1.6
1.2
0.8
0.4
0
3 6 18 24
Time (h)

Figure 14. HG increases IKKβ phosphorylation in human MDMs. Human MDMs were exposed to 5 mM (NG) or 25 mM (HG) glucose for 3-24 hours. Equal amounts of solubilized protein were separated by SDS-PAGE and immunoblotted with the indicated antibodies. IKKβ serves as loading control. Immunoblots from one donor sample are shown. Densitometric data from 4 separate donor samples, normalized to loading control, are graphically presented as means ± S.E.M. Each donor sample was assessed in an individual experiment. * denotes $p<0.05$ between indicated pairs, as assessed by two-way ANOVA with Tukey post-hoc tests.

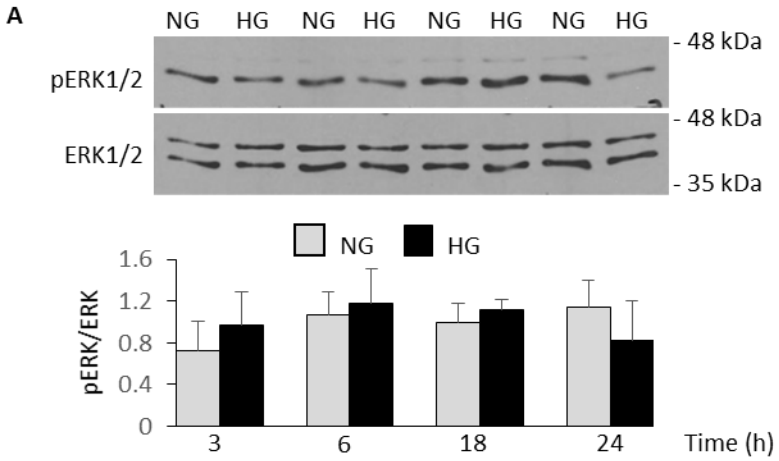
A
NG HG NG HG NG HG NG HG
pERK1/2
- 48 kDa
ERK1/2
- 48 kDa
- 35 kDa
NG HG
pERK/ERK
1.6
1.2
0.8
0.4
0
3 6 18 24
Time (h)

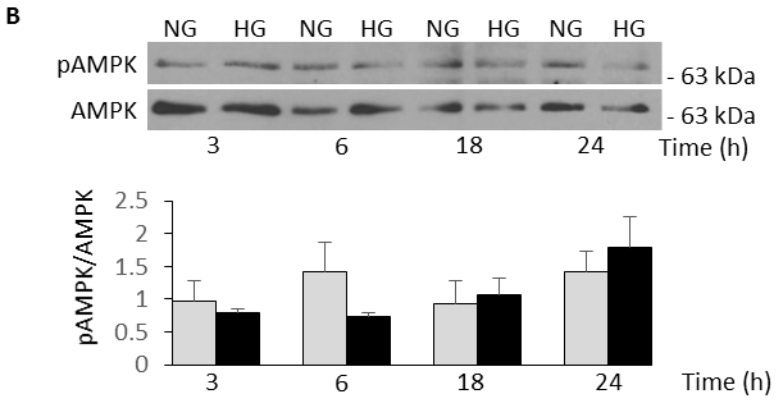
B
NG HG NG HG NG HG NG HG
pAMPK
- 63 kDa
AMPK
- 63 kDa
3 6 18 24
Time (h)
pAMPK/AMPK
2.5
2
1.5
1
0.5
0
3 6 18 24
Time (h)

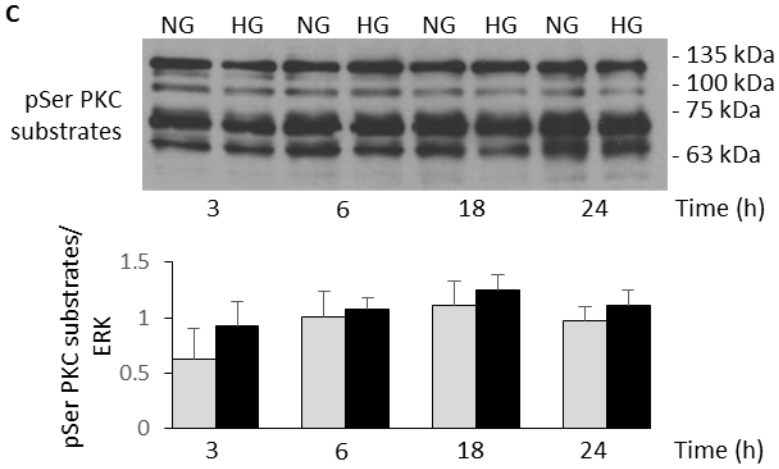
C
NG HG NG HG NG HG NG HG
pSer PKC substrates
- 135 kDa
- 100 kDa
- 75 kDa
- 63 kDa
3 6 18 24
Time (h)
pSer PKC substrates/ ERK
1.5
1
0.5
0
3 6 18 24
Time (h)

Figure 15. HG does not affect the phosphorylation levels of ERK1/2, AMPK, or PKC substrates. Human MDMs were exposed to 5 mM (NG) or 25 mM (HG) glucose for 3-24 hours. Equal amounts of solubilized protein were separated by SDS-PAGE and immunoblotted with the indicated antibodies. ERK1/2 (A and C) and AMPK (B) serve as loading controls. Immunoblots from one donor sample are shown. Densitometric data from 4 separate donor samples, normalized to loading control, are graphically presented as means ± S.E.M. Each donor sample was assessed in an individual experiment.

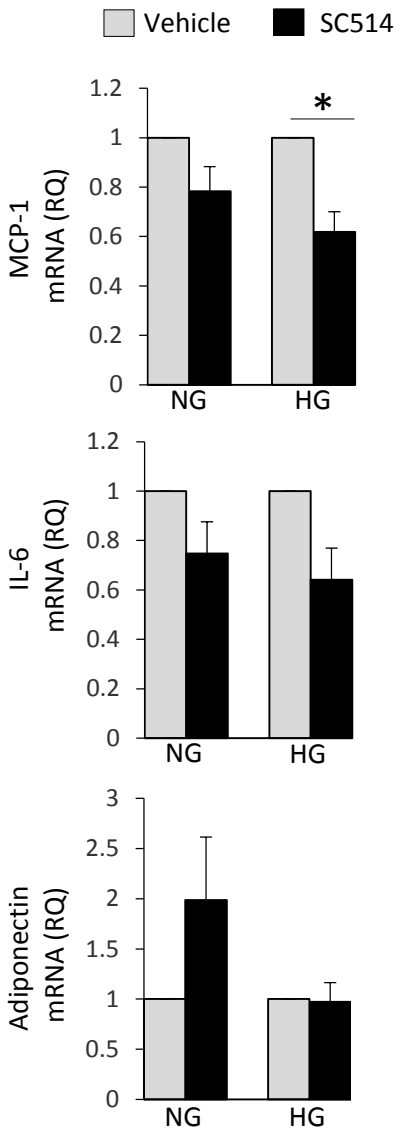
Vehicle
SC514
MCP-1 mRNA (RQ)
1.2
1
0.8
0.6
0.4
0.2
0
*
NG
HG
IL-6 mRNA (RQ)
1.2
1
0.8
0.6
0.4
0.2
0
NG
HG
Adiponectin mRNA (RQ)
3
2.5
2
1.5
1
0.5
0
NG
HG

Figure 16. Sc-514 suppresses HG-MacCM-induced MCP-1 mRNA expression in human differentiated adipocytes. MacCM was generated over 24 hours in 5 mM glucose (NG) or 25 mM glucose (HG) in the presence of DMSO (vehicle) or 1 µM sc-514. Human abdominal subcutaneous preadipocytes were induced to differentiate for 14 days using these various media. RNA was isolated, then quantified by-real time PCR, using indicated primers. Levels were normalized to endogenous 18S RNA, and expressed as a function of the respective vehicle MacCM condition. Results are expressed as the means ± S.E.M. of 4 separate experiments, where each donor sample was assessed in an individual experiment. * denotes $p < 0.05$ between indicated pair, as assessed by two-way ANOVA with Tukey post-hoc tests. RQ stands for relative quantification.

4. DISCUSSION

4.1 Effect of HG on human adipogenesis

As explained earlier (Section **1.4**), AT remodeling is a dynamic process that includes two distinct mechanisms, hyperplasia and hypertrophy. Hyperplastic (i.e., intact adipogenesis) and hypertrophic (i.e., reduced adipogenesis) AT expansion contributes significantly to developing metabolically healthy versus metabolically unhealthy obesity, respectively (Klöting et al., 2010). About 80-90% of individuals with diabetes are obese (Lau et al., 2013); the effects of high glucose conditions on adipogenesis are not fully understood, with only a few reports in the literature. To address this, I measured differentiation parameters under NG versus HG conditions.

Using an *in vitro* human primary model system I showed that HG does not affect adipogenesis, as assessed by TG accumulation and by protein expression of several standard adipogenic genes. These data are consistent with Collins *et al*. who reported no difference in TG accumulation when human preadipocytes were differentiated in 17.5 mM glucose versus 5 mM glucose (Collins et al., 2011). Another group, using the human SGBS preadipocyte cell line, also saw no effect of HG on adipogenesis as assessed by TG accumulation (Verrijn Stuart et al., 2012). SGBS preadipocytes, as noted in Section **1.7.1** have an unknown genetic abnormality and may not accurately represent primary human preadipocytes. These two reports were not as comprehensive as my studies. They were limited to assessment of TG accumulation, and did not evaluate expression of adipogenic genes. In contrast, others have shown that HG (25 mM) enhances the differentiation of primary human preadipocytes compared to NG, as assessed by adipogenic gene expression. However, their experimental approach was quite different, in that they performed their studies in the absence of usual

differentiation inducers of dexamethasone, IBMX, and a PPARγ ligand. Therefore, the actual rates of differentiation were very low (Aguiari et al., 2008). Overall, my findings indicate that hyperglycemic conditions do not affect adipogenesis according to standard markers of differentiation. The question that remained was whether HG conditions during differentiation exerted other effects on the resulting adipocytes.

4.2 Effect of HG on ChREBP expression

Since ChREBP (discussed in section **1.7.2**) is a glucose sensing transcription factor in adipocytes, it was possible that it might be affected by HG conditions. In particular, the regulation of the recently identified ChREBP-β isoform was of interest (Herman et al., 2012). Changes in expression of ChREBP as a function of differentiation were first analyzed in NG versus HG conditions. ChREBP-α mRNA expression rapidly increased with differentiation and to the same extent under NG or HG conditions. This is consistent with one study that reported ChREBP mRNA increased during the differentiation of human preadipocyte (from VAT and SAT) in NG conditions (Hurtado del Pozo et al., 2011). They used commercially designed probes for ChREBP to quantify ChREBP mRNA. However, since the nucleotide sequence of their probe was not provided, it is unclear whether the mRNA they measured was only ChREBP-α, or total ChREBP (ChREBP-α and -β together). They did not assess HG conditions on ChREBP gene expression during adipogenesis. Recently, ChREBP-α mRNA expression was reported to increase in mouse 3T3-L1 adipocytes that were differentiated under HG (25 mM) conditions. These studies were not performed in NG conditions; therefore direct comparison of HG versus NG cannot be made (Witte et al., 2015).

My studies revealed that upon differentiation, ChREBP-β mRNA increased to a greater extent under HG versus NG conditions. This is the first time ChREBP-β specifically has been assessed in human adipocytes in this context. In contrast, ChREBP-β gene expression was nearly undetectable in mouse 3T3-L1 adipocytes differentiated in HG (25 mM) conditions. Studies in NG conditions were not performed, preventing further comparisons (Witte et al., 2015). There may be a species-dependent differences in the regulation of ChREBP-β gene expression during adipogenesis.

Analysis of ChREBP-α protein were detected in cytoplasmic and nuclear fractions of differentiated human adipocytes under NG and HG conditions. Total levels and relative distribution of ChREBP-α were similar in both conditions. Herman *et al*. reported that ChREBP-α protein is predominantly cytosolic (Herman et al., 2012), but assessed this with an artificial system by transfecting HEK392T cells with Flag-tagged ChREBP-α. With this system, they reported no effect of HG in the levels of ChREBP-α in the cytoplasm or nucleus. Their conclusions were drawn based on qualitative (immunofluorescent) analysis with no quantification of ChREBP-α protein levels (Herman et al., 2012).

ChREBP-β (under NG and HG conditions) was only detected in the nuclear fraction of differentiated adipocytes in my studies, similar to what was reported by Herman *et al*. (Herman et al., 2012). It is known that the N-terminus (including the low-glucose inhibitory domain; LID) deletion of ChREBP-α leads to increased nuclear localization and enhanced transcriptional activity. This is consistent with the truncated isoform ChREBP-β, which also lacks LID, being predominantly nuclear and having higher activity than ChREBP-α (Li et al., 2008; Herman et al., 2012).

The nuclear ChREBP-β protein level was significantly higher in adipocytes that were differentiated under HG versus NG conditions, in agreement with the HG-induced enhancement of ChREBP-β at the mRNA level. It is not entirely clear what regulates the transcription of ChREBP-β in the adipocyte. It has been suggested that the induction of ChREBP-β gene expression follows a two-step mechanism. First, glucose metabolite(s) activate ChREBP-α, which in turn undergoes nuclear localization and induces the transcription of ChREBP-β (Herman et al., 2012). However, the levels of nuclear ChREBP-α protein were similar in the adipocytes under HG versus NG conditions, suggesting nuclear localization of ChREBP-α was not affected. This suggests that the higher level of ChREBP-β expression in differentiated adipocytes under HG conditions may be a result of enhanced ChREBP-α activity. The current literature, based on studies using hepatocytes, suggests the nuclear localization of ChREBP (later recognized to be the ChREBP-α isoform) is mediated by initial dephosphorylation (at Ser 196) by PP2A (Kawaguchi et al., 2001). Once ChREBP localizes to the nucleus, a second PP2A mediated dephosphorylation (Thr 666) occurs, which allows binding of ChREBP to ChoRE binding site (Kawaguchi et al., 2001; Postic et al., 2007). This suggests that translocation and activation of ChREBP-α can be de-coupled. Therefore, it would be useful to assess the phosphorylation levels of nuclear ChREBP-α under HG conditions to gain more insight into its activation state. In addition to dephosphorylation, other glucose-dependent modifications of nuclear ChREBP-α have been reported that enhance its activity including acetylation and O-GlcNAcylation (Bricambert et al., 2010; Guinez et al., 2011). These processes should also be addressed in human adipocytes in future studies, and may shed light on how nuclear ChREBP-α is regulated.

I investigated whether the HG-induced increase in ChREBP-β affected downstream target genes in the differentiated human adipocytes but mRNA expression of several lipogenic genes that are ChREBP targets, including ACC1, SCD, and FAS (Eissing et al., 2013) were not altered. The reason for a lack of a response is unknown, but it is consistent with the absence of a change in TG accumulation that was observed during adipogenesis with HG compared to NG. One possibility may be that even if the protein expression of ChREBP-β was enhanced by HG, excess ChREBP-β alone may not be sufficient to carry out its downstream transcriptional activities of these lipogenic target genes. As described in Section **1.7.2**, ChREBP transcriptional activity is highly dependent on transcriptional partner Max-like protein X (Mlx) (Filhoulaud et al., 2013). In hepatocytes, dominant negative form of Mlx (unable to bind to DNA but can still interact with ChREBP), can blunt 60% of glucose-responsive genes in HG conditions; and FAS, SCD1, and ACC were among these genes (Ma et al., 2006; Ma et al., 2005).

In addition to the lipogenic genes, a ChoRE sequence also occurs in the GLUT4 gene promoter region (Ma et al., 2006). Enhancement of GLUT4 mRNA expression in adipocytes differentiated in HG versus NG was observed. The fold-increase of GLUT4 mRNA expression was positively correlated with ChREBP-β mRNA fold-increase, suggesting that there may be a link between ChREBP-β and GLUT4 mRNA expression. A higher level of ChREBP-β expression in AT is associated with improved systemic insulin sensitivity (Eissing et al., 2013). Both VAT and SAT from obese and obese-diabetic subjects with HOMA-IR scores of 4.6 and 8.6 respectively, exhibited reduced ChREBP-β and GLUT4 gene expression, (Eissing et al., 2013; Garvey et al., 1991). These data suggest increased ChREBP-β in the adipocyte promotes whole body insulin sensitivity, although the

mechanism by which this occurs has not been identified. Weight loss led to enhanced systemic insulin sensitivity, increased GLUT4, and lipogenic mRNA expression in SAT of obese patients (Eissing et al., 2013). They also observed an increase in ChREBP-α mRNA; however ChREBP-β mRNA was below detection levels.

Furthermore, a class of endogenous lipids (palmitic-acid-9-hydroxy-stearicacid; 9-PAHSA) with anti-diabetic and anti-inflammatory effects was enhanced in the AT of adipocyte specific GLUT4 overexpressing mice with upregulated ChREBP expression (Yore et al., 2014). These effects were blunted in mice lacking ChREBP, suggesting that these lipids may be involved in ChREBP-β mediated increased insulin sensitivity (Yore et al., 2014).

HG is known to inhibit insulin signaling and insulin-stimulated glucose uptake in adipocytes (Gao et al., 2010; Buren et al., 2003) although this was not directly assessed in my thesis. It is possible the higher level of GLUT4 mRNA expression, related to the increase in ChREBP-β , could potentially be a compensatory (protective) response against these negative effects of HG. My study is limited in that I have not determined if GLUT4 protein is also elevated, and whether its translocation by insulin is altered.

4.3 Effect of HG-MacCM on adipogenesis

Effects of macrophages on preadipocytes are of interest, given the increase in adipose tissue macrophages (derived from peripheral blood monocytes) that occurs in the obese state (Weisberg et al., 2003). Various preadipocyte and macrophage cell lines have been used to demonstrate an anti-adipogenic effect (Constant et al., 2006; Lacasa et al., 2007; Keophiphath et al., 2009; Ide et al., 2011). Studies on human primary MDMs and primary

human preadipocytes are less frequent, and the effect of HG on these interactions has not been investigated.

My data show that HG-MacCM inhibits some components of the adipocyte differentiation program more severely than does NG-MacCM. Inhibition of TG accumulation and PPARγ protein levels occurred only with HG-MacCM, while FAS was suppressed in NG- and HG-MacCM. Another group reported that FAS activity in 3T3-L1 mouse differentiated adipocytes was reduced upon endocytosis of a factor released by macrophages called apoptosis inhibitor of macrophage (AIM). AIM had no effect on PPARγ mRNA expression in these mature adipocytes (Kurokawa et al., 2010). The expression level of FAS was not measured; therefore it is not clear whether the reduced FAS activity was due to lower FAS expression. AIM exposure to 3T3-L1 preadipocytes during adipogenesis however, led to reduced PPARγ mRNA expression (Kurokawa et al., 2010). Using a FAS inhibitor, C57, one study showed reduced PPARγ mRNA expression at an early and late stage of adipogenesis (Liu et al., 2004). It has been suggested that reduced FAS activity may reduce the synthesis of lipids that may act as endogenous PPARγ ligands (Farmer, 2006). However, in my studies, reduced FAS expression under NG-MacCM did not affect PPARγ expression. It may be that other regulators are involved in the relationship between FAS and PPARγ in human primary cell cultures

An anti-adipogenic effect of MDMs on human preadipocytes was previously reported (Lacasa et al., 2007). Their experimental protocol differed from mine in several ways. They placed MDMs in RPM1 at a glucose concentration of 11 mM for 24 hours, and then added 1 volume of MacCM (RPMI; 11 mM glucose) to 3 volumes of preadipocyte medium (DMEM: F12; 17 mM glucose) containing adipogenic inducers, resulting in a final

concentration of 15.5 mM glucose. Another difference was that this group pooled MacCM from several donors, compared to my approach of assessing MacCM from individual donors. Since I used MacCM from individual donors, it is possible that effect of the MacCM across different experiments may have contributed to some of the variation I observed. With their protocol, TG accumulation was reduced, as was mRNA expression of adipogenic markers (PPARγ, C/EBPα, SREBP-1c, FAS, CD36, leptin, adiponectin, but not C/EBPβ) (Lacasa et al., 2007). Although these findings partially support my data in respect to the effects of MacCM on adipogenesis, direct comparisons cannot be made since the generation of MacCM were in different glucose concentrations.

I assessed the inflammatory profile of adipocytes differentiated in HG- versus NG-MacCM. My data indicate HG-MacCM is a more potent inducer of adipocyte inflammation than NG-MacCM, resulting in higher levels of IL-6 and MCP-1 mRNA, as well as lower levels of ant-inflammatory adiponectin mRNA. However, since protein and mRNA levels do not always match, a limitation of my thesis is that the corresponding protein levels are not known (Vogel and Marcotte, 2012).

This pro-inflammatory action of HG-MacCM is comparable to what has been observed by others using MacCM generated from LPS-treated MDMs (Lacasa et al., 2007). In this study, MacCM generated in 11 mM glucose did not elicit inflammatory responses in the differentiated adipocytes. To achieve a pro-inflammatory response in the adipocyte, MacCM was required to be generated with LPS treated MDMs. In my data, HG alone was sufficient in activating macrophages and could potentially mimic the effects of LPS treatment.

Another interpretation for the elevated pro-inflammatory response might relate to the stage of differentiation of the preadipocytes undergoing adipogenesis in the HG-MacCM. Our lab has shown that human preadipocyte express more IL-6 (Antunes et al., 2006) and MCP-1 (not published) mRNA than adipocytes. The reduction of PPARγ protein levels in HG-MacCM may have resulted in more preadipocyte like cell culture, which could have contributed to increases in IL-6 and MCP-1 and the decrease in adiponectin.

4.4 Identifying anti-adipogenic factors secreted by MDMs upon HG exposure

The question of what factors macrophages release when they respond to HG has been examined previously in the context of atherosclerosis. Effects on endothelial cell adhesion markers (E-selectin) and on the expression of lipid-related and growth factors receptors have been observed, and they could play a role in plaque progression (Chen et al., 2011; Li et al., 2004; Fukuhara-Takaki et al., 2005; Inaba et al., 1996; Moheimaniet al., 2011). With HG treatment of MDMs in my studies, there was a small increase in mRNA levels of ICAM-1 and ICAM-3; closely related cell adhesion molecules involved in cell inflammation responses (Fawcett et al., 1992). HG exposure to MDMs however, did not affect the mRNA expression of pro-inflammatory markers, IL-1β, MCP-1, and TNFα. Consistent with my findings, others reported that HG alone is insufficient to induce IL-1β mRNA expression, and only did so when combined with high palmitate concentrations (Kratz et al., 2014). Although another study found higher TNFα protein levels in HG-MacCM, the degree of the elevation was not provided (Sartippour et al., 1998). Although the expression of inflammatory genes was not increased by HG, there was a substantial reduction in PPARγ protein levels in MDMs exposed to HG compared to NG. In the macrophage, PPARγ acts an anti-inflammatory factor that inhibits cell activation (Ricote et al., 1998). A reduction in

PPARγ in human MDMs has been seen by others at the mRNA level (Sartippour et al., 2000; Ni et al., 2010). Whereas others reported that HG exposure to human MDMs did not elicit any changes in PPARγ mRNA expression (Senanayake et al., 2007). These differences may possibly be due to differences in experimental conditions, such as glucose exposure times.

My investigations did not identify a cytokine(s) released from macrophages that may be responsible for the anti-adipogenic effect of HG-MacCM. It should be noted that the scope of my search has not been exhaustive. It remains possible to identify potential cytokines by other means, such as performing polyA RNA sequencing or secretomic analysis.

It is possible that the HG-mediated macrophage secreted factor(s) may not be a cytokine(s). Other candidates could be bioactive lipids such as eicosanoids or platelet activating factor (Nathan, 1987). For example, exposure of BMDM to HG (25 mM) led to increased production of pro-inflammatory prostaglandin (PG) E_2 and PGD_2 (Kanter et al., 2012). In particular, PGE_2 can suppress adipogenesis by attenuating PPARγ function (Fujimori, 2012). PGE_2 can also inhibit adipocyte production of adiponectin (Hardwick et al., 2014). Further studies should investigate the levels of bioactive lipids that may be produced by MDMs under HG versus NG conditions, and assess whether these factors are required for the HG-MacCM effects on preadipocytes.

It is also possible that factors in HG-MacCM might be stimulating PG production by preadipocytes. PGs are produced by preadipocytes and the profile of the PGs depends on the microenvironment of the cell (Michaud et al., 2014A). For example, $PGF_{2\alpha}$, an anti-adipogenic PG, is synthesized by SAT and VAT preadipocytes upon pro-inflammatory stimulation (Michaud et al., 2014B). Furthermore, production of this PG was stimulated

when the polyol pathway was increased. Therefore, in my study, it is possible that HG-induced macrophage secreted factors may increase anti-adipogenic PGs such as $PGF_{2\alpha}$ in preadipocytes.

Another group of potential macrophage secreted factors that should be evaluated in the future are microRNAs (miRNAs), which are small noncoding RNAs that can modulate the expression of many target genes (Liu and Abraham, 2013). For example, stimulated RAW 264.7 macrophages secrete more miR-155 compared to unstimulated cultures, in a time-dependent manner (Bala et al., 2011). Overexpression of miR-155 in preadipocytes partially inhibited the differentiation of 3T3-L1 preadipocytes, assessed by PPARγ protein levels and TG accumulation (Liu et al., 2011). This suggest miRNAs may affect adipogenesis; however studies have not yet shown if inhibiting miRNAs in macrophages would alter the effects of MacCM on adipogenesis.

4.5 Signaling pathways activated by HG in MDMs

Hyperglycemia can mediate cellular responses through five main mechanisms: (1) aberrant activation of PKC isoforms which are upstream of IKK, (2) increased polyol pathway, (3) increased intracellular AGE (advanced glycation end products) formation, (4) increased RAGE (receptor for AGE) expression, and (5) hyperactivity of the hexosamine pathway (Giacco and Brownlee, 2010).

In MDMs, HG increased ROS production and induced PKC activation (Li et al., 2004; Inaba et al., 1996). These HG-mediated signaling events are positioned upstream of IKK. HG stimulated IKKβ phosphorylation and IκBα degradation in human MDMs, and this could be linked to the reduction of PPARγ protein levels in MDMs exposed to HG versus NG that I observed. Studies have suggested a mechanism involving the activation of IKK

(due to TNFα stimulation) followed by degradation of IκBα and suppression of PPARγ activity in HEK293 cells. They showed PPARγ activity was reduced due to increased nuclear export of PPARγ mediated by histone deacetylase 3 (HDAC3) when IκBα was degraded (Gao et al., 2006). Nuclear export of PPARγ may lead to its proteolytic degradation.

I determined whether HG-induced IKKβ activation in MDMs was required for HG-MacCM to augment gene expression associated with adipocyte inflammation. Sc-514, a molecule that blocks IKKβ action by inhibiting the phosphorylation/degradation of IκBα (Kishore et al., 2003), partly reduced the stimulatory effect of HG-MacCM on MCP-1 mRNA expression in differentiated adipocytes. This suggests HG-induced IKKβ activation is needed for MDMs to produce and release factors into HG-MacCM that can enhance MCP-1 expression in differentiated adipocytes. There were no effects of sc-514 on IL-6 or adiponectin levels, suggesting HG-induced pathways in MDMs other than IKKβ are operating. This work is limited in that activation of NF-κB via IKK phosphorylation was not determined, but should be a subject to future work. Also, it should be noted that pharmacological inhibitors have inherent limitations of specificity. For example, although sc514 is widely used as an inhibitor of IKK, it has been shown to also inhibit other kinases (eg. dual specificity tyrosine-phosphorylation-regulated kinase 3 and Aurora B), although more weakly than IKKβ (Bain et al., 2007).

I also examined other potential signaling pathways in MDMs that might have been activated by HG which could lead to release of pro-inflammatory factors. Using ERK1/2 and PKCβ_2 inhibitors, one study reversed HG (30 mM)-induced induction of LOX-1 expression in MDMs. HG-mediated increase in LOX-1 may lead to increased uptake of oxidised LDL

in macrophages. A higher uptake of oxidized LDL activates and induces pro-inflammatory cytokine responses in macrophages (Janabi et al., 2000). I attempted to assess whether ERK1/2 and PKCβ_2 are activated by HG in MDMs, but no changes in ERK1/2 phosphorylation or cPKC substrate phosphorylation were observed in MDMs treated with HG versus NG in my studies.

Other hyperglycemia-stimulated pathways (listed above) might lead MDMs to secrete factors that promote adipocyte inflammation. The HG conditioning period used in this thesis (24 hours) was too short to allow AGE or RAGE formation (Brownlee et al., 1984). In the polyol pathway, glucose is enzymatically reduced to sorbitol by aldose reductase using NADPH as a co-factor in the reaction. Sorbitol is in turn oxidized to fructose by sorbitol dehydrogenase, with NAD+ reduced to NADH. A decrease in cytosolic NADPH and an increase in cytosolic NADH/NAD+ promotes ROS production and oxidative stress (Giacco and Brownlee, 2010). The hexosamine pathway leads to increased intracellular glycosylation of transcription factors, such as Sp1, which may alter their responses and lead to changes in the release of macrophage secreted factors (Giacco and Brownlee, 2010).

AMPK is a known energy sensing protein complex involved in lipid metabolism (Kahn et al., 2005). It can be activated when cellular AMP/ATP ratio rise such as the cases of low glucose. Although HG has been shown to decrease AMPK activity in myocytes and hepatocytes, there are no reports on whether this occurs in macrophages (Ruderman and Prentki, 2004). When MDMs were exposed to HG, AMPK phosphorylation levels after 6 hours were reduced, although this reduction did not reach statistical significance-perhaps due to variability between donor responses. The variability may be due in part to sex differences, as AMPK activation was inhibited more robustly in MDMs from two male donors than the

two female donors. Indeed, a sex specific regulation of AMPK activation was shown in skeletal muscle; following exercise, AMPK activity increased significantly with a concomitant increase in the AMP/ATP ratio in men but not women (Roepstorff et al., 2006).

4.6 Proposed model

Adipogenesis is not altered by hyperglycemic conditions; preadipocytes differentiate similarly under HG (red box) versus NG (blue box) conditions (**Figure 17A**). HG conditions inhibit insulin signaling and insulin stimulated glucose uptake in differentiated adipocyte (Gao et al., 2010; Buren et al., 2003). Although preadipocytes differentiated to the same extent, adipocytes differentiated in HG conditions expressed more ChREBP-β. It is unknown if ChREBP-β is helping retain insulin sensitivity in the adipocytes exposed to HG by increasing GLUT4 expression (**Figure 17B**).

Some macrophage secreted factors generated under HG conditions alter adipogenesis more severely than those generated under NG. Also, HG-mediated macrophage secreted factors promote a more pro-inflammatory phenotype in differentiated adipocytes. These macrophage secreted factors remain unknown. Reduced adipogenic capacity and inflammatory adipocyte phenotype are associated with hypertrophied and dysfunctional AT expansion (Klöting et al., 2010). As such, HG conditions influencing the interactions between macrophages and preadipocyte may lead to loss of healthy functional AT (**Figure 17C**).

In MDMs, HG leads to ROS production and aberrant PKC activation (Li et al., 2004; Inaba et al., 1996). These signaling events are upstream of IKK activation leading to subsequent degradation of IκBα and nuclear translocation of pro-inflammatory transcription

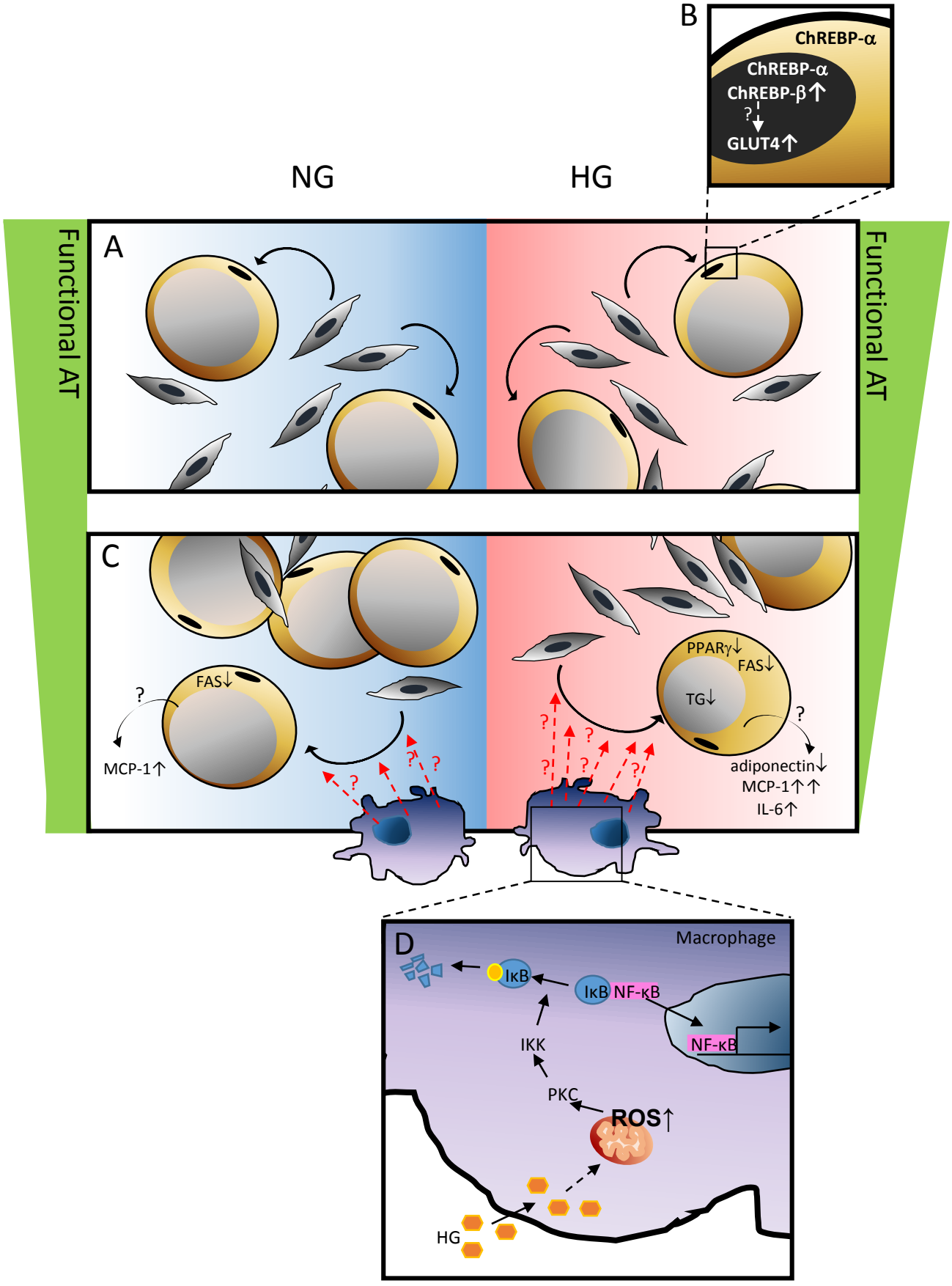
B
ChREBP-α
ChREBP-α
ChREBP-β↑
?
GLUT4↑
NG
HG
Functional AT
Functional AT
A
C
FAS↓
?
MCP-1↑
PPARγ↓
FAS↓
TG↓
?
adiponectin↓
MCP-1↑↑
IL-6↑
D
Macrophage
IκB
IκB
NF-κB
NF-κB
IKK
PKC
ROS↑
HG

Figure 17. Proposed model depicting the effects of HG and HG-exposed macrophage secreted factors on human adipogenesis. (A) Preadipocytes differentiate into mature adipocytes similarly under normal glucose (NG) versus high glucose (HG) conditions. (B) Adipocyte differentiated under HG conditions express higher levels of ChREBP-β. The increase in ChREBP-β may account for the increased GLUT4 mRNA expression noted in adipocytes exposed to HG. Whether these adipocytes are more sensitive to insulin remains to be determined. (C) Macrophages exposed to HG release factors that lead to 1) partial inhibition of adipogenesis, and 2) a shift to a more pro-inflammatory pattern of adipocyte gene expression. (D) HG activates IKKβ in the macrophage, and this activation is partially required for the ability of conditioned medium from HG-exposed macrophages to promote the inflammatory effects described in (C). IKKβ is thought to be acting via NF-κB, but this has not been confirmed.

factor, NF-κB (**Figure 17D**). HG-mediated activation of IKK led to macrophage secreted factors that partially promoted inflammatory responses in adipocytes.

CONCLUSIONS

AT remodeling (hyperplastic or hypertrophic expansion) plays an important role in adipose tissue function (Sun et al., 2011). Impaired adipogenic capacity may lead to dysfunctional, hypertrophic AT expansion, which is associated with inflammation and insulin resistance (Klöting et al., 2010). Adipogenesis is an important part of AT remodeling; however the effects of high glucose conditions on adipogenesis have not been clearly investigated. Using a human primary model system, I showed that HG alone does not affect adipogenesis. The HG-induced differentiated adipocytes have higher levels of mRNA and protein expression of the glucose sensing transcription factor ChREBP-β. Lipogenic gene targets were unaffected, but GLUT4 mRNA expression was increased. More work is needed to determine if GLUT4 protein and its insulin-stimulated translocation is altered.

Macrophages are an important component of AT remodeling in obesity (Sun et al., 2011). A positive relationship exists between adipocyte size and ATM content in AT of rodents and humans, suggesting a link between hypertrophied AT expansion and macrophage infiltration (Weisberg et al., 2003). It was previously shown by us and by others that MacCM attenuates adipogenesis; a component of AT remodeling that may tip the balance between healthy hyperplastic to unhealthy hypertrophic expansion (Constant et al., 2006; Lacasa et al., 2007; Torres-Leal and Fonseca-Alaniz, 2012). My work re-examined these finding under a diabetic setting and using for the first time, human primary preadipocytes and human primary MDMs. My data highlights an important interaction between HG-mediated macrophage secreted factors and increased adipocyte inflammation as

well as partially reduced adipogenic capacity, both of which are associated with hypertrophic AT remodeling leading to dysfunctional AT (Klöting et al., 2010).

My studies indicate that HG augments the effect of MacCM to inhibit adipocyte differentiation and to increase inflammation. They raise the possibility that macrophage interactions with preadipocytes and adipose tissue remodeling *in vivo* may be modulated in the presence of hyperglycemia (**Figure 17**). It should be noted also that my studies and published work by others were all performed in an *in vitro* cell culture conditions which can underestimate the complexity of adipogenesis part of AT remodelling *in vivo*. Future studies should aim to identify factors released by human macrophages under HG versus NG conditions that influence preadipocyte responses, and whether these factors can be targeted for a therapeutic potential.

REFERENCES

Agha-Jaffar, R., Oliver, N., Johnston, D., and Robinson, S. (2016). Gestational diabetes mellitus: does an effective prefention strategy exist? Nat. Rev. Endocrinol. 2016 Jun 24 doi: 10.1038/nrendo.2016.88. [Epub ahead of print].

Aguiari, P., Leo, S., Zavan, B., Vindigni, V., Rimessi, A., Bianchi, K., Franzin, C., Cortivo, R., Rossato, M., Vettor, R., Abatangelo, G., Pozzan, T., Pinton, P., and Rizzuto, R. (2008). High glucose induces adipogenic differentiation of muscle-derived stem cells. Proc. Natl. Acad. Sci. U. S. A. *105*, 1226-1231.

Ahl, S., Guenther, M., Zhao, S., James, R., Marks, J., Szabo, A., and Kidambi, S. (2015). Adiponectin levels differentiate metabolically healthy vs unhealthy among obese and nonobese white individuals. J. Clin. Endocrinol. Metab. *100*, 4172-4180.

Antunes, T.T., Gagnon, A., Chen, B., Pacini, F., Smith, T.J., and Sorisky, A. (2006). Interleukin-6 release from human abdominal adipose cells is regulated by thyroid-stimulating hormone: effect of adipocyte differentiation and anatomic depot. Am. J. Physiol. Endocrinol. Metab. *290*, E1140-1144.

Arden, C., Tudhope, S.J., Petrie, J.L., Al-Oanzi, Z.H., Cullen, K.S., Lange, A.J., Towle, H.C., and Agius, L. (2012). Fructose 2, 6-bisphosphate is essential for glucose-regulated gene transcription of glucose-6-phosphatase and other ChREBP target genes in hepatocytes. Biochem. J. *443*, 111-123.

Arner, E., Westermark, P.O., Spalding, K.L., Britton, T., Ryden, M., Frisen, J., Bernard, S., and Arner, P. (2010). Adipocyte turnover: relevance to human adipose tissue morphology. Diabetes. *59*, 105-109.

Atlantis, E., and Baker M. (2008). Obesity effects on depression: systematic review of epidemiological studies. Int. J. Obes. (Lond). *32*, 881-891.

Bain, J., Plater, L., Elliott, M., Shpiro, N., Hastie, C.J., McLauchlan, H., Klevernic, I., Arthur, J.S., Alessi, D.R., and Cohen, P. (2007). The selectivity of protein kinase inhibitors: a further update. Biochem. J. *408*, 297-315.

Bala, S., Marcos, M., Kodys, K., Csak, T., Catalano, D., Mandrekar, P., and Szabo, G. (2011). Up-regulation of microRNA-155 in macrophages contributes to increased tumor necrosis factor {alpha} (TNF{alpha}) production via increased mRNA half-life in alcoholic liver disease. J. Biol. Chem. *286*, 1436-1444.

Bilkovski., R., Schulte, D.M., Oberhauser, F., Mauer, J., Hampel, B., Gutschow, C., Krone, W., and Laudes, M. (2011). Adipose tissue macrophages inhibit adipogenesis of mesenchymal precursor cells via wnt-5a in humans. Int. J. Obes. (Lond). *35*, 1450-1454.

Bjorbaek, C., and Kahn, B.B. (2004). Leptin signaling in the central nervous system and the periphery. Recent. Prog. Horm. Res. *59*, 305-331.

Blüher, M. (2010). The distinction of metabolically 'healthy' from 'unhealthy' obese individuals. Curr. Opin. Lipidol. *21*, 38-43.

Bradley, R.L., Fisher, F.F., and Maratos-Flier, E. (2008). Dietary fatty acids differentially regulate production of TNF-alpha and IL-10 by murine 3T3-L1 adipocytes. Obesity. *16*, 938-944.

Bremer, A.A., Mietus-Snyder, M., and Lustig, R.H. (2012). Toward a unifying hypothesis of metabolic syndrome. Pediatrics. *129*, 557-570.

Bricambert, J., Miranda, J., Benhamed, F., Girard, J., Postic, C., and Dentin, R. (2010). Salt-inducible kinase 2 links transcriptional coactivator p300 phosphorylation to the prevention of ChREBP dependent hepatic steatosis in mice. J. Clin. Invest. *120*, 4316-4331.

Brownlee, M., Vlassara, H., and Cerami, A. (1984). Nonenzymatic glycosylation and the pathogenesis of diabetic complications. Ann. Intern. Med. *101*, 527-537.

Buren, J., Liu, H.X., Lauritz, J., and Eriksson, J.W. (2003). High glucose and insulin in combination cause insulin receptor substrate-1 and -2 depletion and protein kinase B desensitisation in primary cultured rat adipocytes: possible implications for insulin resistance in type 2 diabetes. Eur. J. Endocrinol. *148*, 157-167.

Calle, E.E., Rodriguez, C., Walker-Thurmond, K., and Thun, M.J. (2003). Overweight, obesity, and mortality from cancer in a prospectively studied cohort of US adults. N. Engl. J. Med. *348*, 1625-1638.

Canadian Diabetes Association Clinical Practice Guidelines Expert Committee. Canadian Diabetes Association (2013). Clinical Practice Guidelines for the Prevention and Management of Diabetes in Canada. Can. J. Diabetes. *37*, S1-S212.

Canadian Diabetes Cost Model. (2015). Estimated diabetes statistics in Canada.

Cannon, B., Hedin, A., and Nedergaard, J. (1982). Exclusive occurrence of thermogenin antigen in brown adipose tissue. FEBS. Lett. *150*, 129-132.

Cao, Z., Umek, R.M., and McKnight, S.L. (1991). Regulated expression of three C/EBP isoforms during adipose conversion of 3T3-L1 cells. Genes. Dev. *5*, 1538-1552.

Chang, Y.C., Sheu, W.H., Chien, Y.S., Tseng, P.C., Lee, W.J., and Chiang, A.N. (2013). Hyperglycemia accelerates ATP-binding cassette transporter A1 degradation via an ERK-dependent pathway in macrophages. J. Cell. Biochem. *114*, 1364-1373.

Chen, T.C., Chien, S.J., Kuo, H.C., Huang, W.S., Sheen, J.M., Lin, T.H., Yen, C.K., Sung, M.L., and Chen, C.N. (2011). High glucose-treated macrophages augment E-selectin expression in endothelial cells. J. Biol. Chem. *286*, 25564-25573.

Chuang, C.C., Yang, R.S., Tsai, K.S., Ho, F.M., and Liu, S.H. (2007). Hyperglycemia enhances adipogenic induction of lipid accumulation: involvement of extracellular signal-regulated protein kinase 1/2, phosphoinositide 3-kinase/Akt, and peroxisome proliferator-activated receptor gamma signaling. Endocrinology. *148*, 4267-4275.

Cinti, S., Mitchell, G., Barbatelli, G., Murano, I., Ceresi, E., Faloia, E., Wang, S., Fortier, M., Greenberg, A.S., and Obin, M.S. (2005). Adipocyte death defines macrophage

localization and function in adipose tissue of obese mice and humans. J. Lipid. Res. *46*, 2347-2355.

Collier, J.J., Zhang, P., Pedersen, K.B., Burke, S.J., Haycock, J.W., and Scott, D.K. (2007). c-Myc and ChREBP regulate glucose-mediated expression of the L-type pyruvate kinase gene in INS-1-derived 832/13 cells. Am. J. Physiol. Endocrinol. Metab. *293*, E48-E56.

Collins, J.M., Neville, M.J., Pinnick, K.E., Hodson, L., Ruyter, B., van Dijk, T.H., Reijngoud, D.J., Fielding, M.D., and Frayn, K.N. (2011). De novo lipogenesis in the differentiating human adipocyte can provide all fatty acids necessary for maturation. J. Lipid. Res. *52*, 1683-1692.

Constant, V.A., Gagnon, A., Yarmo, M., and Sorisky, A. (2008). The antiadipogenic effect of macrophage-conditioned medium depends on ERK1/2 activation. Metabolism. *57*, 465-472.

Constant, V.A., Gagnon, A., Yarmo, M., and Sorisky, A. (2008). The antiadipogenic effect of macrophage-conditioned medium depends on ERK1/2 activation. Metabolism. *57*, 465-472.

Cypess, A.M., Lehman, S., Williams, G., Tal, I., Rodman, D., Goldfine, A.B., Kuo, F.C., Palmer, E.L., Tseng, Y.H., Doria, A., Kolodny, G.M., and Kahn, C.R. (2009). Identification and importance of brown adipose tissue in adult humans. N. Engl. J. Med. *360*, 1509-1517.

Dalmas, E., Clément, K., and Guerre-Millo, M. (2011). Defining macrophage phenotype and function in adipose tissue. Trends. Immunol. *32*, 307-314.

Danforth, E., Jr. (2000). Failure of adipocyte differentiation causes type II diabetes mellitus? Nat. Genet. *26*, 13.

Decaunes, P., Esteve, D., Zakaroff-Girard, A., Sengenes, C., Galitzky, J., and Bouloumie, A. (2011). Adipose-derived stromal cells: cytokine expression and immune cell contaminants. Methods. Mol. Biol. *702*, 151-161.

Dentelli. P., Barale, C., Togliatto, G., Trombetta, A., Olgasi, C., Gili, M., Riganti, C., Toppino, M., and Brizzi, M.F. (2013). A diabetic milieu promotes OCT4 and NANOG production in human visceral-derived adipose stem cells. Diabetologia. *56*, 173-184.

Dentin, R., Langin, D., and Postic, C. (2012). Hidden variant of ChREBP in fat links lipogenesis to insulin sensitivity. Cell. Metab. *15*, 795-797.

Eissing, L., Scherer, T., Tödter, K., Knippschild, U., Greve, J.W., Buurman, W.A., Pinnschmidt, H.O., Rensen, S.S., Wolf, A.M., Bartelt, A., Heeren, J., Buettner, C., and Scheja, L. (2013). De novo lipogenesis in human fat and liver is linked to ChREBP-β and metabolic health. Nat. Commun. *4*, 1528.

Eligini, S., Brioschi, M., Fiorelli, S., Tremoli, E., Banfi, C., and Colli, S. (2015). Human monocyte-derived macrophages are heterogenous: Proteomic profile of different phenotypes. J. Proteomics. *124*, 112-123.

Eligini, S., Crisci, M., Bono, E., Songia, P., Tremoli, E., Colombo, G.I., and Colli, S. (2013). Human monocyte-derived macrophages spontaneously differentiated in vitro show distinct phenotypes. J. Cell. Physiol. *228*, 1464-1472.

Fajas L1, Auboeuf D, Raspé E, Schoonjans K, Lefebvre AM, Saladin R, Najib J, Laville M, Fruchart JC, Deeb S, Vidal-Puig A, Flier J, Briggs MR, Staels B, Vidal H, Auwerx J. (1997). The organization, promoter analysis, and expression of the human PPARgamma gene. J. Biol. Chem. *272*, 18779-18789.

Farmer, S.R. (2006). Transcriptional control of adipocyte formation. Cell. Metab. *4*, 263-273.

Farooqi, I.S., Keogh, J.M., Yeo, G.S., Lank, E.J., Cheetham, T., and O'Rahilly, S. (2003). Clinical spectrum of obesity and mutations in the melanocortin 4 receptor gene. N. Engl. J. Med. *348*, 1085-1095.

Fawcett, J., Holness, C.L., Needham, L.A., Turley, H., Gatter, K.C., Mason, D.Y., Mason, D.Y., and Simmons, D.L. (1992). Molecular cloning of ICAM-3, a third ligand for LFA-1, constitutively expressed on resting leukocytes. Nature. *360*, 481-484.

Filhoulaud, G., Guilmeau, S., Dentin, R., Girard, J., and Postic, C. (2013). Novel insights into ChREBP regulation and function. Trends. Endocrinol. Metab. *24*, 257-268.

Foufelle, F., Gouhot, B., Pégorier, J.P., Perdereau, D., Girard, J., and Ferré, P. (1992). Glucose stimulation of lipogenic enzyme gene expression in cultured white adipose tissue. A role for glucose 6-phosphate. J Biol Chem. *267*, 20543-20556.

Frayn K.N., Karpe F., Fielding B.A., Macdonald I.A., and Coppack S.W. (2003). Int. J. Obes. Relat. Metab. Disord. *27*, 875-888.

Freemerman, A.J., Johnson, A.R., Sacks, G.N., Milner, J.J., Kirk, E.L., Troester, M.A., Macintyre, A.N., Goraksha-Hicks, P., Rathmell, J.C., and Makowski, L. (2014). Metabolic reprogramming of macrophages: glucose transporter 1 (GLUT1)-mediated glucose metabolism drives a proinflammatory phenotype. J. Biol. Chem. *289*, 7884-7896.

Fujimori, K. (2012). Prostaglandins as PPARγ Modulators in Adipogenesis. PPAR Res. *2012*, 527607.

Fukuhara-Takaki, K., Sakai, M., Sakamoto, Y., Takeya, M., and Horiuchi, S. (2005). Expression of class A scavenger receptor is enhanced by high glucose in vitro and under diabetic conditions in vivo: one mechanism for an increased rate of atherosclerosis in diabetes. J. Biol. Chem. *280*, 3355-3364.

Gagnon, A., and Sorisky, A. (1998). The effect of glucose concentration on insulin-induced 3T3-L1 adipose cell differentiation. Obes. Res. *6*, 157-163.

Gagnon, A., Foster, C., Landry, A., and Sorisky, A. (2013). The role of interleukin 1β in the anti-adipogenic action of macrophages on human preadipocytes. J. Endocrinol. *217*, 197-206.

Gagnon, A., Yarmo, M.N., Landry, A., and Sorisky, A. (2012). Macrophages alter the differentiation-dependent decreases in fibronectin and collagen I/III protein levels in human preadipocytes. Lipids. *47*, 873-880.

Galic S., Oakhill J.S., and Steinberg G.R. (2010). Adipose tissue as an endocrine organ. Mol. Cell. Endocrinol. *316*, 129-139.

Gao, C.L., Zhu, C., Zhao, Y.P., Chen, X.H., Ji, C.B., Zhang, C.M., Zhu, J.G., Xia, Z.K., Tong, M.L., and Guo, X.R. (2010). Mitochondrial dysfunction is induced by high levels of glucose and free fatty acids in 3T3-L1 adipocytes. Mol. Cell. Endocrinol. *320*, 25-33.

Gariepy G., Nitka D., and Schmitz N. (2009). The association between obesity and anxiety disorders in the population: a systematic review and meta-analysis. Int. J. Obes. (Lond). *34*, 407-419.

Garvey, W.T., Maianu, L., Huecksteadt, T.P., Birnbaum, M.J., Molina, J.M., and Ciaraldi, T.P. (1991) Pretranslational suppression of a glucose transporter protein causes insulin resistance in adipocytes from patients with non-insulin dependent diabetes mellitus and obesity. J. Clin. Invest. *87*, 1072-1081.

Ge, Q., Huang, N., Wynn, R.M., Li, Y., Du, X., Miller, B., Zhang, H., and Uyeda, K. (2012). Structural characterization of a unique interface between carbohydrate response element-binding protein (ChREBP) and 14-3-3β protein. J. Biol. Chem. *287*, 41914-41921.

Gesta, S., Tseng, Y.H., and Kahn, C.R. (2007). Developmental origin of fat: tracking obesity to its source. Cell. *131*, 242-256.

Giacco, F., and Brownlee, M. (2010). Oxidative stress and diabetic complications. Circ. Res. *107*, 1058-1070.

Girard, J., Ferré, P., and Foufelle, F. (1997). Mechanisms by which carbohydrates regulate expression of genes for glycolytic and lipogenic enzymes. Annu. Rev. Nutr. *17*, 325-52.

Goossens G.H., and Blaak E.E. (2015). Adipose tissue dysfunction and impaired metabolic health in human obesity: a matter of oxygen?. Front. Endocrinol. *6*, 55.

Gordon, S. (2003). Alternative activation of macrophages. Nat. Rev. Immunol. *3*, 23-35.

Green, H., and Meuth, M. (1974). An established pre-adipose cell line and its differentiation in culture. Cell. *3*, 127-133.

Gregoire, F.M., Smas, C.M., and Sul, H.S. (1998). Understanding adipocyte differentiation. Physiol. Rev. *78*, 783-809.

Guinez, C., Filhoulaud, G., Rayah-Benhamed, F., Marmier, S., Dubuquoy, C., Dentin, R., Moldes, M., Burnol, A.F., Yang, X., Lefebvre, T., Girard, J., and Postic, C. (2011) O-GlcNAcylation increases ChREBP protein content and transcriptional activity in the liver. Diabetes. *60*, 1399-1413.

Hardwick, J.P., Eckman, K., Lee, Y.K., Abdelmegeed, M.A., Esterle, A., Chilian, W.M., Chiang, J.Y., and Song, B.J. (2013). Eicosanoids in metabolic syndrome. Adv. Pharmacol. *66*, 157-266.

Harms M., and Seale P. (2013). Brown and beige fat: development, function and therapeutic potential. Nat. Med. *19*, 1252-1263.

Hauner, H. (2005). Secretory factors from human adipose tissue and their functional role. Proc. Nutr. Soc. *64*, 163-169.

Heilbronn L., Smith S.R., and Ravussin E. (2004). Failure of fat cell proliferation, mitochondrial function and fat oxidation results in ectopic fat storage, insulin resistance and type 2 diabetes mellitus. Int. J. Obesity. *28*, S12-S21.

Herman, M.A., Peroni, O.D., Villoria, J., Schön, M.R., Abumrad, N.A., Blüher, M., Klein, S., and Kahn BB. (2012). A novel ChREBP isoform in adipose tissue regulates systemic glucose metabolism. Nature. *484*, 333-338.

Hotamisligil, G.S., Arner, P., Caro, J.F., Atkinson, R.L., and Spiegelman, B.M. (1995). Increased adipose tissue expression of tumor necrosis factor-alpha in human obesity and insulin resistance. J. Clin. Invest. *95*, 2409-2415.

Hua, K.F., Wang, S.H., Dong, W.C., Lin, C.Y., Ho, C.L., and Wu, T.H. (2012). High glucose increases nitric oxide generation in lipopolysaccharide-activated macrophages by enhancing activity of protein kinase C-α/δ and NF-κB. Inflamm. Res. *61*, 1107-1116.

Hurtado del Pozo, C., Vesperinas-García, G., Rubio, M.Á., Corripio-Sánchez, R., Torres-García, A.J., Obregon, M.J., and Calvo, R.M. (2011). ChREBP expression in the liver, adipose tissue and differentiated preadipocytes in human obesity. Biochim. Biophys. Acta. *1811*, 1194-1200.

Ibrahim M.M. (2010). Subcutaneous and visceral adipose tissue: structural and functional differences. Obes. Rev. *11*, 11-8.

Inaba, T., Ishibashi, S., Gotoda, T., Kawamura, M., Morino, N., Nojima, Y., Kawakami, M., Yazaki, Y., and Yamada, N. (1996). Enhanced expression of platelet-derived growth factor-beta receptor by high glucose. Involvement of platelet-derived growth factor in diabetic angiopathy. Diabetes. *45*, 507-512.

Ingalls, A.M., Dickie, M.M., and Snell, G.D. (1950). Obese, a new mutation in the house mouse. J. Hered. *41*, 317-318.

Janabi, M., Yamashita, S., Hirano, K., Sakai, N., Hiraoka, H., Matsumoto, K., Zhang, Z., Nozaki, S., and Matsuzawa, Y. (2000). Oxidized LDL-induced NF-kappa B activation and subsequent expression of proinflammatory genes are defective in monocyte-derived macrophages from CD36-deficient patients. Arterioscler. Thromb. Vasc. Biol. *20*, 1953-1960.

Johnson A.M., and Olefsky J.M. (2013). The origins and drivers of insulin resistance. Cell. *152*, 673-684.

Johnson, W.D., Jr., Mei, B., and Cohn, Z.A. (1977). The separation, long-term cultivation, and maturation of the human monocyte. J. Exp. Med. *146*, 1613-1626.

Jung U.J., and Choi M.S. (2014). Obesity and its metabolic complications: the role of adipokines and the relationship between obesity, inflammation, insulin resistance, dyslipidemia and nonalcoholic fatty liver disease. Int. J. Mol. Sci. *15*, 6184-6223.

Kabashima, T., Kawaguchi, T., Wadzinski, B.E., and Uyeda, K. (2003). Xylulose 5-phosphate mediates glucose-induced lipogenesis by xylulose 5-phosphate-activated protein phosphatase in rat liver. Proc. Natl. Acad. Sci. U. S. A. *100*, 5107-5112.

Kadl, A., Meher, A.K., Sharma, P.R., Lee, M.Y., Doran, A.C., Johnstone, S.R., Elliott, M.R., Gruber, F., Han, J., Chen, W., Kensler, T., Ravichandran, K.S., Isakson, B.E., Wamhoff, B.R., and Leitinger, N. (2010). Identification of a novel macrophage phenotype that develops in response to atherogenic phospholipids via Nrf2. Circ. Res. *107*, 737-746.

Kahn B.B., and Flier J.S. (2000). Obesity and insulin resistance. J. Clin. Invest. *106*, 473-481.

Kahn, B.B., Alquier, T., Carling, D., and Hardie, D.G. (2005). AMP-activated protein kinase: ancient energy gauge provides clues to modern understanding of metabolism. Cell. Metab. *1*, 15-25.

Kanda, H., Tateya, S., Tamori, Y., Kotani, K., Hiasa, K., Kitazawa, R., Kitazawa, S., Miyachi, H., Maeda, S., Egashira, K., and Kasuga, M. (2006). MCP-1 contributes to macrophage infiltration into adipose tissue, insulin resistance, and hepatic steatosis in obesity. J. Clin, Invest. *116*, 1494-1505.

Kanter, J.E., Kramer, F., Barnhart, S., Averill, M.M., Vivekanandan-Giri, A., Vickery, T., Li, L.O., Becker, L., Yuan, W., Chait, A., Braun, K.R., Potter-Perigo, S., Sanda, S., Wight, T.N., Pennathur, S., Serhan, C.N., Heinecke, J.W., Coleman, R.A., and Bornfeldt, K.E. (2012). Diabetes promotes an inflammatory macrophage phenotype and atherosclerosis through acyl-CoA synthetase 1. Proc. Natl. Acad. Sci. U. S. A. *109*, E715-724.

Kaplan, M., Tendler, Y., Mahamid, R., Shiner, M., Aviram, M., and Hayek, T. (2010). High glucose upregulates C-reactive protein synthesis in macrophages. Clin. Chem. *56*, 1036-1038.

Kawaguchi, T., Takenoshita, M., Kabashima, T., and Uyeda, K. (2001) Glucose and cAMP regulate the L-type pyruvate kinase gene by phosphorylation dephosphorylation of the ChREBP. Proc. Natl. Acad. Sci. U.S.A. *98*, 13710-13715.

Keophiphath, M., Achard, V., Henegar, C., Rouault, C., Clement, K., and Lacasa, D. (2009). Macrophage-secreted factors promote a profibrotic phenotype in human preadipocytes. Mol. Endocrinol. *23*, 11-24.

Kim J.B., Wright H.M., Wright M., and Spiegelman B.M. (1998). ADD1/SREBP1 activates PPARg through the production of endogenous ligand. Proc. Natl. Acad. Sci. *95*, 4333-4337.

Kim, J.B., and Spiegelman, B.M. (1996). ADD1/SREBP1 promotes adipocyte differentiation and gene expression linked to fatty acid metabolism. Genes. Dev. *10*, 1096-1107.

Kishore, N., Sommers, C., Mathialagan, S., Guzova, J., Yao, M., Hauser, S., Huynh, K., Bonar, S., Mielke, C., Albee, L., Weier, R., Graneto, M., Hanau, C., Perry, T., and Tripp, C.S. (2003). A selective IKK-2 inhibitor blocks NF-kappa B-dependent gene expression in interleukin-1 beta-stimulated synovial fibroblasts. J. Biol. Chem. *278*, 32861-32871.

Kitade, H., Sawamoto, K., Nagashimada, M., Inoue, H., Yamamoto, Y., Sai, Y., Takamura, T., Yamamoto, H., Miyamoto, K., Ginsberg, H.N., Mukaida, N., Kaneko, S., and Ota, T. (2012). CCR5 plays a critical role in obesity-induced adipose tissue inflammation and insulin resistance by regulating both macrophage recruitment and M1/M2 status. Diabetes. *61*, 1680-1690.

Klöting, N., Fasshauer, M., Dietrich, A., Kovacs, P., Schon, M.R., Kern, M., Stumvoll, M., and Blüher, M. (2010). Insulin-sensitive obesity. Am. J. Physiol. Endocrinol. Metab. *299*, E506-515.

Kratz, M., Coats, B.R., Hisert, K.B., Hagman, D., Mutskov, V., Peris, E., Schoenfelt, K.Q., Kuzma, J.N., Larson, I., Billing, P.S., Landerholm, R.W., Crouthamel, M., Gozal, D., Hwang, S., Singh, P.K., and Becker, L. (2014). Metabolic dysfunction drives a mechanistically distinct proinflammatory phenotype in adipose tissue macrophages. Cell. Metab. *20*, 614-625.

Krauss R.M., Winston M., Fletcher B.J., and Grundy S.M. (1998). Obesity impact on cardiovascular disease. Circulation. *98*, 1472-1476.

Kurokawa, J., Arai, S., Nakashima, K., Nagano, H., Nishijima, A., Miyata, K., Ose, R., Mori, M., Kubota, N., Kadowaki, T., Oike, Y., Koga, H., Febbraio, M., Iwanaga, T., and Miyazaki, T. (2010). Macrophage-derived AIM is endocytosed into adipocytes and decreases lipid droplets via inhibition of fatty acid synthase activity. Cell. Metab. *11*, 479-492.

Kursawe, R., Caprio, S., Giannini, C., Narayan, D., Lin, A., D'Adamo, E., Shaw, M., Pierpont, B., Cushman, S.W., and Shulman, G. (2013). Decreased transcription of ChREBP-α/β isoforms in abdominal subcutaneous adipose tissue of obese adolescents with prediabetes or early type 2 diabetes: associations with insulin resistance and hyperglycemia. Diabetes. *62*, 837-844.

Lacasa, D., Taleb, S., Keophiphath, M., Miranville, A., and Clément, K. (2007). Macrophage-secreted factors impair human adipogenesis: involvement of proinflammatory state in preadipocytes. Endocrinology. *148*, 868-877.

Laemmli, U.K. (1970). Cleavage of structural proteins during the assembly of the head of bacteriophage T4. Nature. *227*, 680-685.

Lafontan, M. (2008). Advances in adipose tissue metabolism. Int. J. Obes. *32*, S39-S51.

Lau, D.C., and Teoh, H. (2013). Benefits of modest weight loss on the management of type 2 diabetes mellitus. Can. J. Diabetes. *37*, 128-134.

Lee M.J., Wu Y., and Fried S.K. (2010). Adipose tissue remodeling in pathophysiology of obesity. Curr. Opin. Clin. Nutr. Metab. Care. *13*, 371-376.

Li, L., Sawamura, T., and Renier, G. (2004). Glucose enhances human macrophage LOX-1 expression: role for LOX-1 in glucose-induced macrophage foam cell formation. Circ. Res. *94*, 892-901.

Li, M.V., Chang, B., Imamura, M., Poungvarin, N., and Chan, L. (2006). Glucose-dependent transcriptional regulation by an evolutionarily conserved glucose-sensing module. Diabetes. *55*, 1179-1189.

Li, M.V., Chen, W., Harmancey, R.N., Nuotio-Antar, A.M., Imamura, M., Saha, P., Taegtmeyer, H., and Chan, L. (2010). Glucose-6-phosphate mediates activation of the carbohydrate responsive binding protein (ChREBP). Biochem. Biophys. Res. Commun. *395*, 395-400.

Li, M.V., Chen, W., Poungvarin, N., Imamura, M., and Chan, L. (2008). Glucose-mediated transactivation of carbohydrate response element-binding protein requires cooperative actions from Mondo conserved regions and essential trans-acting factor 14-3-3. Mol. Endocrinol. *22*, 1658-1672.

Lin, Y., Berg, A.H., Iyengar, P., Lam, T.K., Giacca, A., Combs, T.P., Rajala, M.W., Du, X., Rollman, B., Li, W., Hawkins, M., Barzilai, N., Rhodes, C.J., Fantus, I.G., Brownlee, M., and Scherer, P.E. (2005). The hyperglycemia-induced inflammatory response in adipocytes: the role of reactive oxygen species. J Biol Chem. *280*, 4617-4626.

Liu, G., and Abraham, E. (2013). MicroRNAs in immune response and macrophage polarization. Arterioscler. Thromb. Vasc. Biol. *33*, 170-177.

Liu, L.H., Wang, X.K., Hu, Y.D., Kang, J.L., Wang, L.L., and Li, S. (2004). Effects of a fatty acid synthase inhibitor on adipocyte differentiation of mouse 3T3-L1 cells. Acta. Pharmacol. Sin. *25*, 1052-1057.

Liu, S., Yang, Y., and Wu, J. (2011). TNFα-induced up-regulation of miR-155 inhibits adipogenesis by down-regulating early adipogenic transcription factors. Biochem. Biophys. Res. Commun. *414*, 618-624.

Lu, C., Kumar, P.A., Fan, Y., Sperling, M.A., and Menon, R.K. (2010). A novel effect of growth hormone on macrophage modulates macrophage-dependent adipocyte differentiation. Endocrinology. *151*, 2189-2199.

Lumeng, C.N., Bodzin, J.L., and Saltiel, A.R. (2007A). Obesity induces a phenotypic switch in adipose tissue macrophage polarization. J. Clin. Invest. *117*, 175-184.

Lumeng, C.N., DelProposto, J.B., Westcott, D.J., and Saltiel, A.R. (2008). Phenotypic switching of adipose tissue macrophages with obesity is generated by spatiotemporal differences in macrophage subtypes. Diabetes. *57*, 3239-3246.

Lumeng, C.N., Deyoung, S.M., and Saltiel, A.R. (2007C). Macrophages block insulin action in adipocytes by altering expression of signaling and glucose transport proteins. Am. J. Physiol. Endocrinol. Metab. *292*, E166-174.

Lumeng, C.N., Deyoung, S.M., Bodzin, J.L., and Saltiel, A.R. (2007B). Increased inflammatory properties of adipose tissue macrophages recruited during diet-induced obesity. Diabetes. *56*, 16-23.

Lumeng, C.N., Liu, J., Geletka, L., Delaney, C., Delproposto, J., Desai, A., Oatmen, K., Martinez-Santibanez, G., Julius, A., Garg, S., and Yung, R.L. (2011). Aging is associated with an increase in T cells and inflammatory macrophages in visceral adipose tissue. J. Immunol. *187*, 6208-6216.

Ma, L., Robinson, L.N., and Towle, H.C. (2006). ChREBP*Mlx is the principal mediator of glucose-induced gene expression in the liver. J. Biol. Chem. *281*, 28721-28730.

Ma, L., Tsatsos, N.G., and Towle, H.C. (2005). Direct role of ChREBP*Mlx in regulating hepatic glucose-responsive genes. J. Biol. Chem. *280*, 12019-12027.

Malyshev, I., and Malyshev, Y. (2015). Current Concept and Update of the Macrophage Plasticity Concept: Intracellular Mechanisms of Reprogramming and M3 Macrophage "Switch" Phenotype. Biomed. Res. Int. *2015*, 341308.

Michaud, A., Lacroix-Pépin, N., Pelletier, M., Daris, M., Biertho, L., Fortier, M.A., and Tchernof, A. (2014A). Expression of genes related to prostaglandin synthesis or signaling in human subcutaneous and omental adipose tissue: depot differences and modulation by adipogenesis. Mediators. Inflamm. *2014*, 451620.

Michaud, A., Lacroix-Pépin, N., Pelletier, M., Veilleux, A., Noël, S., Bouchard, C., Marceau, P., Fortier, M.A., and Tchernof, A. (2014B). Prostaglandin (PG) F2 alpha synthesis in human subcutaneous and omental adipose tissue: modulation by inflammatory cytokines and role of the human aldose reductase AKR1B1. PLoS. One. *9*, e90861.

Moura, L.I., Silva, L., Leal, E.C., Tellechea, A., Cruz, M.T., and Carvalho, E. (2013). Neurotensin modulates the migratory and inflammatory response of macrophages under hyperglycemic conditions. Biomed. Res. Int. *2013*, 941764.

Mueller, E., Drori, S., Aiyer, A., Yie, J., Sarraf, P., Chen, H., Hauser, S., Rosen, E.D., Ge, K., Roeder, R.G., and Spiegelman, B.M. (2002). Genetic analysis of adipogenesis through peroxisome proliferator-activated receptor gamma isoforms. J. Biol. Chem. *277*, 41925-41930.

Mukherjee R., Jow L., Croston G.E., and Paterniti J.R. Jr. (1997). Identification, characterization, and tissue distribution of human peroxisome proliferator-activated receptor (PPAR) isoforms PPARgamma2 versus PPARgamma1 and activation with retinoid X receptor agonists and antagonists. J. Biol. Chem. *272*, 8071-8076.

Myers, M. G., Cowley, M. A., and Münzberg, H. (2008). Mechanisms of leptin action and leptin resistance. Annu. Rev. Physiol., *70*, 537-556.

Nathan, C.F. (1987). Secretory products of macrophages. J. Clin. Invest. *79*, 319-326.

Navaneelan, T., and Janz, T. (2014). Adjusting the scales: Obesity in the Canadian population after correcting for respondent bias. Health at a Glance. May. Statistics Canada Catalogue no. 82-624-X.

Ni, H.X., Yu, N.J., and Yang, X.H. (2010). The study of ginsenoside on PPARgamma expression of mononuclear macrophage in type 2 diabetes. Mol. Biol. Rep. *37*, 2975-2979.

Norris, D.A., Morris, R.M., Sanderson, R.J., and Kohler, P.F. (1979). Isolation of functional subsets of human peripheral blood monocytes. J. Immunol., *123*, 166-172.

O'Hara, A., Lim, F.L., Mazzatti, D.J., and Trayhurn, P. (2012). Stimulation of inflammatory gene expression in human preadipocytes by macrophage-conditioned medium: upregulation of IL-6 production by macrophage-derived IL-1b. Mol. Cell. Endocrinol. *349*, 239-247.

Oh, D.Y., Morinaga, H., Talukdar, S., Bae, E.J., and Olefsky, J.M. (2012). Increased macrophage migration into adipose tissue in obese mice. Diabetes. *61*, 346-354.

Ohashi, K., Parker, J.L., Ouchi, N., Higuchi, A., Vita, J.A., Gokce, N., Pedersen, A.A., Kalthoff, C., Tullin, S., Sams, A., Summer, R., and Walsh, K. (2010). Adiponectin promotes macrophage polarization toward an anti-inflammatory phenotype. J. Biol. Chem. *285*, 6153-6160.

Oñate B., Vilahur G., Ferrer-Lorente R., Ybarra J., Díez-Caballero A., Ballesta-López C., Moscatiello F., Herrero J., and Badimon L. (2012). The subcutaneous adipose tissue reservoir of functionally active stem cells is reduced in obese patients. FASEB. *26*, 4327-4336.

Oram, J.F., and Vaughan, A.M. (2006). ATP-Binding cassette cholesterol transporters and cardiovascular disease. Circ. Res. *99*, 1031-1043.

Ortega Martinez de Victoria, E., Xu, X., Koska, J., Francisco, A.M., Scalise, M., Ferrante, A.W., Jr., and Krakoff, J. (2009). Macrophage content in subcutaneous adipose tissue: associations with adiposity, age, inflammatory markers, and whole-body insulin action in healthy Pima Indians. Diabetes. *58*, 385-393.

Ouchi, N., Higuchi, A., Ohashi, K., Oshima, Y., Gokce, N., Shibata, R., Akasaki, Y., Shimono, A., and Walsh, K. (2010). Sfrp5 is an anti-inflammatory adipokine that modulates metabolic dysfunction in obesity. Science. *329*, 454-457.

Ouchi, N., Parker, J.L., Lugus, J.J., and Walsh, K. (2011). Adipokines in inflammation and metabolic disease. Nat. Rev. Immunol. *11*, 85-97.

Ouellet V., Labbé S.M., Blondin D.P., Phoenix S., Guérin B., Haman F., Turcotte E.E., Richard D., and Carpentier A.C. (2012). J. Clin. Invest. *122*, 545-552.

Patsouris, D., Li, P.P., Thapar, D., Chapman, J., Olefsky, J.M., and Neels, J.G. (2008). Ablation of CD11c-positive cells normalizes insulin sensitivity in obese insulin resistant animals. Cell. Metab. *8*, 301-339.

Postic, C., Dentin, R., Denechaud, P.D., and Girard, J. (2007). ChREBP, a transcriptional regulator of glucose and lipid metabolism. Annu. Rev. Nutr. *27*, 179-192.

Proença, A.R., Sertié, R.A., Oliveira, A.C., Campaãa, A.B., Caminhotto, R.O., Chimin, P., and Lima, F.B. (2014). New concepts in white adipose tissue physiology. Braz. J. Med. Biol. Res. *47*, 192-205.

Public Health Agency of Canada. (2011). Diabetes in Canada: Facts and figures from a public health perspective.

Reshef, L., Olswang, Y., Cassuto, H., Blum, B., Croniger, C.M., Kalhan, S.C., Tilghman, S.M., and Hanson, R.W. (2003). Glyceroneogenesis and the triglyceride/fatty acid cycle. J. Biol. Chem. *278*, 30413-30416.

Ricote, M., Li, A.C., Willson, T.M., Kelly, C.J., and Glass, C.K. (1992). The peroxisome proliferator-activated receptor-gamma is a negative regulator of macrophage activation. Nature. *391*, 79-82.

Rodríguez-Prados, J.C., Través, P.G., Cuenca, J., Rico, D., Aragonés, J., Martín-Sanz, P., Cascante, M., and Boscá, L. (2010). Substrate fate in activated macrophages: a comparison between innate, classic, and alternative activation. J. Immunol. *185*, 605-614.

Roepstorff, C., Thiele, M., Hillig, T., Pilegaard, H., Richter, E.A., Wojtaszewski, J.F., and Kiens, B. (2006). Higher skeletal muscle alpha2AMPK activation and lower energy charge and fat oxidation in men than in women during submaximal exercise. J. Physiol. *574*, 125-138.

Rosen, E.D., Hsu, C.H., Wang, X., Sakai, S., Freeman, M.W., Gonzalez, F.J., and Spiegelman, B.M. (2002). C/EBPalpha induces adipogenesis through PPARgamma: a unified pathway. Genes. Dev. *16*, 22-26.

Ruan, H., Hacohen, N., Golub, T.R., Van Parijs, L., Lodish, H.F. (2002). Tumor necrosis factor-alpha suppresses adipocyte-specific genes and activates expression of preadipocyte genes in 3T3-L1 adipocytes: nuclear factor-kappaB activation by TNF-alpha is obligatory. Diabetes. *51*, 1319-1336.

Ruderman, N., and Prentki, M. (2004). AMP kinase and malonyl-CoA: targets for therapy of the metabolic syndrome. Nat. Rev. Drug. Discov. *3*, 340-351.

Saely C.H., Geiger K., and Drexel H. (2012). Brown versus white adipose tissue: a mini-review. Gerontology. *58*, 15-23.

Saini, V. (2010). Molecular mechanisms of insulin resistance in type 2 diabetes mellitus. World. J. Diabetes. *1*, 68-75.

Sakiyama, H., Wynn, R.M., Lee, W.R., Fukasawa, M., Mizuguchi, H., Gardner, K.H., Repa, J.J., and Uyeda, K. (2008). Regulation of nuclear import/export of carbohydrate response element-binding protein (ChREBP): interaction of an alpha-helix of ChREBP with the 14-3-3 proteins and regulation by phosphorylation. J. Biol. Chem. *283*, 24899-24908.

Sartippour, M.R., and Renier, G. (2000). Differential regulation of macrophage peroxisome proliferator-activated receptor expression by glucose : role of peroxisome

proliferator-activated receptors in lipoprotein lipase gene expression. Arterioscler. Thromb. Vasc. Biol. *20*, 104-110.

Sartippour, M.R., Lambert, A., Laframboise, M., St-Jacques, P., and Renier, G. (1998). Stimulatory effect of glucose on macrophage lipoprotein lipase expression and production. Diabetes. *47*, 431-438.

Senanayake, S., Brownrigg, L.M., Panicker, V., Croft, K.D., Joyce, D.A., Steer, J.H., Puddey, I.B., and Yeap, B.B. (2007). Monocyte-derived macrophages from men and women with Type 2 diabetes mellitus differ in fatty acid composition compared with non-diabetic controls. Diabetes. Res. Clin. Pract. *75*, 292-300.

Skurk, T., and Hauner, H. (2012). Primary culture of human adipocyte precursor cells: expansion and differentiation. Methods. Mol. Biol. *806*, 215-226.

Smas, C.M., and Sul, H.S. (1995) Control of adipocyte differentiation. Biochem. J. *309*, 697-710.

Spalding, K.L., Arner, E., Westermark, P.O., Bernard, S., Buchholz, B.A., Bergmann, O., Blomqvist, L., Hoffstedt, J., Naslund, E., Britton, T., Concha, H., Hassan, M., Rydén, M., Frisén, J., and Arner, P. (2008). Dynamics of fat cell turnover in humans. Nature. *453*, 783-787.

Speakman J.R., and O'Rahilly S. (2012). Fat: an evolving issue. Dis. Model. Mech. *5*, 569-573.

Spiegelman, B.M., and Ginty, C.A. (1983). Fibronectin modulation of cell shape and lipogenic gene expression in 3T3-adipocytes. Cell. *35*, 657-666.

Steinberg, G.R. (2009). Role of the AMP-activated protein kinase in regulating fatty acid metabolism during exercise. Appl. Physiol. Nutr. Metab. *34*, 315-322.

Stienstra, R., Duval, C., Keshtkar, S., van der Laak, J., Kersten, S., and Muller, M. (2008). Peroxisome proliferator-activated receptor gamma activation promotes infiltration of alternatively activated macrophages into adipose tissue. J. Biol. Chem. *283*, 22620-22627.

Strissel, K.J., Stancheva, Z., Miyoshi, H., Perfield, J.W., 2nd, DeFuria, J., Jick, Z., Greenberg, A.S., and Obin, M.S. (2007). Adipocyte death, adipose tissue remodeling, and obesity complications. Diabetes. *56*, 2910-2918.

Suganami, T., Nishida, J., and Ogawa, Y. (2005). A paracrine loop between adipocytes and macrophages aggravates inflammatory changes: role of free fatty acids and tumor necrosis factor alpha. Arterioscler. Thromb. Vasc. Biol. *25*, 2062-2068.

Sun K., Kusminski C.M., and Scherer P.E. (2011) Adipose tissue remodeling and obesity. J. Clin. Invest. *121*, 2094-2101.

Suzawa, M., Takada, I., Yanagisawa, J., Ohtake, F., Ogawa, S., Yamauchi, T., Kadowaki, T., Takeuchi, Y., Shibuya, H., Gotoh, Y., Matsumoto, K., and Kato, S. (2003). Cytokines suppress adipogenesis and PPAR-gamma function through the TAK1/TAB1/NIK cascade. Nat. Cell. Biol. *5*, 224-230.

Tam, C.S., Tordjman, J., Divoux, A., Baur, L.A., and Clément, K. (2012). Adipose tissue remodeling in children: the link between collagen deposition and age-related adipocyte growth. J. Clin. Endocrinol. Metab. *97*, 1320-1327.

Tchoukalova, Y., Koutsari, C., and Jensen, M. (2007). Committed subcutaneous preadipocytes are reduced in human obesity. Diabetologia. *50*, 151-157.

Thompson, K. and Towle, H.C. (1991). Localization of the carbohydrate response element of the rat L-type pyruvate kinase gene. J. Biol. Chem. *266*, 8679-8882.

Tontonoz, P., Graves, R.A., Budavari, A.I., Erdjument-Bromage, H., Lui, M., Hu, E., Tempst, P., and Spiegelman, B.M. (1994). Adipocyte-specific transcription factor ARF6 is a heterodimeric complex of two nuclear hormone receptors, PPAR gamma and RXR alpha. Nucleic. Acids. Res. *22*, 5628-5634.

Tung, Y.C., and Yeo, G.S. (2011). From GWAS to biology: lessons from FTO. Ann. N. Y. Acad. Sci. *1220*, 162-171.

Turer A.T., and Scherer P.E. (2012). Adiponectin: mechanistic insights and clinical implications. Diabetologia. *55*, 2319-2326.

Ukkola O., and Santaniemi M. (2002). Adiponectin: a link between excess adiposity and associated comorbidities?. J. Mol. Med. *80*, 696-702.

van de Veerdonk, F.L., and Netea, M.G. (2010). Diversity: a hallmark of monocyte society. Immunity. *33*, 289-291.

van der Lans A.A., Hoeks J., Brans B., Vijgen G.H., Visser M.G., Vosselman M.J., Hansen J., Jörgensen J.A., Wu J., Mottaghy F.M., Schrauwen P., and van Marken Lichtenbelt W.D. (2013). Cold acclimation recruits human brown fat and increases nonshivering thermogenesis. J. Clin, Invest. *123*, 3395-3403.

van Marken Lichtenbelt, W.D., Vanhommerig, J.W., Smulders, N.M., Drossaerts, J.M., Kemerink, G.J., Bouvy, N.D., Schrauwen, P., and Teule, G.J. (2009). Cold-activated brown adipose tissue in healthy men. N. Engl. J. Med. *360*, 1500-1508.

Vats, D., Mukundan, L., Odegaard, J.I., Zhang, L., Smith, K.L., Morel, C.R., Wagner, R.A., Greaves, D.R., Murray, P.J., and Chawla, A. (2006). Oxidative metabolism and PGC-1beta attenuate macrophage-mediated inflammation. Cell. Metab. *4*, 13-24.

Verrijn Stuart, A.A., Schipper, H.S., Tasdelen, I., Egan, D.A., Prakken, B.J., Kalkhoven, E., and de Jager W. (2012). Altered plasma adipokine levels and in vitro adipocyte differentiation in pediatric type 1 diabetes. J. Clin. Endocrinol. Metab. *97*, 463-472.

Virtanen, K.A., Lidell, M.E., Orava, J., Heglind, M., Westergren, R., Niemi, T., Taittonen, M., Laine, J., Savisto, N.J., Enerback, S., and Nuutila, P. (2009). Functional brown adipose tissue in healthy adults. N. Engl. J. Med. *360*, 1518-1525.

Vogel, C., snf Marcotte, E.M. (2012). Insights into the regulation of protein abundance from proteomic and transcriptomic analyses. Nat. Rev. Genet. *13*, 227-232.

Wabitsch, M., Brenner, R.E., Melzner, I., Braun, M., Moller, P., Heinze, E., Debatin, K.M., and Hauner, H. (2001). Characterization of a human preadipocyte cell strain with high capacity for adipose differentiation. Int. J. Obes. Relat. Metab. Disord. *25*, 8-15.

Wajchenberg B.L. (2000). Subcutaneous and visceral adipose tissue: their relation to the metabolic syndrome. Endocr. Rev. *21*, 697-738.

Wang, W., Zhang, X., Zheng, J., and Yang, J. (2010). High glucose stimulates adipogenic and inhibits osteogenic differentiation in MG-63 cells through cAMP/protein kinase A/extracellular signal-regulated kinase pathway. Mol. Cell. Biochem. *338*, 115-122.

Weisberg, S.P., Hunter, D., Huber, R., Lemieux, J., Slaymaker, S., Vaddi, K., Charo, I., Leibel, R.L., and Ferrante, A.W., Jr. (2006). CCR2 modulates inflammatory and metabolic effects of high-fat feeding. J. Clin. Invest. *116*, 115-124.

Weisberg, S.P., McCann, D., Desai, M., Rosenbaum, M., Leibel, R.L., and Ferrante, A.W., Jr. (2003). Obesity is associated with macrophage accumulation in adipose tissue. J. Clin. Invest. *112*, 1796-1808.

Wells, J.C., and Fewtrell, M.S. (2006). Measuring body composition. Arch. Dis. Child. *91*, 612-617.

Wentworth, J.M., Naselli, G., Brown, W.A., Doyle, L., Phipson, B., Smyth, G.K., Wabitsch, M., O'Brien, P.E., and Harrison, L.C. (2010). Pro-inflammatory CD11c+CD206+ adipose tissue macrophages are associated with insulin resistance in human obesity. Diabetes. *59*, 1648-1656.

Wernstedt Asterholm, I., Tao, C., Morley, T.S., Wang, Q.A., Delgado-Lopez, F., Wang, Z.V., and Scherer, P.E. (2014). Adipocyte inflammation is essential for healthy adipose tissue expansion and remodeling. Cell. Metab. *20*, 103-118.

WHO (2004). The global burden of disease. Geneva, World Health Organization, 2004:2008 update.

Wilson P.W., D'Agostino R.B., Sullivan L., Parise H., and Kannel W.B. (2002). Overweight and obesity as determinants of cardiovascular risk: the Framingham experience. Arch. Intern. Med. *162*, 1867-1872.

Witte, N., Muenzner, M., Rietscher, J., Knauer, M., Heidenreich, S., Nuotio-Antar, A.M., Graef, F.A., Fedders, R., Tolkachov, A., Goehring, I., and Schupp, M. (2015). The Glucose Sensor ChREBP Links De Novo Lipogenesis to PPARγ Activity and Adipocyte Differentiation. Endocrinology. *156*, 4008-4019.

Wu Z., Rosen E.D., Brun R., Hauser S., Adelmant G., Troy A.E., McKeon C., Darlington G.J., and Spiegelman B.M. (1999). Cross-regulation of C/EBP alpha and PPAR gamma controls the transcriptional pathway of adipogenesis and insulin sensitivity. Mol. Cell. *3*, 151-158.

Wu, D., Molofsky, A.B., Liang, H.E., Ricardo-Gonzalez, R.R., Jouihan, H.A., Bando, J.K., Chawla, A., and Locksley, R.M. (2011). Eosinophils sustain adipose alternatively activated macrophages associated with glucose homeostasis. Science. *332*, 243-247.

Xu, H., Barnes, G.T., Yang, Q., Tan, G., Yang, D., Chou, C.J., Sole, J., Nichols, A., Ross, J.S., Tartaglia, L.A., and Chen, H. (2003). Chronic inflammation in fat plays a crucial role in the development of obesity-related insulin resistance. J. Clin. Invest. *112*, 1821-1830.

Yamashita, H., Takenoshita, M., Sakurai, M., Bruick, R.K., Henzel, W.J., Shillinglaw, W., Arnot, D., and Uyeda, K. (2001). A glucose-responsive transcription factor that regulates carbohydrate metabolism in the liver. Proc. Natl. Acad. Sci. U. S. A. *98*, 9116-9121.

Yarmo, M.N., Gagnon, A., and Sorisky, A. (2010). The anti-adipogenic effect of macrophage-conditioned medium requires the IKKbeta/NF-kappaB pathway. Horm. Metab. Res. *42*, 831-836.

Yeh, W.C., Cao, Z., Classon, M., and McKnight, S.L. (1995). Cascade regulation of terminal adipocyte differentiation by three members of the C/EBP family of leucine zipper proteins. Genes. Dev. *9*, 168-181.

Yore, M.M., Syed, I., Moraes-Vieira, P.M., Zhang, T., Herman, M.A., Homan, E.A., Patel, R.T., Lee, J., Chen, S., Peroni, O.D., Dhaneshwar, A.S., Hammarstedt, A., Smith, U., McGraw, T.E., Saghatelian, A., and Kahn, B.B. (2014). Discovery of a class of endogenous mammalian lipids with anti-diabetic and anti-inflammatory effects. Cell. *159*, 318-332.

Zeyda, M., Gollinger, K., Kriehuber, E., Kiefer, F.W., Neuhofer, A., and Stulnig, T.M. (2010). Newly identified adipose tissue macrophage populations in obesity with distinct chemokine and chemokine receptor expression. Int. J. Obes. *34*, 1684-1694.

Zhang J., Fu M., Cui T., Xiong C., Xu K., Zhong W., Xiao Y., Floyd D., Liang J., Li E., Song Q., and Chen Y.E. (2004). Selective disruption of PPARgamma 2 impairs the development of adipose tissue and insulin sensitivity. Proc. Natl. Acad. Sci. USA. *101*, 10703-10708.

Zhang, Y., Proenca, R., Maffei, M., Barone, M., Leopold, L., and Friedman, J.M. (1994). Positional cloning of the mouse obese gene and its human homologue. Nature. *372*, 425-432.

Zuo, Y., Qiang, L., and Farmer, S.R. (2006). Activation of C/EBPalpha expression by C/EBPbeta during adipogenesis requires a PPARgamma-associated repression of HDAC1 at the C/EBPalpha gene promoter. J. Biol. Chem. *281*, 7960-7967.

CURRICULUM VITAE

VIAN PESHDARY

Education

PhD. Biochemistry
University of Ottawa, Ottawa, ON
Jan 2012 – present

MSc. Biochemistry
University of Ottawa, Ottawa, ON
Sept 2009 – Dec 2011

BSc. Biochemistry
University of Ottawa, Ottawa, ON
Sept 2004 – May 2009

Employment

Contractor, Health Canada
(Jan 2016 – April 2016)

Laboratory of Dr. Ella Atlas, Department of Endocrine Toxicology, Ottawa ON

- Cultured INS-1E rat pancreatic beta cells and optimized conditions for glucose stimulated insulin release with exposure to flame retardants
- Cultured 3T3-L1 mouse preadipocyte cells and assessed adipogenesis in response to flame retardant treatment

Laboratory Instructor, University of Ottawa

Faculty of Science, Department of Biochemistry, Ottawa ON

Courses:
- "Introduction to Biochemistry II", Winter sessions 2011 – 2015
- "Molecular Biology Laboratory", Fall sessions 2012 – 2014
- "Introduction to Biochemistry I", Winter sessions 2009 – 2014

- Taught topics in the field of chemistry, biochemistry and molecular biology relevant to laboratory sessions
- Taught and mentored students in biochemical techniques
- Supervised laboratory sessions

- Evaluated laboratory reports, take home assignments, and laboratory performance
- Guided and evaluated students individually during final project, protocol compilation and project oral presentation
- Proctored practical and written exams

Head-Laboratory Instructor, University of Ottawa
Faculty of Science, Department of Biochemistry, Ottawa ON

Course:
- "Introduction to Biochemistry I", Winter session 2010

- Trained and mentored junior lab instructors
- Supervised and overlooked laboratory sessions
- Prepared consensus laboratory report and marking scheme for all lab demonstrators to follow and use

Teacher, University of Ottawa
Faculty of Science, Department of Biochemistry, Ottawa ON

Mini-Course**:**
- "Detectives in Genes", every first week of May 2006 – 2009

- Prepared teaching plans
- Taught basic biology, chemistry and biochemistry to elite elementary and high school students (grades 8-12)
- Supervised laboratory sessions

Instructor: "Celebrating Science" workshop, University of Ottawa
(2007, 2008)

Faculty of Science, Department of Biochemistry, Ottawa ON

- Science instructor,
- Taught grade 11 and 12 high school students techniques used for extraction of Green Fluorescent Protein from transformed *E.coli*.

Laboratory Technician, University of Ottawa

(2006 – 2009)

The laboratory of Dr. Steffany Bennett, Ottawa ON

- Genotyped and handled various mouse colonies
- Performed animal (intraperitoneal injection, tissue dissection, etc.) work for graduate students,
- Carried on individual projects and laboratory tasks
- Limited access to ordering and in regular communication with industry representatives

Volunteering/ Extracurricular Activities

Ottawa Sport and Social Club (OSSC)
(Winter 2015)
Ottawa ON

Play soccer with 7 other team members for a recreational co-ed sports league.

Multiple Sclerosis Society of Canada
(2014)
Ottawa ON

Friendly visitor, accompany and assist clients during social outings and events that are planned by the society. Help create a positive and encouraging environment for clients.

Child Sponsor, Plan Canada
(2012 – Present)

Child sponsor, providing financial support and correspondence for an adolescent child and her community to help establish better living environment and to enhance positive opportunities

Science Demonstrator, Let's Talk Science
(2012 – 2014)
Ottawa ON

Science presenter/demonstrator, with a partner demonstrated in class hands-on activities to convey scientific materials to public and First Nations elementary and kindergarten classrooms

Scholarships and Awards

First place winner of the graduate student poster presentation at Group for Research in Inflammation and Pathogenesis (GRIP) poster symposia
(2014)

University of Ottawa Dean's Scholarship
(2012)

University of Ottawa Biochemistry, Microbiology and Immunology Soft- Funded Scholarship
(2009 – 2011)

University of Ottawa Entrance Scholarship
(2004 – 2005)

Queen Elizabeth II Reaching For the Top Scholarship, ON
(2004)

Publication

Kennedy KAM, Porter T, Mehta V, Ryan SD, Price F, **Peshdary V**, Karamboulas C, Savage J, Drysdae T, Li S-C, Bennett SAL, Skerjanc IS. (2009) Retinoic acid can enhance skeletal muscle specification and bypass inhibition by Bone Morphogenetic Protein 4 but not by dominant negative beta-catenin**.** BMC Biology, 7: 67.

Publication in press

V. Peshdary, A. Gagnon, and A. Sorisky. (2016) Anti-adipogenic and pro-inflammatory effects of human monocyte-derived macrophages are enhanced by high glucose concentration. Canadian Journal of Diabetes.

Conferences

Poster presented and showcased in a guided audio tour at American Diabetes Association 75th Scientific Sessions, Boston, MA; June 5 - June 9, 2015.

V. Peshdary, A.M. Gagnon, and A. Sorisky (2015) Medium from Human Monocyte-derived Macrophage Conditioned in High, but Not Normal, Glucose Inhibits Triacylglycerol Accumulation and Peroxisome Proliferator-Activated Receptor γ Expression in Differentiating Human Preadipocytes,

Poster presentation at American Diabetes Association 73rd Scientific Sessions, Chicago, IL; June 21 - 25, 2013,

V. Peshdary, A.M. Gagnon, and A. Sorisky (2013) High glucose promotes triacylglycerol accumulation during the differentiation of human subcutaneous abdominal preadipocytes into adipocytes.

Poster presentation at Society of Neurosciences Conference, Washington, DC; 2008

V. Peshdary, S. Imbeault, K. Wurts, L. G. Gauvin, S. A. L. Bennett, and S. Fai. (2008) 3D modeling of connexin expression in postnatal neural progenitor cells.

Laboratory Skills

Molecular Genetics: Genetic cloning (PCR, RT–PCR, qRT–PCR, ligation, restriction enzyme digests, recombination, transformation), primer design and optimization, DNA and RNA purification, plasmid amplification (MINI preps), *in situ* hybridization, immunofluorescence staining of frozen tissue.

***In Vitro* Work:** Culturing and differentiating human primary preadipocytes and macrophage cell line. Isolating and differentiating blood derived human monocytes. Cultureing and differentitating mouse 3T3-L1 preadipocyte cells. Culturing INS-1E rat pancreatic beta cells.

***In Vivo* Work:** Mouse perfusion, mouse brain (hippocampus, posterior cortex, etc.) dissection, mouse body (heart, lung, and liver) dissection, mouse brain sectioning, mouse brain synaptosome extraction and purification, Morris water Maze (MWM) behavior analysis

Proteomic and Lipidomic: Western blotting, protein and lipid extraction, TUNEL assay, glucose stimulated insulin secretion (GSIS) assay

Microscopy: Light microscopy and Fluorescent microscopy

Computing: Photoshop, Clone Manager**,** Graph Pad In Stat, Graph Pad Prism, Delta Graph**,** Pymol**,** Fly Lab**,** Microsoft word and Microsoft Excel**,** Autodesk Maya and Adobe Premiere Pro CS4